Drought-Stress-Related Reprogramming of Gene Expression in Barley Involves Differential Histone Modifications at ABA-related Genes

Dissertation

zur Erlangung des akademischen Grades

doctor rerum naturalium

(Dr. rer. nat.)

vorgelegt der

Naturwissenschaftlichen Fakultät I - Biowissenschaften -

der Martin-Luther-Universität Halle-Wittenberg

vorgelegt von

Frau Charlotte Ost

geb. am 18.01.1990 in Berlin

Gutachter:

Prof. Dr. Klaus Humbeck

Prof. Dr. Zofia Szweykowska-Kulińska

Prof. Dr. Edgar Peiter

Tag der öffentlichen Verteidigung: 02.04.2024

Table of Contents

Parts of this work were published in the following article:

Ost, C., Cao, H. X., Nguyen, T. L., Himmelbach, A., Mascher, M., Stein, N., & Humbeck, K. (2023). Drought-Stress-Related Reprogramming of Gene Expression in Barley Involves Differential Histone Modifications at ABA-Related Genes. *International Journal of Molecular Sciences*, *24*(15), 12065. DOI: 10.3390/ijms24151206

Abbreviations

AAO3	Aldehyde oxidase
ABA	Abscisic Acid
ABFs	ABRE-binding factors
ABI1	ABA senstive 1
adj.	adjusted
AHG3	ABA hypersensitive germination 3
AP2.4	Apetala2.4
AREB	ABA-responsive Element Binding factors
ATG	start codon ATG
ATX1	Arabidopsis TRITHORAX-like factor
BAC	bacterial artificial chromsome
BAM	Binary Alignment Map
BED	Browser Extensible Data
bp	base pair
BWA	Burrows-Wheeler-Alignment
bZIP TF	basic leucine zipper domain transcription factor
CBC	cap-binding complex
ChIP	Chromatin Immunoprecipitation
ChIP-Seq	ChIP followed by NGS
Chl	Chlorophyll
CMT3	Chromomethylase 3
COMPASS-like	complex proteins associated with Set1
COP1	constitutive photomorgenic 1
CPB	CREB-binding protein
CPM	counts per million reads
CREB	cAMP response element-binding protein
CT	Control
CYP	Cytochrome P450
das	days after sowing
DEG	Differentially Expressed Gene
DME	Demeter
DMG	Differentially Methylated Gene
DML2	Demeter-like 2
DMR	Differentially Methylated Region
DMS	differentially methylated sites
DMTs	histone demethylases
DNA	Desoxyribonucleic Acid
DNMT1	DNA (cytosine-5)-methyltransferase 1
DRE/CRT	dehydration-responsive element/C-repeat
DREB2	DRE/CRT-binding protein 2
DRM1	Domain rearranged methyltransferase 1
DS	drought stress
e.g.	for example
EDTA	Ethylenediaminetetraacetic acid
Fv	variable fluorescence
Gb	Gigabase

GNATs	GNC5-related acetyltrasnferase
GNC5	General control nondepressible 5
GO	Gene Ontology
GS2	glutamine synthetase
HAB1	Homology to ABI1
HAI1	Highly ABA-induced PP2C1
HAT	Histone Acetyltransferase
HC	High Confidence
HD2	histone-deacetylase 2
HDAC	Histone Deacetylase
HDACs	histone deacetylase
HDM	Histone Demethylase
HKMT	Histone lysine Methyltransferase
HSP	heat shock protein
HSTF	heat shock transcription factor
ICME	Isoprenylcysteine alpha-carbonyl methylesterase
IGV	Integrative Genomics Viewer
Kb	Kilobases
KYP	KRYPTONITE
LC	Low Confidence
LEA	late embryogenesis abundant
LTR	Long Terminal Repeat
MCSU	Molybdenum cofactor sulfurase
MET1	Methyltransferase 1
MSAP	methylation-sensitive amplification polymorphism
MYST	Moz, Ybf2/Sas3, Sas2 and Tip60
NADPH	Nicotinamide adenine dinucleotide phosphate
NbPHAN	Nicotiana benthamiana Phantastica
NCED3	Nine-cis-epoxycarotenoid dioxygenase 3
NGS	Next Generation Sequencing
OST1	open stomata 1
P5CS2	Delta-1-pyrroline-5-carboxylate synthetase enzyme
PCA	Principal Component Analysis
PIC	preinitiation complex
PMSF	phenylmethylsulfonyl fluoride
PP2C	protein phosphatase 2C
PRMTs	protein arginine methyltransferases
PRO	promotor
PSII	Photosystem II
PYL	Pyrabactin resistance-like
PYR	Pyrabactin resistance
qRT-PCR	quantitative Real-Time Polymerase Chain Reaction
RAP2.4	Related to AP2.4
RCAR	Regulatory component of the abscsisc acid receptor
RD29A	Responsive to desiccation 29A
RdDM	RNA-directed DNA-methylation
REST	Relative Expression Software Tool
RNA	Ribonucleic Acid
ROS	Reactive Oxygen Species

ROS1	Repressor of silencing 1
rpm	Revolutions per minute
RT	room temperature
RWC	relative water content
SAM	Sequence Alignment/Map
SDS	Sodium dodecyl sulfate
SET	Su(var)3-9, Enhancer-of-zeste, and Trithorax
SIR2	silent information regulator 2
siRNAs	small interfering RNAs
SLAC1	S-type anion channel
SnRK2	sucrose non-fermenting 1-related kinase 2-type protein kinases
SUVH5	Suppressor of variegation 3-9 homolog 5
SWEET	sugar will eventually be exported transporter
TE	Transposable Element
TES	Transcription End Site
TF	Transcritpion Factor
TFIID	Transcription factor II D
TPM	Transcript per Kilobase Million
TSS	Transcription Start Site
WGBS	Whole Genome Bisulfite Sequencing
v	version
ZEP	Zeaxanthin epoxidase

Summary

Plants respond to drought by the major reprogramming of gene expression, enabling the plant to survive this threatening environmental condition. The phytohormone abscisic acid (ABA) serves as a crucial upstream signal, inducing this multifaceted process. In this present work, the drought response in barley plants (*Hordeum vulgare*, cv. Morex) was analyzed at the epigenome, the transcriptome and the methylome levels. To be more specific, the genome-wide responses of the crop plant *H. vulgare* to early drought stress at the level of H3K4 trimethylation, H3K9 acetylation and H3K9 dimethylation were investigated. After a ten-day drought period, during which the soil water content was reduced by about 35%, the relative chlorophyll content, as well as the photosystem II efficiency of the barley leaves, decreased by about 10%. Furthermore, drought-related genes such as *HvS40*, *HvA1, Hsp17* and *P5CS2* were already induced compared to the well-watered controls. Global ChIP-Seq was performed and by applying stringent exclusion criteria, 129 genes loaded with H3K4me3, 2008 genes loaded with H3K9ac and 107 genes labelled with H3K9me2 in response to drought were identified. Interestingly, the H3K9ac mark showed a more flexible and dynamic response to the stress than H3K4me3. Strikingly, especially histones in the promoter and ATG-region of genes involved in ABA-related stress responses were acetylated at H3K9 in response to the stress, including 26 protein phosphatases 2C (PP2Cs), indicating epigenetic regulation of ABA-related drought stress responses in the crop plant barley. Parallel stringent RNA-Seq and qRT-PCR analyses revealed that some of these genes were also induced during drought treatment, but on the other hand, many genes upregulated during drought did not show loading with these euchromatic marks. While Whole Genome Bisulfite Sequencing (WGBS) revealed no significant global changes in the DNA methylation during early drought stress, 339 hypo- and 376 hypermethylated differentially methylated genes (DMGs) could be detected. In summary, these results indicate that epigenetic control, at least during the early phase of drought stress response investigated in this work, specifically targets genes involved in ABA-biosynthesis and -response.

Zusammenfassung

Pflanzen reagieren auf Trockenheit mit einer umfassenden Reprogrammierung der Genexpression, die es der Pflanze ermöglicht, diese bedrohliche Umweltbedingung zu überleben. Das Phytohormon Abscisinsäure (ABA) dient als entscheidendes Upstream-Signal, das diesen vielschichtigen Prozess in Gang setzt. In der vorliegenden Arbeit wurde die Reaktion auf Trockenheit in Gerstenpflanzen (*Hordeum vulgare,* cv. Morex) auf der Ebene des Epigenoms, des Transkriptoms und des Methyloms analysiert. Genauer gesagt wurden die genomweiten Reaktionen der Nutzpflanze *H. vulgare* auf frühen Trockenstress auf der Ebene der H3K4-Trimethylierung, H3K9-Acetylierung und H3K9-Dimethylierung untersucht. Nach einer zehntägigen Dürreperiode, in der der Wassergehalt des Bodens um etwa 35% reduziert wurde, sanken der relative Chlorophyllgehalt sowie die Photosystem-II-Effizienz der Gerstenblätter um etwa 10%. Darüber hinaus waren Trockenstress-relevante Gene wie *HvS40*, *HvA1*, *Hsp17* und *P5CS2* im Vergleich zu den gut bewässerten Kontrollen bereits deutlich induziert. Es wurde eine globale ChIP-Seq-Untersuchung durchgeführt und durch die Anwendung strenger Ausschlusskriterien wurden 129 Gene, die mit H3K4me3 markiert waren, 2008 Gene, die mit H3K9ac markiert waren, und 107 Gene, die mit H3K9me2 als Reaktion auf die Trockenheit markiert waren, identifiziert. Interessanterweise zeigte die H3K9ac-Markierung eine flexiblere und dynamischere Reaktion auf den Stress als H3K4me3. Auffallend ist, dass vor allem Histone im Promotor und in der ATG-Region von Genen, die an ABA-bezogenen Stressreaktionen beteiligt sind, als Reaktion auf den Stress mit H3K9 acetyliert wurden, darunter 26 Proteinphosphatasen 2C (PP2Cs), was auf eine epigenetische Regulierung von ABA-bezogenen Stressreaktionen in der Kulturpflanze Gerste hinweist. Parallele stringente RNA-Seq- und qRT-PCR-Analysen ergaben, dass einige dieser Gene auch während der Trockenstressbehandlung induziert werden, aber andererseits zeigten viele Gene, die während des Trockenstresses hochreguliert wurden, keine Markierung mit diesen euchromatischen Modifikationen. Während die Ganzgenom-Bisulfit-Sequenzierung (WGBS) keine signifikanten globalen Veränderungen im Ausmaß der DNA-Methylierung während des frühen Trockenstresses ergab, konnten 339 hypo- und 376 hypermethylierte differentiell methylierte Gene (DMGs) nachgewiesen werden. Zusammenfassend belegen diese Ergebnisse, dass die Trockenstressantwort der Pflanzen auch auf epigenetischer Ebene reguliert wird und dass die epigenetische Kontrolle, zumindest in der frühen Phase der in dieser Arbeit untersuchten Reaktion auf Trockenstress, speziell auf Gene abzielt, die an der ABA-Biosynthese und -Reaktion beteiligt sind.

1 Introduction

1.1 Drought stress

The sessile lifestyle of plants burdens numerous challenges for plants and one of them is the accessibility of water. Water shortage leads to drought stress affecting the plant on a morphological, physiological and molecular level during every stage of development. Focusing on crop plants as a major food source for humans and animals, drought leads to reduced yield as reviewed in Dietz et al. (2021).

The quality of stress can be divided into mild, moderate and severe stress and previous studies mainly focused on severe stress, which ultimately leads to death of the plant (Cominelli et al., 2005; Yuan et al., 2005; Rampino et al., 2006; Zhu et al., 2007; Zhang et al., 2008). In recent years it became obvious that the response of plants to drought is attuned to the severity of drought and that moderate stress is more likely to occur in natural environment (Harb et al., 2010; Clauw et al., 2015; Chen et al., 2021). Since drought is a severe threat, plants have developed several strategies to adapt to this unfavorable condition and thereby to survive in such adverse environment. These strategies include maintaining stomatal conductance by osmotic adjustment due to the accumulation of osmolytes like proline, sugars and phenols (Ferchichi et al., 2018; Turner, 2018) or altering of the root system (Wasson et al., 2012; Uga et al., 2013; Lynch et al., 2014). On a molecular level, the perception of drought leads to a response pathway including signal transduction, hormonal and biochemical adaptions and reprogramming of gene expression on transcriptional level including epigenetic mechanisms. The drought response in plants was extensively studied and there are nice reviews (Zhu, 2016; Gong et al., 2020). The following chapter will shortly summarize several mechanisms of drought stress response.

1.1.1 Abscisic acid (ABA) and its role in stress responses

The phytohormone abscisic acid (ABA) exhibits a multitude of roles in the life cycle of a plant including, amongst other things, seed dormancy and development, flowering, embryo morphogenesis and leaf senescence (Dar et al., 2017). Besides its involvement in developmental processes, ABA is the main phytohormone functioning in the perception and response to abiotic stress. Drought induces the synthesis of ABA, which in turn triggers the expression of stress related genes. The identification of several genes upregulated during drought but not responding to endogenous ABA treatment lead to the hypothesis of ABA-independent and ABA-dependent signaling in response to drought stress (Yamaguchi-Shinozaki & Shinozaki, 2005; Shinozaki & Yamaguchi-Shinozaki, 2007; Yoshida et al., 2014). In the ABA-dependent signaling pathway, sequence analyses of ABA–induced genes revealed

specific cis-elements in the promotor of these genes, called ABA-responsive elements (ABREs) (Busk & Pagès, 1998; Narusaka et al., 2003). ABRE-binding proteins/ABRE-binding factors (AREBS/ABFs) are basic leucine zipper-type transcription factors that are activated through phosphorylation by the sucrose non-fermenting 1-related kinase 2-type protein kinases (SnRK2). They are able to bind to the ABRE elements and thereby inducing gene expression, e.g. of the dehydration responsive gene *rd29b* (Uno et al., 2000; Fujita et al., 2005, 2013; Furihata et al., 2006; Nakashima et al., 2006). In a similar way, the ABA-independent pathway includes the dehydration-responsive element/C-repeat (DRE/CRT) which is recognized by the DRE-/CRT-binding protein 2 (DREB2) transcription factors (Yoshida et al., 2014). Recent findings suggest a crosstalk between both pathways, e.g. SnRK2s participate in gene regulation in ABA-dependent and independent pathway (Fujita et al., 2009, 2013).

1.1.2 Stomatal closure and the role of ABA

One of the first responses to the perception of water shortage is stomatal closing, thereby minimizing the loss of water through stomata but also reducing photosynthetic action through diminished CO_2 uptake. Stomata consist of two guard cells surrounding a pore in the epidermis of plants and their opening width is regulated through changes in the turgor pressure by external (e.g. CO_2 level, water level) and internal stimuli (such as phytohormones and reactive oxygen species (ROS)) (Schroeder et al., 2001; Qi et al., 2018).

Beside its numerous functions in plant abiotic and biotic stress responses, the hormone ABA plays a major role in the stomatal opening and closure. Occurring drought leads to an accumulation of ABA due to changes in gene expression associated with ABA biosynthesis (Kim et al., 2010; Dar et al., 2017), e.g. the ABA synthesis enzymes 9-cis epoxycarotenoid dioxygenase 3 *(NCED3),* zeaxanthin epoxidase *(ZEP),* aldehyde oxidase *(AAO3)* and molybdenum cofactor sulfurase *(MCSU)* are upregulated. Newly synthesized ABA interacts with the protein family PYRABACTIN RESISTANCE/PYRABACTIN RESISTANCE-LIKE/REGULATORY COMPONENTS OF THE ABSCISIC ACID RECEPTOR (PYR/PYL/RCAR) which function as ABA receptors and thereby inhibit clade A protein phosphatases 2Cs (PP2Cs) (Ma et al., 2009; Park et al., 2009; Cutler et al., 2010; Raghavendra et al., 2010). The inhibition of PP2Cs leads to an activation of the sucrose non-fermenting 1-related kinase 2-type protein kinases (SnRK2), including the open stomata 1 (OST1)/SnRK2-6 and the S-type anion channel (SLAC1) which function in the induction of stomatal closure (Mustilli et al., 2002; Geiger et al., 2009; Lee et al., 2009; Lim et al., 2015; Ullah et al., 2017; Hsu et al., 2021) (Fig. 1).

2
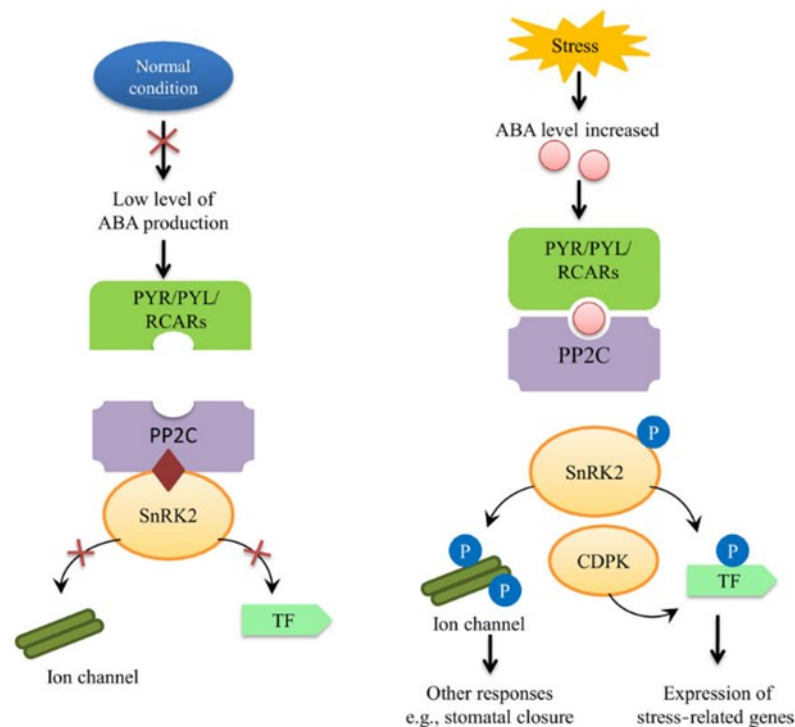
Figure 1. Model of the stress-signaling pathway mediated by ABA. Under non-stress conditions, ABA levels are low and the protein phosphatases 2C (PP2C) suppress the activity of the sucrose non-fermenting 1-related kinase 2-type protein kinases (SnRK2). With the detection of water shortage, the rising ABA level is perceived by the PYR/PYL/RCARs receptors which in turn inhibit the activity of the PP2Cs. SnRK2s are activated and thereby the activation of downstream transcription factors. Adapted from Ullah et al. (2017).

1.1.3 Protein phosphatase 2C (PP2C)

Protein serine/threonine phosphatases dephosphorylate proteins and can be separated into the phosphoprotein phosphatases (PPP) family including PP1, PP2A and PP2B and the phosphoprotein metallophosphatase (PPM) family which comprises the $Mg2+$ and $Mn2+$-dependent type 2C protein phosphatases (PP2C) (Cohen, 1997; Singh et al., 2010). In *Arabidopsis thaliana*, 76 PP2Cs were identified and classified into 11 subclades (A-K) (Kerk et al., 2002; Schweighofer et al., 2004). One of the main functions of the PP2Cs in plants is the involvement in signaling pathways, especially ABA stress signaling, e.g., the earlier mentioned stomatal closure. Discovery of the first plant PP2C ABA insensitive 1 (ABI1) and its homologue ABI2 due to mutant studies, depicts a role as a negative regulator in ABA signaling towards abiotic stress and during development for clade A PP2Cs (Koornneef et al., 1984; Leung et al., 1994, 1997; Rodriguez et al., 1998; Sheen, 1998; Gosti et al., 1999; Merlot et al., 2001; Singh & Pandey, 2012; Fuchs et al., 2013). Besides ABI1 and ABI2, AHG3 (ABA Hypersensitive Germination 3), HAB1 (Homology to ABI1 1), HAB2 (Homology to ABI1 2), HAI1 (Highly ABA-Induced PP2C1), HAI2, HAI3 and AHG1 (ABA Hypersensitive Germination 1) belong to clade A (Rodriguez et al., 1998; Saez et al., 2004; Yoshida et al., 2006; Nishimura et al., 2007; Fujita et al., 2009).

Interestingly, several ABA receptor RCARs are downregulated during stress whereas some of the PP2Cs are upregulated (Szostkiewicz et al., 2010; Chan, 2012). Especially, PP2Cs of the clade A are reported to be enhanced towards rising ABA levels or stress stimuli involving ABA synthesis (Fujita et al., 2011). Several studies e.g., in rice and *A. thaliana* could confirm these findings (Xue et al., 2008; Singh et al., 2010). Suggestions were made, that specific ratios between ABA receptors and PP2Cs are important to help the plant to adjust to enriched ABA levels (Raghavendra et al., 2010; Szostkiewicz et al., 2010; Chan, 2012).

1.2 Higher order control: Epigenetic modifications

Recent studies revealed that responses of plants to environmental stress involve higher-order epigenetic regulatory mechanisms, such as differential histone modifications and DNA methylation, affecting chromatin structure (reviewed in Kim, 2021). In the following chapters, epigenetic mechanisms are explained in more detail.

1.2.1 Chromatin structure

The DNA is wrapped around specific proteins, together forming nucleosomes, the structural unit of chromatin (Vergara & Gutierrez, 2017). Each nucleosome is an octamer consisting of two copies of histone subunits H2A, H2B, H3 and H4 and is associated with 145-147 bp of DNA wrapped around (Luger et al., 1997; Arya & Schlick, 2009; Asensi-Fabado et al., 2017). The chromatin structure defines the accessibility of the DNA for transcription and therefore gene expression (Asensi-Fabado et al., 2017). These nucleosomes can be densely packed which leads to an inaccessible, transcriptionally inactive form (heterochromatin) or openly packed, leading to transcriptionally active euchromatin. Heterochromatin is present in the centromere and the surrounding pericentromere and depicts a late replication during the cell cycle (Lima-De-Faria & Jaworska, 1968; Baker et al., 2015). The chromatin status is dynamic and determined by different epigenetic mechanisms, such as DNA methylation, non-coding RNAs, covalent histone modifications and ATP-depending chromatin remodeling (Fig. 2). In this research, the focus will lay on histone modifications and DNA methylation.
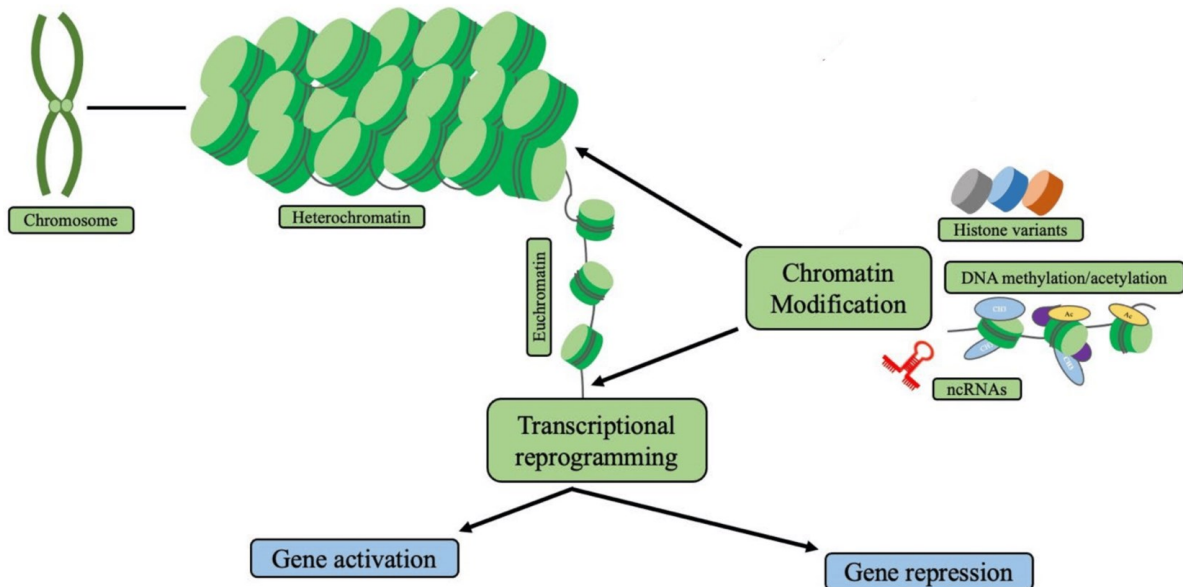
Figure 2. Chromatin structure and regulation. Shown is the highly condensed, transcriptionally inactive heterochromatin and the active, openly packed euchromatin. Different epigenetic mechanisms like histone variants/modifications, DNA methylation and non-coding RNAs modify and change the chromatin structure and thereby regulate gene expression. Adapted and modified from Halder et al. (2022).

1.2.2 Histone modifications

Histone modifications are characterized by post-translationally modifying the N-terminal tails of histones by specific enzymes which are adding different side groups (e.g. methyl, acetyl or phosphate) at different levels (e.g. mono-, di or tri-methylation) or removing them (Asensi-Fabado et al., 2017). Thereby the chromatin status is altered which in turn affects the accessibility of the DNA (e.g. for regulatory proteins) and the gene transcription (Pikaard & Scheid, 2014; Allis & Jenuwein, 2016). The most studied marks are acetylation or methylation on histone H3 at lysine residues. The methylation of N-terminal histone tails can be associated with either activating or repressing genes whereas acetylation is usually activating (Berger, 2007; Kouzarides, 2007; He et al., 2011). Acetylation and methylation of the lysine residues of histone H3 are the best studied modifications and their global changes in response to stress have been reported in various plants (Hu et al., 2019). Histone acetylation is reversible and dynamically maintained by the antagonistic action of histone acetyltransferase (HATs) and histone deacetylase (HDACs) (Pandey et al., 2002; Pikaard & Scheid, 2014; Zheng et al., 2019; Yang et al., 2020). The modification changes the charge of the lysine and therefore weakens the interaction between the modified histone and the DNA and leads to an open chromatin form, promoting gene transcription (Imhof & Wolffe, 1998; Marmorstein & Zhou, 2014; Sharma et al., 2019).

1.2.2.1 Histone methylation

The methylation of the lysine or arginine residues is catalyzed by histone lysine methyltransferases (HKMTs) or protein arginine methyltransferases (PRMTs), respectively. Since the methylation status is dynamic, the methylation can be erased by histone demethylases (DMTs) (Liu et al., 2010; Black et al., 2012). The methylation of lysine can be grouped into mono-, di- and trimethylation. For histone H3, it is known so far, that the methylation of H3K9 or H3K27 is linked to transcriptional repression and the methylation of H3K4, H3K36 and H3K79 is associated with transcriptional activation (Berger, 2007). For example, in *A. thaliana*, the trimethylation of H3K27 acts as repressive mark towards gene expression whereas the trimethylation of H3K4 is often associated with activating gene expression (Berr et al., 2011; Zheng & Chen, 2011).

1.2.2.1.1 H3K4 trimethylation

H3K4 trimethylation is one of the most intensive studied histone modifications and is linked to transcriptional activation, but the mechanisms behind this reaction are still not fully understood yet. H3K4me3 is mostly found in euchromatic regions and cytological examinations revealed that its enrichment occurs mainly on chromosome arms (Houben et al., 2003; Carchilan et al., 2007; Roudier et al., 2011). At genic location, H3K4me3 is found to be distributed around the transcription start site (TSS) (Bernstein et al., 2002; Zhang et al., 2006; Li et al., 2008; van Dijk et al., 2010). The HKMTs which catalyze the methylation of H3K4 contain a SET (Su(var)3-9, Enhancer-of-zeste, and Trithorax) domain where Trithorax is a subunit of the COMPASS-like (complex proteins associated with Set1) complex (Schuettengruber et al., 2011; Shilatifard, 2012). In *A. thaliana*, five Trithorax-like (ATX, class III SET-domain) proteins could be identified (Avramova, 2009; Tamada et al., 2009; Guo et al., 2010), which are proposed to interact with the COMPASS-like complex which deposits trimethylation at H3K4 (Jiang et al., 2011). Mutation analysis in ATX1 revealed a dual role, in which the protein is important for the assembly of the preinitiation complex (PIC) at promotors of target genes, influencing their expression and, on the other hand, its ability to trimethylate H3K4 seems to promote the transcription elongation (Ding et al., 2011b; Foroozani et al., 2021). In barley, *HvTX1*, a putative ATX1/ATX2 homologue, was identified which shows elevated expression during seed development and drought stress (Papaefthimiou & Tsaftaris, 2012). Li et al. (2016) unraveled a potential function of H3K4me3 and its methyltransferase in mRNA splicing involving the mRNA cap-binding complex (CBC). The CBC forms complexes with the COMPASS-like to integrate histone methylations with mRNA cap preservation and pre-mRNA processing at target genes (Li et al., 2016).

1.2.2.1.2 H3K9 dimethylation

The acetylation of H3K9 is described as transcriptional activating (Kurdistani et al., 2004; Bernstein et al., 2005) which is opposed to the methylation of this residue inactivating transcription. Dimethylation of H3K9 is associated with silenced chromatin in animals and yeast (Jenuwein & Allis, 2001; Bernatavichute et al., 2008) and silenced transposable elements (TE) and repetitive DNA in the heterochromatin of plants (Jackson et al., 2002, 2004; Malagnac et al., 2002; Bernatavichute et al., 2008). Histone lysine methyltransferases like KRYPTONITE/SUPPRESSOR OF VARIEGATION3-9 HOMOLOG 4 (KYP/SUVH4), SUVH5 and SUVH6 are important catalysators for the methylation of the residues (Jackson et al., 2002; Jasencakova et al., 2003; Ebbs et al., 2005; Ebbs & Bender, 2006). By using the Chromatin immunoprecipitation (ChIP) method, it has been shown that the H3K9me2 mark is mainly located at the chromocenters in comparison to the distribution of transcriptional activating histone modifications (Jackson et al., 2004; Mathieu et al., 2005; Fuchs et al., 2006). Several studies confirmed a link between H3K9me2 and DNA methylation, especially in the CHG context (Jackson et al., 2004; Mathieu et al., 2005; Bernatavichute et al., 2008; Du et al., 2012), e.g., mutations in the histone methyltransferase KRYPTONITE decrease the methylation of H3K9 and DNA methylation resulting in less gene silencing (Jackson et al., 2004).

1.2.2.2 Histone acetylation

The acetylation is executed by transferring an acetyl group of acetyl-CoA to the ε-amine group of N-terminal lysine residues (Hu et al., 2019), thereby changing the chromatin structure and facilitating gene transcription. This process is catalyzed by histone acetyltransferases (HATs) and can be reversed by histone deacetylases (HDACs). Because of its flexible reversibility, histone acetylation and deacetylation plays an important role in a variety of developmental steps and stress responses such as flowering, osmotic/oxidative stress and cell aging (Imai et al., 2000; He et al., 2003; Ausín et al., 2004; Brunet et al., 2004; De Nadal et al., 2004; Kim et al., 2004; Tian et al., 2005). Down-regulation of the *A. thaliana* histone deacetylase 1 (*AtHD1*) lead to various developmental effects like early senescence, ectopic expression of silenced genes, suppression of apical dominance and sterility, suggesting a global role in regulation (Tian & Chen, 2001).

Based on their cellular distribution, plant HATs can be sorted into two groups, type A and type B (Brownell & Allis, 1996; Roth et al., 2001). Plant type B HATs are located in the cytoplasm, catalyzing histone acetylation at lysine 5 and 12 of histone H4 (Parthun et al., 1996; Verreault et al., 1998). In maize, a type B HAT has been characterized, interestingly, its localization is not only limited to the cytoplasm, but also shows a significant proportion in the nuclei, proposing a potential function in the nucleus (Eberharter et al., 1996; Lusser et al., 1999). Type

A HATs include four groups of protein families: the general control non-depressible 5 (GNC5)-related acetyltransferases (GNATs), the MOZ, Ybf2/Sas3, Sas2 and Tip60-related (briefly MYST) HATs, cAMP response element-binding protein (CREB)-binding protein (CBP)/p300 family and the TATA-binding protein-associated factor (TAF1) (Sterner & Berger, 2000; Pandey et al., 2002; Carrozza et al., 2003). They are functioning at nuclear histones and therefore being directly involved in chromatin assembly and gene transcription (Carrozza et al., 2003; Chen & Tian, 2007). HDACs in plants are grouped into three types: reduced potassium dependency 3/histone deacetylase 1 (RPD3/HDA1) superfamily, plant-specific histone-deacetylase 2 (HD2) and the silent information regulator 2 (SIR2) (Pandey et al., 2002).

1.2.2.2.1 H3K9 acetylation

The acetylation of K9 of H3 is a well-studied mark in a variety of organisms where it is strongly associated with transcriptional activation (Kurdistani et al., 2004; Schübeler et al., 2004; Bernstein et al., 2005; Pokholok et al., 2005; Roh et al., 2005). In plants, H3K9ac functions in developmental processes like flowering, light-responsive gene expression, fruit formation, de-etiolation and the circadian clock (Ausín et al., 2004; Benhamed et al., 2006; Charron et al., 2009; Zhou et al., 2010; Malapeira et al., 2012; Hu et al., 2021). Moreover, a rising number of studies describe an important role of acetylation of H3 towards responses in biotic and abiotic stress (Tsuji et al., 2006; Kim et al., 2008; Hu et al., 2019; An et al., 2022). The distribution of H3K9ac at genomic loci is towards the 5' end with a peak at the ATG (Zhou et al., 2010).

1.2.2.3 Drought-stress-induced changes in histone methylation and acetylation

Recent studies revealed a link between gene expression in response to abiotic stress and alterations in histone modifications and DNA methylation, depicting fast and dynamic changes in histone marks towards the upcoming stress as well as more stable and progressive changes in the histone context (Kim et al., 2008, 2015; Kim et al., 2012; Luo et al., 2012). However, the exact link between epigenetic modifications and transcriptional regulations/responses and in which order they influence each other is not fully understood yet (Kim et al., 2015; Asensi-Fabado et al., 2017).

Using Chromatin immunoprecipitation followed by Next generation sequencing (ChIP-Seq), genome-wide distribution patterns of mono-, di- and trimethylation of H3K4 in *A. thaliana* under drought stress were conducted and it could be shown that in contrast to the moderately changed H3K4me1 and H3K9me2 marks, H3K4me3 changed prominently corresponding with up- and downregulated genes (van Dijk et al., 2010). Furthermore, dehydration and ABA-inducible genes showed a broader distribution of H3K4me3 over the gene body. In another genome-wide study in rice under drought stress, the transcript level of a subset of stress-

responsive genes could be positively correlated with the modification level of H3K4me3 (Zong et al., 2013). Forestan et al. (2020) applied mild prolonged stress on *Zea mays* followed by a recovery phase while examining changes in the H3K4me3, H3K9ac and H3K27me3 level with an additional focus on transcript level changes. It could be shown that between 25- 30% of genes marked with H3K4me3 or H3K9ac are also upregulated during drought whereas the H3K27me3 mark showed no correlation (Forestan et al., 2020). In the grass *Brachypodium distachyon,* combined ChIP-Seq and transcriptome data could identify genes upregulated during PEG-6000-simulated drought stress and associated with increased H3K9ac level (Song et al., 2020).

On gene level, real time qPCR analysis with drought stressed rice seedlings showed an elevated expression of four *HATs* (*OsHAC703*, *OsHAG703*, *OsHAF701*, *OsHAM701*) and supporting Western-blot analysis revealed an enrichment of acetylation on H3K9, K18 and K27 as well as H4K5 in parallel to the increased *OsHATs* expression (Fang et al., 2014). Loss of function studies of the earlier mentioned *A. thaliana* TRITHORAX-like factor ATX1 which trimethylates H3K4 leads to decreased levels of H3K4me3 at 9-cis epoxycarotenoid dioxygenase 3 (*NCED3*), a key enzyme in ABA biosynthesis, in drought stressed *A. thaliana* plants, resulting in reduced ABA concentration (Ding et al., 2011a). Furthermore, it could be shown, that during dehydration, *NCED3* showed increased enrichment of nucleosomal H3K4me3 (Ding et al., 2011b). In two studies, Kim et al. (2008, 2012) showed enriched H3K4me3 and H3K9ac levels at the drought-inducible genes *RD20* and *RD29A* where the enrichment levels correlated with the intensity of the stress (moderate vs severe). Interestingly, during dehydration, the H3K9ac mark diminished fast and robustly while H3K4me3 decreased progressively (Kim et al., 2012).

1.2.3 DNA methylation

Besides histone modifications and chromatin remodeling, DNA methylation determines the structure of the chromatin and its accessibility (reviewed in Zhang, Lang, & Zhu, 2018). One of the main functions of DNA methylation is the maintenance of the genome stability due to silencing transposons and repetitive DNA (Yoder et al., 1997; Chan et al., 2005). A second important function is regulating gene expression. Methylation of the coding region of genes does not affect gene expression in most cases (Zilberman et al., 2007; Cokus et al., 2008) whereas DNA methylation of the promotor region prohibits gene transcription (Park et al., 1996; Stam et al., 1998; Jones et al., 1999; Chan et al., 2005) e.g. by inhibiting the binding of transcription factors (Domcke et al., 2015). While in *A. thaliana* about 5% of the genes are methylated in the promotor region, over one third of the gene bodies is methylated (Zhang et al., 2006; Zhang et al., 2018). Gene body methylation is mainly located at exons and the most

abundant methylation context is CG (Zhang et al., 2006; Cokus et al., 2008; Lister et al., 2008; Takuno & Gaut, 2013). Interestingly, genes exhibiting gene body methylation are generally longer in comparison to unmethylated genes and in most cases constitutively expressed (Zhang et al., 2006; Takuno & Gaut, 2013).

DNA methylation is characterized by DNA methyltransferases adding a methyl group from S-adenosyl-L-methionine to a nucleotide, mainly cytosine, forming 5-methylcytosine (Richards, 1997; Klose & Bird, 2006; Lister et al., 2008; Law & Jacobsen, 2010). The methylation of cytosine bases appears in plants in the symmetric CG and CHG context (in which H = A, T or C) and in the asymmetric CHH context (Zhang et al., 2006; Henderson & Jacobsen, 2007; Lister et al., 2008). In a genome-wide bisulfite sequencing (WGBS) in *A. thaliana*, Cokus et al. (2008) could observe global methylation levels of 24% for CG, 6.7% for CHG and 1.7% for CHH. In a similar study, the percentage of the global methylcytosines was examined, resulting in the highest fraction of methylcytosines in the CG context (55%), followed by the CHG context (23%) and the CHH context (22%) (Lister et al., 2008). Both studies could show that all three contexts of DNA methylation in *A. thaliana* are mostly enriched in the repeat-rich pericentromeric regions. Through the RNA-directed DNA-methylation (RdDM) pathway, involving small interfering RNAs (siRNAs), DNA methylation in plants is established (reviewed in Matzke and Mosher 2014; Zhang, Lang, and Zhu 2018). Next to *de novo* DNA methylation, methylation maintenance and DNA demethylation are involved in the methylation process (Elhamamsy, 2016). In plants, the DNA (cytosine-5) -methyltransferase 1 (DNMT1) homolog METHYLTRANSFERASE 1 (MET1) maintains the CG methylation (Chan et al., 2005). The DNA methyltransferases CHROMOMETHYLASE 3 (CMT3) and CMT2 maintain the CHG methylation (Lindroth et al., 2001; Stroud et al., 2014) and the CHH methylation in addition with the DOMAIN REARRANGED METHYLTRANSFERASE 1 (DRM1) and DRM2 is perpetuated through the RdDM pathway (Stroud et al., 2013). DNA methylation is a reversible modification and demethylation can occur either active or passive. DNA glycosylases like DEMETER (DME), DEMETER-LIKE 2 or 3 (DML2 or 3) as well as the REPRESSOR OF SILENCING 1 (ROS1) take part in the erasure of the 5-methylcytosine (Choi et al., 2002; Agius et al., 2006; Gehring et al., 2006; Penterman et al., 2007; Ortega-Galisteo et al., 2008).

Although the role of DNA methylation in response to abiotic stress has been studied in several plant species like *A. thaliana*, rice, maize, winter wheat and barley (Khan et al., 2013; C. Jiang et al., 2014; Eichten & Springer, 2015; Secco et al., 2015; Yong-Villalobos et al., 2015; Chwialkowska et al., 2016), the mechanism behind DNA methylation modulating stress response is not yet fully understood (Liu & He, 2020). One of the first extensive studies of the methylome in barley under drought-stress in leaves and roots, using the methylation-sensitive amplification polymorphism (MSAP) method followed by sequencing, depicts high and generally stable methylation levels in the barley genome under water-deficient conditions (Chwialkowska et al., 2016). Nonetheless, several differentially methylated sites between control and drought were identified. In upland cotton, whole genome bisulfite sequencing (WGBS) revealed a hypermethylation pattern for all three contexts due to drought which declined to nearly normal levels after rewatering (Lu et al., 2017). In *Populous trichocarpa*, methylation levels significantly enhanced due to drought treatment and it has been observed that methylation 100 bp upstream of the Transcription Start Site (TSS) repressed gene expression. In contrast, methylation 100-2000bp upstream of TSS or at the gene body was positively correlated with gene expression (Liang et al., 2014). Two studies in rice examined the changes in methylation levels in different rice cultivars (drought-sensitive vs drought-tolerant) and could show significant changes in methylation levels especially in the drought-sensitive lines (Garg et al., 2015; Wang et al., 2016). The results indicated a potential correlation between alteration in DNA methylation and stress-related regulation of gene expression, although a huge part of the identified differential expressed genes (DEGs) depicts no significant changes in DNA methylation. Similar results were seen in maize (Wang et al., 2021). In *A. thaliana*, mild drought-stress caused slight changes in the methylome and transcriptome but no significant correlation between DNA methylation alteration and gene expression could be observed (Ganguly et al., 2017; Van Dooren et al., 2020). Furthermore, the stress was applied for multiple generations to detect possible heritable alterations in DNA methylation but only minor transgenerational effects were detected.

1.3 Barley (*Hordeum vulgare* L. cv. Morex) as a model plant

The domesticated barley, *Hordeum vulgare*, belongs to the Poaceae grass family and cultivation started around 10,000 years ago in the Fertile Crescent from its wild relative *Hordeum spontaneum* (Badr et al., 2000; Harwood, 2019).

For this study, the six-rowed malting variety Morex ("**mor**e **ex**tract") was used, which was registered by Rasmussen and Wilcoxson in 1979 (Rasmusson & Wilcoxson, 1979). Barley exhibits a large, diploid genome with a size around 5.1 Gbp distributed on seven chromosomes (2n=14). In 2012, the International Barley Genome Sequencing Consortium (IBGSC)

presented the first genome-wide physical map of Morex (International Barley Genome Sequencing Consortium et al., 2012) which represents more than 95% of the barley genome. About 80% of the barley genome are repetitive elements, which impedes the deciphering of the low-copy regions of the genome. The combination of paired-end sequencing of 87,075 bacterial artificial chromosomes (BACs), followed by constructing super-scaffolds of merged and assembled BACs, population sequencing (PopSeq) and the use of chromosome conformation capture sequencing (Hi-C) resulted in a more detailed barley gene model (Morex V1) representing 98% of the genome and furthermore, including an extensive assembly of the pericentromeric region (Mascher et al., 2017). Shortly after, an improved version 2 (Morex V2) was published (Mascher, 2019; Monat et al., 2019), which was used in this study. The version V2 depicts 32,787 high-confidence genes. The most recent version (Morex V3) (Mascher, 2020; Mascher et al., 2021) depicts 35,827 high-confidence genes, but could not be used in this research because of its later availability.

1.4 Aim of this work

Rising drought periods with decreasing availability of water pose challenges in the near future. To feed the growing population on earth, we require drought-tolerant varieties with efficient water usage. To achieve this goal, it is essential to comprehend the molecular mechanisms by which plants, especially crop plants, can adapt to drought stress. Until now, many studies on plant responses to drought stress have focused on transcriptome and proteome levels. This study aims to uncover additional higher-order stress response mechanisms in the model crop plant barley, with a focus on drought-related genome-wide changes in the epigenome, including differential histone-modifications, alterations in the methylome and the transcriptome.

In detail, the following work packages were planned:

1. Set-up of an experimental approach to analyze responses of barley to drought caused by a stop of irrigation which results in decreasing soil water content (as under natural conditions).

2. Characterization of the drought response by measuring photosynthesis-related parameters and the expression of stress marker genes.

3. Analysis of changes in the transcriptome during drought stress using RNA-Seq including the identification of differentially expressed genes and the analysis of functional classes of these drought-related genes.

4. Analyzing genome-wide changes in histone modifications (H3K9ac, H3K4me3, H3K9me2) in response to drought stress (barley-drought-epigenome) using ChIP-Seq. Functionally annotating genes with differential histone modifications in the promoter or coding sequence.

5. Analysis of genome-wide changes in DNA methylation in response to drought stress using Whole-Genome Bisulfite sequencing (WGBS) at CHG, CHH and CG context (barley-drought-methylome).

6. Integrating RNA-Seq, ChIP-Seq and methylome data.

2 Results

2.1 Experimental system to investigate drought stress responses

2.1.1 Physiological characterization of barley primary leaves under drought stress

Barley plants (cv. Morex) were grown under control and drought stress conditions (stop of irrigation at the 11th day after sowing (das)) in the greenhouse (see Chapter 4.2). The relative water content (RWC) of soil for the control plants was maintained at around 60-65% while the RWC of the drought stressed samples started to decrease at 13th das until reaching a value of 12% at 31st das (Fig. 3A).

To document the physiological status of the control and drought-stressed leaves, photosystem II efficiency (PSII efficiency) and relative chlorophyll content were measured in two-day intervals (Fig. 3B). At day 11, the relative chlorophyll content is at a maximum, indicating that the primary leaf is in its mature, photosynthetically active phase. At day 17 (6 days after stopping irrigation), chlorophyll content clearly started to decrease due to onset of stress-induced senescence until at day 31 almost no chlorophyll is left. The control plants show a relative constant chlorophyll content around 40-45% until day 35. Afterwards the chlorophyll content started to decrease because of the onset of developmental senescence. The course of the PSII efficiency, which reflects the photosynthetic performance, is similar to that of the chlorophyll content. Initially the efficiency is around 0.8 and starts to decrease in the drought-stressed plants at day 19/21 until at day 37 it reaches a value around 0.1. The PSII efficiency of the control plants started to decrease at day 39. Besides the measurement of the chlorophyll content and the PSII efficiency, the development of the control and stressed primary leaves was also documented photographically. Figure 3C shows the primary leaves of the drought-stressed and the control plants over a period of 31 days. Already around day 27 after sowing, the primary leaves of the drought-stressed plants started to get yellow at the tip, which then spread over the whole leaf during the further process of stress-induced senescence, whereas the control primary leaves showed a vital, green color during this time period.
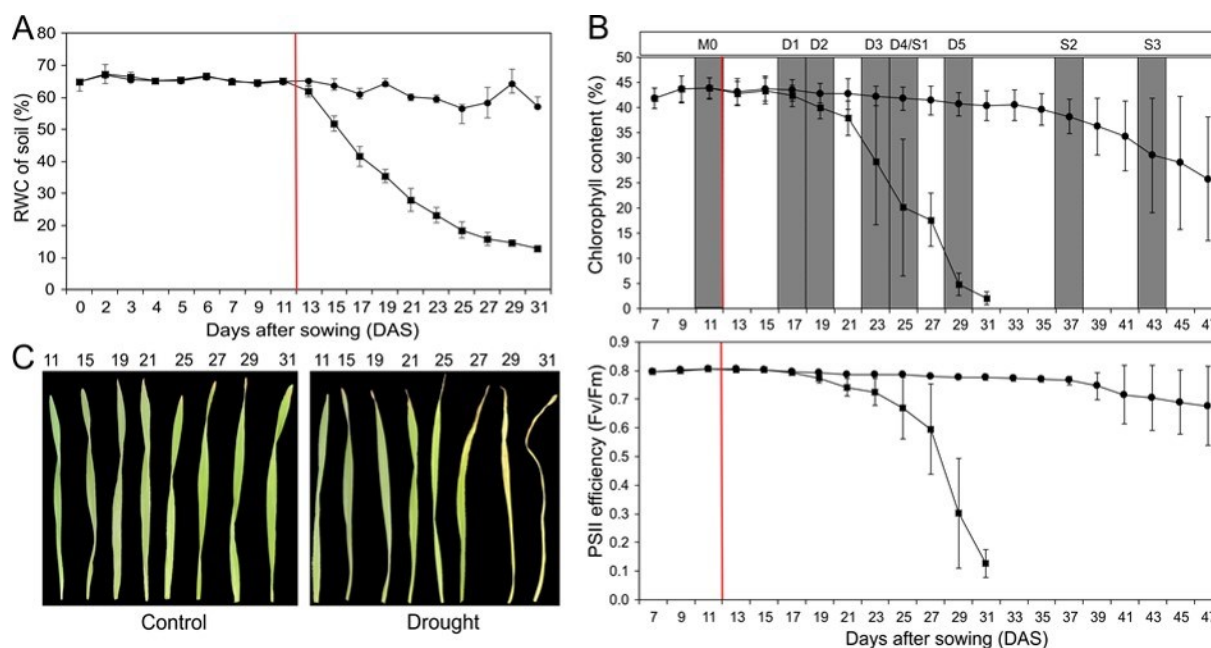
Figure 3. Physiological characterization of barley leaves. (**A**) Relative soil water content of control (■) and drought-stressed (●) plants during a period of 31 days. (**B**) Relative chlorophyll content and PSII efficiency (Fv/Fm = maximum quantum yield) of control and drought-stressed plants over a period of 47 days. The red line marks the starting point of water retention. Developmental stages were defined based on the relative chlorophyll content. The maximum measured value of the chlorophyll content was set as 100%, determined as the mature stage in which the primary leaf is fully developed (M0). Every data point corresponds to the mean values of four to eight independent measurements. (**C**) Photographic documentation of primary leaves under drought stress (right) and control (left) conditions during a period of 31 days. Each data point represents the average value from at least five biological replications, and the error bar shows the mean (±) standard deviation.

The close meshed data reflecting chloroplast function were used to define physiological stages of the different leaf samples. The maximum measured value of the chlorophyll content was set as 100% and defined as the mature stage in which the primary leaf is fully developed. The D1/S1- stage equates to 95% of relative chlorophyll content, D2/S2 to 90%, D3/S3 to 75%, D4/S4 to 50% and D5/S5 to 25% (Fig. 3B). D (drought) indicates the stages of the drought stressed plants and S (senescence) the later stages of the control plants.

15

2.1.2 Molecular analyses of gene expression of selected marker genes

To pinpoint the reprogramming of gene expression during drought stress induced leaf senescence, transcript levels of marker genes for leaf senescence and drought stress (*HvA1, P5CS2, Hsp17*, *HvS40, WRKY21* and *GS2*) were analyzed via qRT-PCR (Fig. 4). These marker genes are the senescence-associated gene *HvS40* (Kleber-Janke and Krupinska 1997; Krupinska et al. 2002, 2014), *HvA1,* encoding a dehydrin of the LEA protein-family (Hong et al., 1988; Straub et al., 1994), *P5CS2,* encoding a delta-1-pyrroline-5-carboxylate synthetase enzyme, involved in proline biosynthesis (Hu et al., 1992; Strizhov et al., 1997; Verbruggen & Hermans, 2008) and *Hsp17,* encoding a stress-related heat shock protein (Guo et al., 2009). *HvS40*, *HvA1*, *P5CS2* and *Hsp17* are known to be clearly upregulated in response to drought-treatment, and to some extent also during developmental senescence. In addition to senescence-associated genes, expression of the senescence-down regulated glutamine synthetase 2 *(HvGS2)* gene (Kamachi et al., 1991; Nagy et al., 2013) was analyzed. This gene is clearly downregulated during drought and its expression is almost zero in later stages of senescence. Drought stress clearly accelerates the down-regulation of *HvGS2*. Furthermore, a recent study in drought-stressed barley plants showed a decreasing expression level in the transcription factor *WRKY21* (Janack et al., 2016). This could be confirmed in the present research.

The aim of this research was to analyze epigenetic and transcriptomic changes associated with a moderate, "natural" drought stress. To prevent later secondary side effects, an early stage of stress was selected, characterized by the initial decrease in physiological parameters and the early reprogramming of stress-related gene expression. This early stage, denoted as D2, exhibited a 10-15% reduction in chlorophyll content compared to M2 and already showed a significant upregulation of stress-related genes.
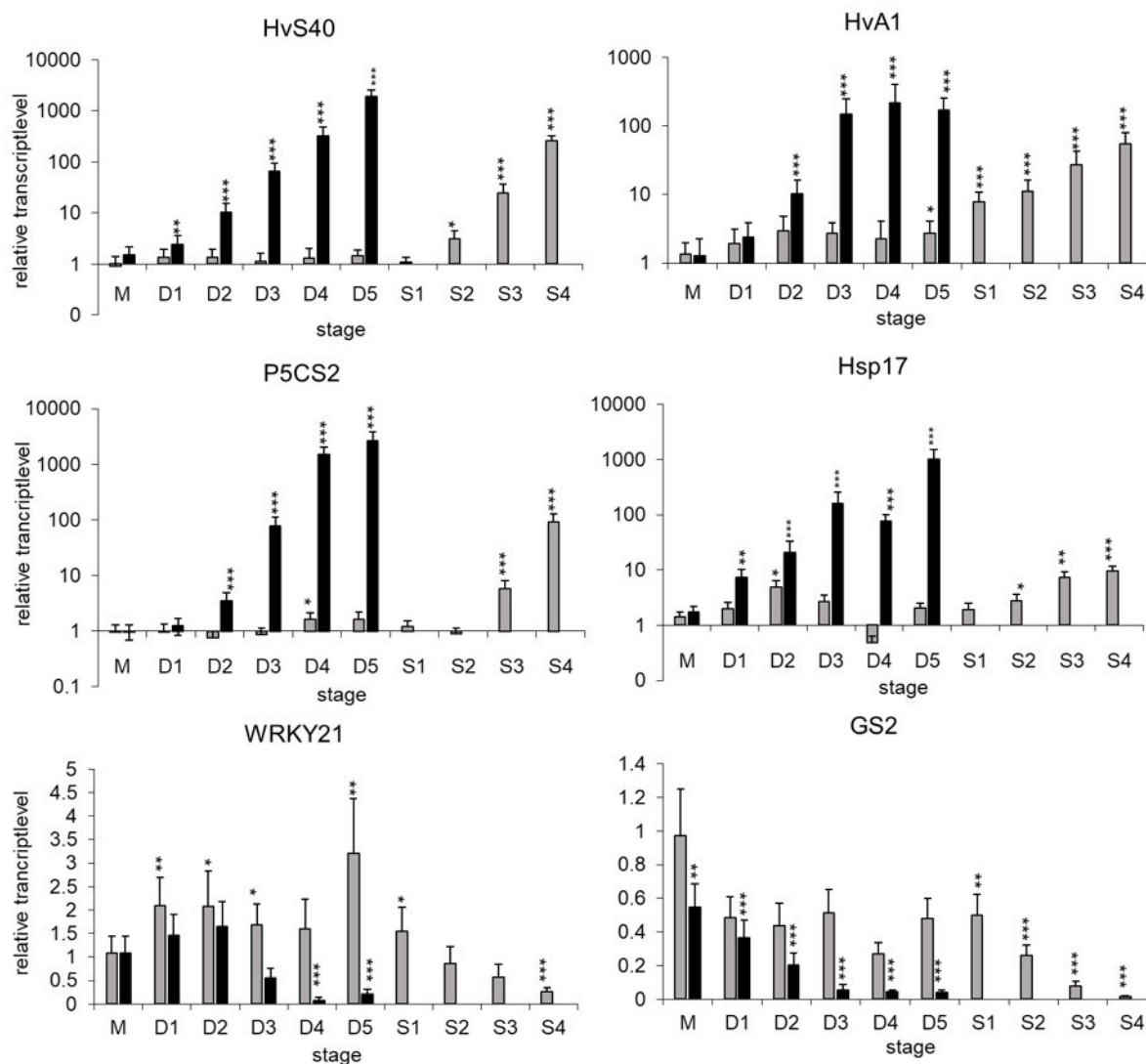
Figure 4. Expression of stress-and senescence-related marker genes. The relative transcript levels of drought-stress-related and senescence-associated genes were measured in mature, nonstressed stage (M) and at different stages during drought stress (D1–D5, represented by (■) and during development under control conditions (▪) of mature leaves at the same days when drought-treated plants are at stages D1–D5 and later at different stages of developmental senescence (S1–S4). Each bar in the graph represents the average value from three separate replications, and the error bars show the ±SE. The asterisks above the graph bar indicate statistically significant differences according to Student's t-test (* $p < 0.05$, ** $p < 0.01$ and *** $p < 0.001$). Mean relative expression levels, standard error and p-values were calculated using the software REST-384 ©2006 (v2.0, Qiagen GmBH, Hilden, Germany).

As a first conclusion, it could be summarized that in an early stage of drought stress while depicting no phenotypical changes yet, the expression of certain drought- and senescence marker genes is already elevated in comparison to the control.

17

2.2 Identification of genome-wide changes in histone modifications during drought stress induced senescence

To analyze genome-wide changes in selected histone modifications during drought stress, Chromatin immunoprecipitation followed by Illumina sequencing (ChIP-Seq) was used. By selecting antibodies against specific histone modifications, it is possible to precipitate the associated chromatin and to identify and quantify the isolated DNA via Next Generation Sequencing (NGS). Two euchromatic histone modifications and one heterochromatic mark were chosen for the ChIP: H3K4me3, H3K9ac and H3K9me2.

2.2.1 Selected time points and sampling

Three time points, namely M0, M2 and D2, were selected for further analysis. M0 represents the mature primary leaf and serves as a control. D2 showing first drought stress-related physiological effects and impacts on stress-related gene expression and it is compared to the control M2 without stress. Leaves harvested at the D2 stage exhibit a 10-15% reduction in chlorophyll content. The ChIP-Seq was performed for each sample with four independent biological replicates.

2.2.2 Mapping results and statistics for the ChIP-Seq

The raw sequence reads were processed by trimming the adapters with cutadapt (see Methods for a detailed description) and reads shorter than 30 bp were discarded. The reads were mapped to the barley cv. Morex pseudomolecules (Morex V2) reference genome using BWA-MEM (Li, 2013). The raw read counts fluctuate between 7 million up to 38 million reads. Since the third replicate was partially re-sequenced, the amount of the raw reads here is higher in comparison to the other replicates. The mapping rates of non-duplicated reads are ranging between 82.94% and 99.31% (Table 1). The mapping rates of the Input (untreated chromatin) samples are generally higher in comparison to the immunoprecipitated samples (IP, antibody-treated chromatin). All four replicates were used for further preliminary analysis.

Table 1. Mapping statistics for the read alignment for every replicate, time point and histone modification.

	Rep	M0 Reads	M0 Mapped (non-dup)	M0 Mapping rate (%)	M2 Reads	M2 Mapped (non-dup)	M2 Mapping rate (%)	D2 Reads	D2 Mapped (non-dup)	D2 Mapping rate (%)
Input	1	22,098,322	21,932,604	99.25	24,023,620	23,858,401	99.31	26,673,886	26,475,769	99.26
	2	9,183,624	9,096,776	99.05	7,684,528	7,614,454	99.09	9,386,624	9,285,551	98.92
	3	34,828,208	33,438,591	96.01	38,941,596	37,444,644	96.16	30,292,424	29,693,892	98.02
	4	14,404,146	14,242,619	98.88	15,063,612	14,869,527	98.71	19,057,296	18,887,111	99.11
H3K4me3	1	22,853,522	21,230,730	92.90	24,165,576	20,847,529	86.27	24,256,014	23,660,496	97.54
	2	12,232,022	11,825,674	96.68	12,910,286	11,593,073	89.80	10,283,494	9,892,678	96.20
	3	27,195,518	26,009,182	95.64	9,914,314	9,502,182	95.84	38,655,214	32,685,390	84.56
	4	21,769,862	19,975,470	91.76	14,604,788	14,008,289	95.92	16,272,548	15,578,149	95.73
H3K9ac	1	22,710,986	20,749,254	91.36	23,205,116	20,157,074	86.86	25,831,310	25,260,949	97.79
	2	9,672,140	8,097,125	83.72	13,048,786	10,891,894	83.47	12,052,420	11,401,428	94.60
	3	10,976,592	10,683,498	97.33	11,911,762	11,683,477	98.08	36,274,874	30,086,881	82.94
	4	19,552,002	19,038,526	97.37	14,840,948	13,202,012	88.96	14,047,186	13,357,287	95.09
H3K9me2	1	17,376,712	16,822,961	96.81	19,239,294	18,301,090	95.12	26,453,710	26,001,257	98.29
	2	9,803,078	9,271,436	94.58	9,436,180	8,560,180	90.72	8,947,726	8,131,917	90.88
	3	30,014,098	28,247,998	94.12	30,601,064	27,868,514	91.07	33,545,198	31,053,237	92.57
	4	23,205,332	22,368,967	96.40	12,734,242	12,427,094	97.59	16,956,056	16,735,182	98.70

2.3 Peak calling with MACS2 – two different ways of analysis

After the alignment and converting the BAM (Binary Alignment Map) files into BED files, the crucial step of the ChIP-Seq was performed: the peak calling. A peak is formed when there is an enrichment of reads at a specific region on the chromosome, indicating an enrichment of the histone modification of interest. MACS2 (Zhang et al., 2008) was chosen as the program for peak identification. In this work, two different methods of analyzing and combining the four independent biological replicates were employed and compared: peak calling for each replicate individually and pooled peak calling with all four replicates.

2.3.1 Peak calling for each replicate individually

For each replicate, the peaks were identified with MACS2 using the Input samples as a background. The detected peaks were intersected with the annotated gene list of the barley genome V2. Table 2 presents the number of detected peaks and associated genes for each modification, time point and replicate. The number of peaks for the H3K4me3 mark ranges from 60,269 to 402,789. Similar peak numbers can be observed for H3K9ac (99,623 to 321,383). The heterochromatic mark H3K9me2 depicts very low peak numbers from only 71 to a maximum of 130,519 peaks. To combine the four replicates for each modification and time point, only genes were retained that appeared in three of the four replicates. The modification H3K4me3 depicts the highest number of genes showing an enrichment in this mark (between

26,231 to 32,902) followed by H3K9ac (between 20,751 and 30,303). The heterochromatic mark H3K9me2 had the least genes (20 to 76).

Table 2. Detected peaks and associated genes for every replicate, time point and histone modification.

	Replicate	M0		M2		D2	
		peaks	genes	peaks	genes	peaks	genes
H3K4me3	1	178,614	35,586	143,963	35,306	304,700	25,965
	2	92,042	33,114	60,269	31,591	85,890	32,553
	3	119,710	35,647	402,789	32,834	112,874	34,109
	4	90,737	32,102	236,357	31,281	270,234	23,774
	in 3 of 4		32,902		29,473		26,231
H3K9ac	1	221,444	34,017	259,749	31,309	321,383	30,465
	2	248,454	31,357	99,623	24,584	101,817	26,919
	3	253,646	34,996	250,863	23,391	112,580	27,981
	4	161,567	33,484	247,248	26,561	264,531	19,306
	in 3 of 4		30,303		20,751		22,675
H3K9me2	1	71,736	1,192	52,871	1,585	72,861	2,853
	2	2,284	68	1,810	126	68,944	1,261
	3	112,292	1,077	130,519	1,425	10,623	276
	4	71	4	64,386	1,836	77,290	1,874
	in 3 of 4		20		76		29

2.3.2 Comparison between genes associated with a histone mark resulting from peak calling with pooled replicates or individually detected

Additionally, to the peak calling for each replicate individually, a pooled peak calling combining all four replicates was performed. The detected peaks were overlapped with the associated gene regions and the resulting gene lists were compared between the two methods (Fig. 5). Interestingly, the majority of the identified histone-modified genes (between 60-90%) are common between the two methods. Only a very small amount (0.01-0.24%) of the genes is specific for the separately treated samples. Obviously, pooling the samples leads to the detection of some more genes associated with the histone marks (between 8.7 and 41.9%). These results suggest continuing working with the results from the pooled peak calling.
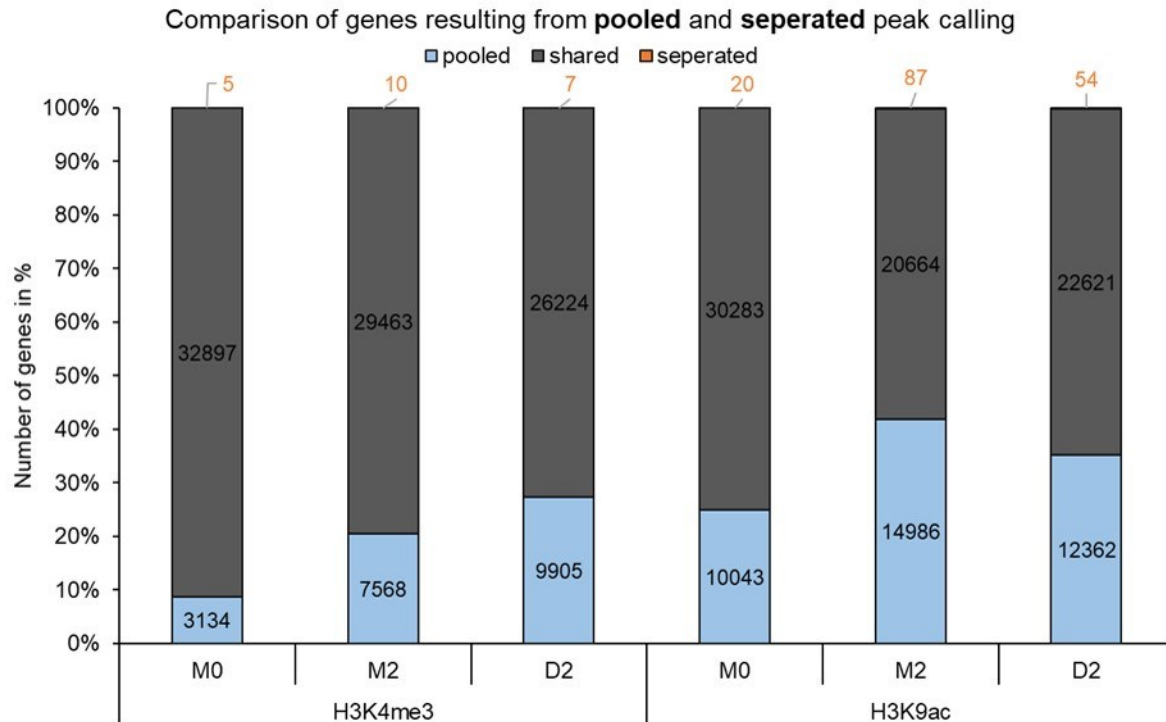
Figure 5. Comparison of the gene lists resulting from the peak calling for pooled replicates and separately treated replicates. Shown are the total numbers of histone-modified genes which are specific for the pooled peak calling (light blue), shared between both methods (grey) and specific for separately peak calling (orange).

2.3.3 Pooled peak calling with MACS2 and peak distribution over the barley chromosomes

As input files, MACS2 expects the IP samples and the Input samples in BAM or BED format. For this analysis the BED format was chosen (for details, see Chapter 4.11). The peak calling was carried out with all four IP samples for every modification and time point and the corresponding Input samples. Figure 6A shows the detected peaks for the pooled samples. For the histone modification H3K4me3, the number of identified peaks ranges from 110,641 to 205,163 between the time points. For the H3K9ac mark, more peaks could be detected (between 288,917 and 317,786). The peak calling for the heterochromatic mark H3K9me2 identified less peaks (between 148,933 and 13,623) in comparison two both of the euchromatic marks.

The resulting list of peaks from MACS2 in BED format can be visualized with the Integrative Genomics Viewer (IGV) (Robinson et al., 2011) program (Fig. 6B). The distribution of the peaks associated with the euchromatic marks show differences between the two euchromatic and the heterochromatic mark. Peaks associated with H3K4me3 and H3K9ac are localized at the telomere-proximal chromosomal regions, resembling the distribution of the barley genes. In

contrast, H3K9me2 is enriched in the low recombining, pericentromeric region (interior of the chromosome), which are rich in e.g., LTR retrotransposons.
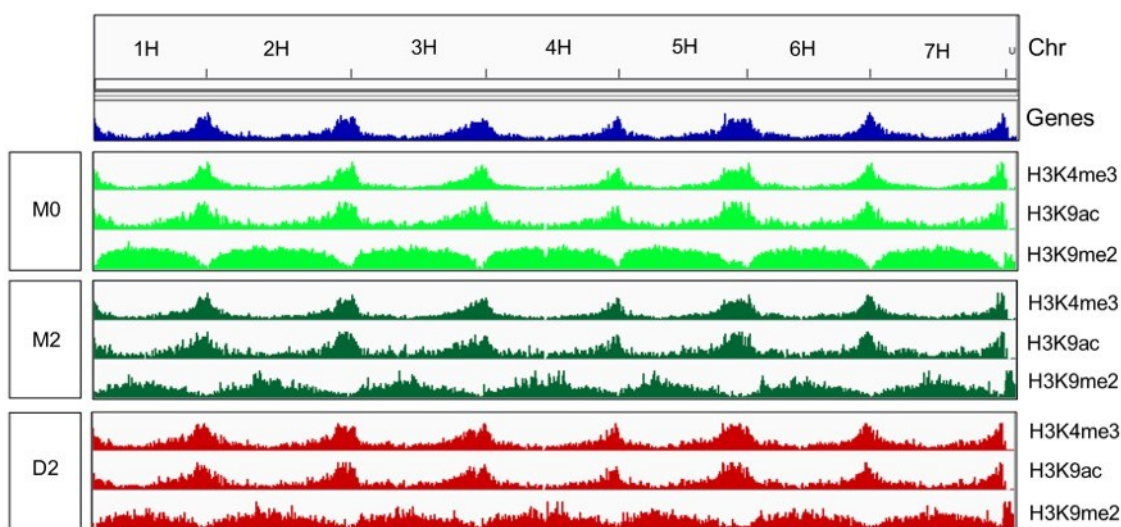
Figure 6. Peak calling numbers and peak distribution. (**A**) Number of peaks resulting from the pooled peak calling with MACS2. (**B**) IGV view of the peak distribution for every modification (H3K4me3, H3K9ac, H3K9me2) and time point (M0 in light green, M2 in dark green, D2 in red and the genes are colored in blue) for the seven chromosomes of barley.

2.3.4 Similarity analysis between replicates and samples

To compare the different data sets within each other, principal component analysis (PCA) was the tool of choice. With deepTools (Ramírez et al., 2014), read coverages of the alignment files of the four replicates for each time point and modification were calculated. The correlation was computed with the Pearson method and visualized in heatmaps (Fig. 7), where one depicts the strongest correlation and zero no correlation. For H3K9me2, the Pearson coefficient varies between 0.64 and 1, showing a similarity between the four replicates. The values for H3K4me3 are generally lower with the lowest at 0.39 in D2, showing a higher variance in the different replicates. Similar results can be seen for the replicates of H3K9ac. Especially the replicates of the drought stress sample depict a higher variance between each other.
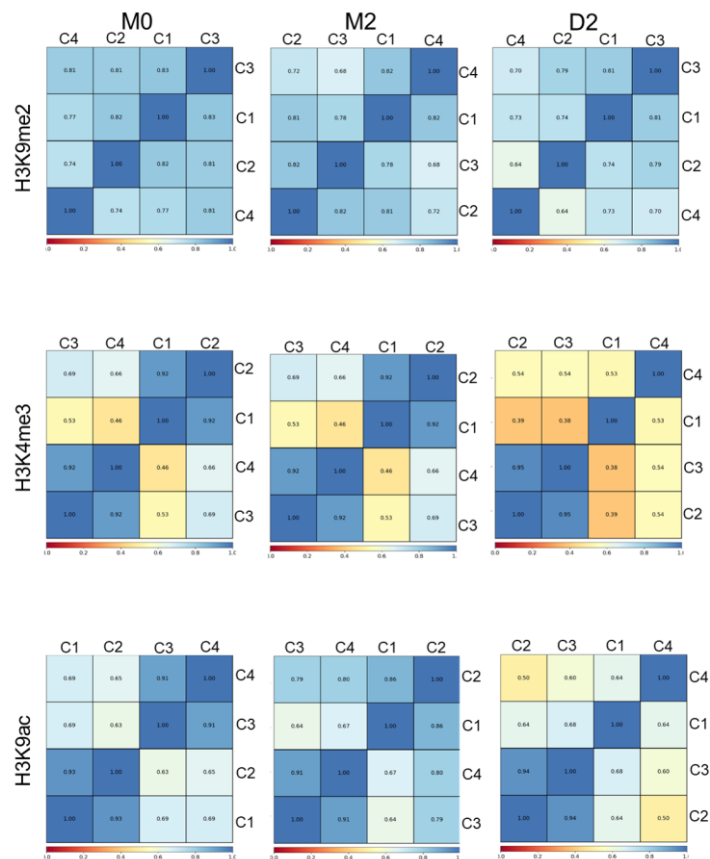
Figure 7. Correlation analysis of the replicates. Heatmaps of the comparison of the replicates for every histone mark and time point using deepTools multiBamSummary and the Pearson correlation method. The calculated correlation coefficient is between one (highest correlation, blue color) and zero (no correlation, red color).

In a next step, all four replicates (C1-C4) and all three time points (M0, M2, D2) for each modification (H3K9me2, H3K4me3 and H3K9ac) were compared with each other (Fig. 8A). No specific clustering is detectable and furthermore, the replicates between the different conditions show high similarities. These results indicate a high similarity in genome-wide loading with the euchromatic marks H3K4me3 and H3K9ac at all time points and conditions at the early phase of stress response. Meaning, that at this early stage, only first specific changes in histone loading occur. Later on, more global changes result in a greater diversity between stressed and control samples. The experimental approach used in this work allows to identify these first epigenetic control steps after onset of drought stress.

However, the overall comparison between H3K9me2, H3K4me3 and H3K9ac of the merged bigwig-files for every time point and condition depicts a stricter clustering of the samples, showing that the onset of drought stress starts to alter the epigenetic loading (Fig. 8B). M0 and M2 of both marks, H3K4me3 and H3K9ac, are close together, while D2 is more separated. The three samples of H3K9ac show a higher similarity to each other than the samples for

H3K4me3. Interestingly, the samples for H3K9me2 show the highest similarity between all three time points.
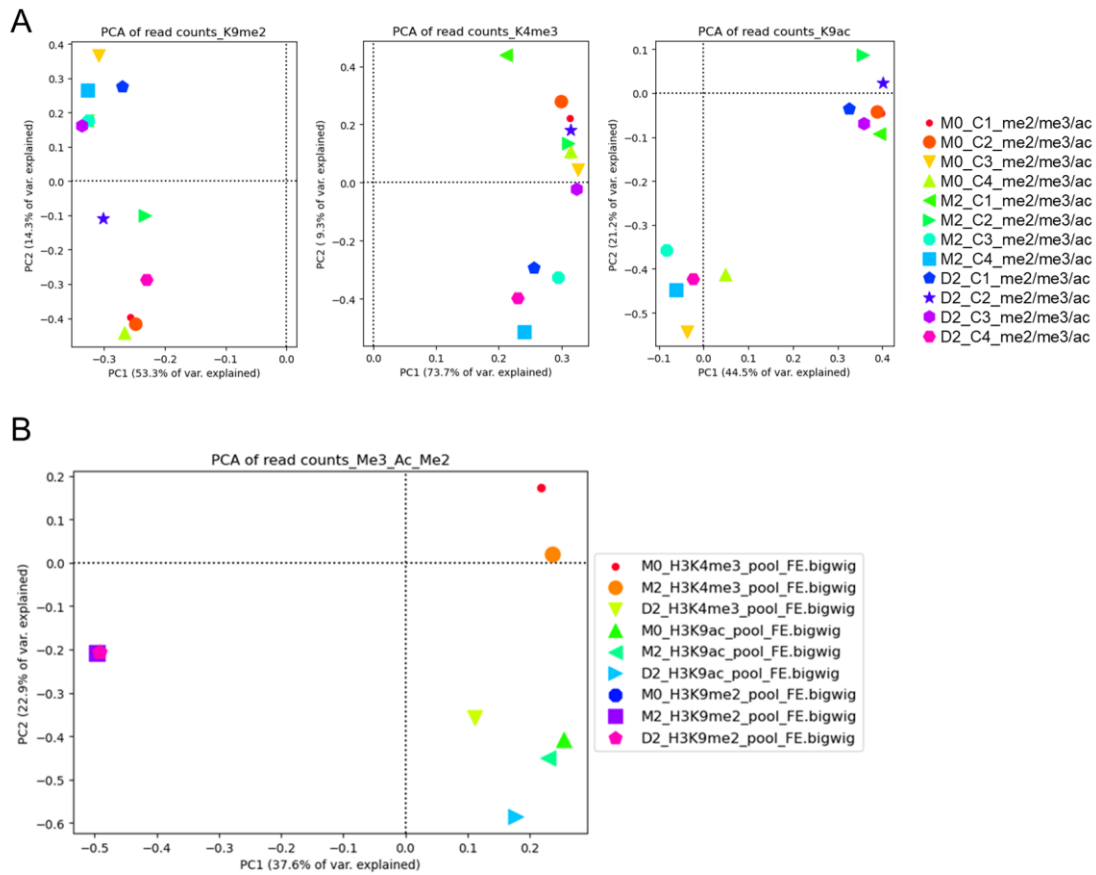
Figure 8. Principal component analysis (PCA) of the samples. (A) PCA of the three time points and their corresponding replicates for every histone modification. (B) PCA of the pooled samples for all three time points and histone modifications combined.

2.3.5 Intersection of ChIP-Seq peaks with annotated barley genes

Before intersecting the peaks with the annotated gene list, the parameter settings were enhanced in order to localize strong peaks for H3K4me3 and H3K9ac. Only peaks with a fold enrichment equal or greater than 10 were chosen. These settings minimize the number of total peaks, but simultaneously diminish weaker peaks. Because of the overall weak peak enrichment, these settings were not chosen for H3K9me2. Table 3 presents the number of peaks and associated genes after the new parameter settings. The peaks were intersected with the annotated gene lists. The annotated genes are separated into genes that are loaded in the range of 250 bp upstream or downstream of start codons (ATG), in the 1000 bp upstream region of start codons (PROMOTOR) or in the genomic sequence between start and stop codons of high-confidence genes (BODY). Trimethylation of H3K4 shows the most peaks (between 18,000 and 33,650 peaks) and associated genes (15,000 to 28,000). For H3K9ac, between 10,000 and nearly 16,000 peaks could be detected and 8,000 to nearly 15,000 corresponding genes. Since H3K9me2 is a heterochromatic mark, which is localized in the non-gene rich parts of the chromosomes, much less genes (between 165 and 1,600) are associated with this histone modification in comparison to the euchromatic marks.

Table 3. Identified peaks and corresponding genes for every time point and modification.

Sample		M0	M2	D2
H3K4me3	peaks	33,650	27,904	18,335
	genes	27,980	24,025	17,154
H3K9ac	peaks	15,813	10,561	15,211
	genes	14,327	9,330	14,134
H3K9me2	peaks	148,933	21,695	13,623
	genes	1,618	292	250

2.3.6 Plotting the read density and adjusting the parameters

Using the program deepTools, mean scores calculated from the signal tracks of the histone enrichment were plotted against the genes associated with a peak. Figure 9 depicts the distribution of the histone signal for M0, M2 and D2 for all three histone modifications.
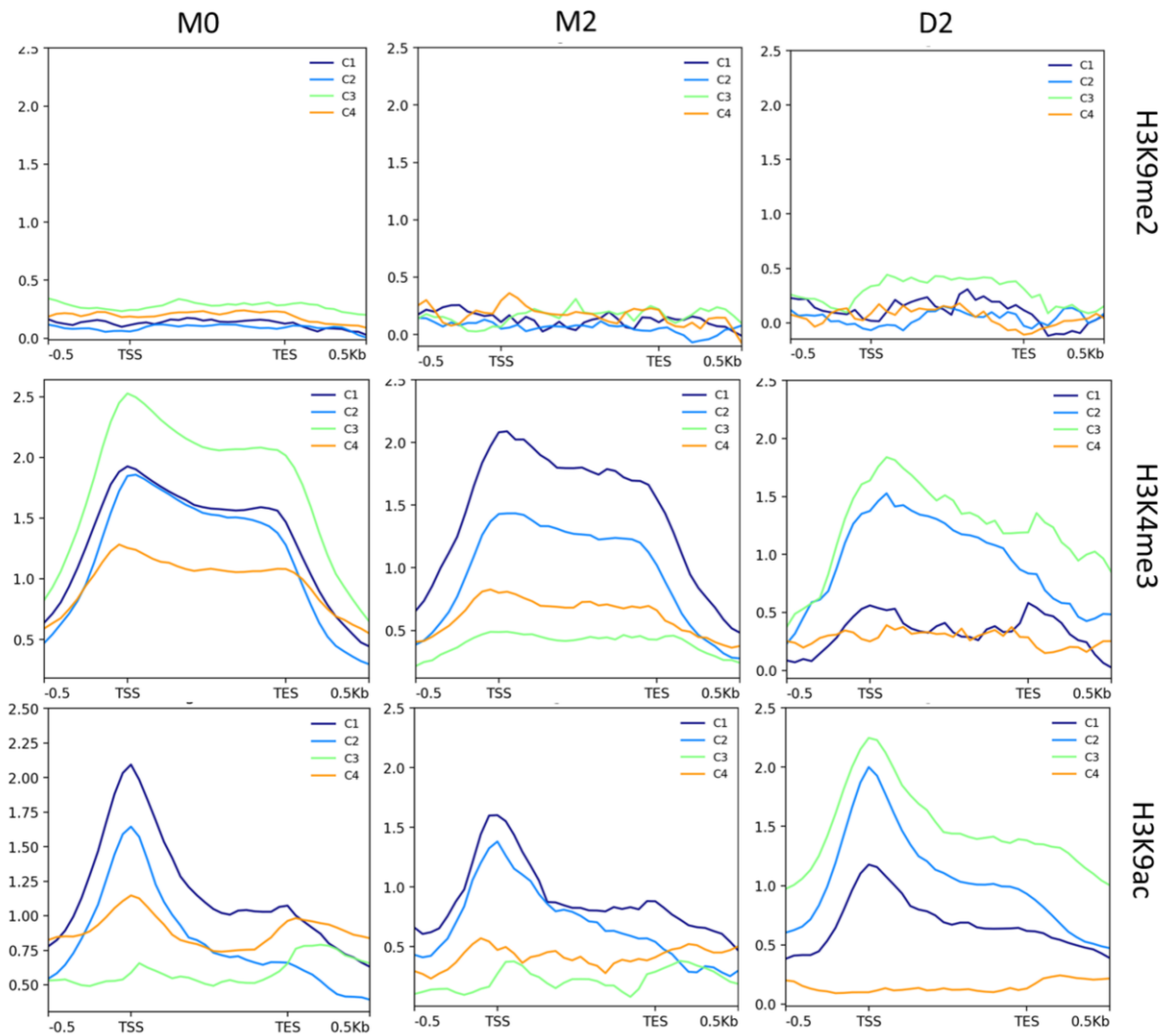
Figure 9. Read density around the TSS of their corresponding genes. Shown for H3K9me2, H3K4me3 and H3K9ac where the y-axis depicts the mean normalized log2 ratio between the signal track of the histone enrichment and the genic regions and the x-axis presents the genomic ranges. Shown are the read densities for all four replicates (C1-C4).

For H3K9me2, the signal distribution over the transcription start site (TSS) and transcription end site (TES) is weak and shows no enrichment in the histone mark. In contrast, in all three conditions (M0, M2 and D2), highest enrichment of H3K4me3 and H3K9ac is around TSS and adjoining gene body. While H3K4me3 shows a broader labeling with high loading over the whole gene body with sharp drop at the transcription end site (TES), H3K9ac is preferentially positioned around TSS. The replicates C3 and especially C4 show a very low signal of read density for the different time points. As a conclusion, the replicate C4 was discarded and a pooled peak calling was executed again for the marks H3K4me3 and H3K9me2. This time, BAM files were used and the q-value were set to 0.05. Again, only peaks with a fold enrichment ≥10 were included and genes were annotated. Table 4 presents the number of peaks and corresponding genes resulting from the peak detecting with three replicates and the q-value

set to 0.05. Slightly less peaks were identified due to the change of settings and enhancing the fold enrichment threshold of peaks to a minimum of 10 reduced the number of peaks majorly. This set of genes was finally used for further analysis.

Table 4. Identified peaks and genes with 3 replicates (C1-C3) and q-value set to 0.05.

Sample		M0	M2	D2
	peaks	62,975	64,735	54,050
H3K4me3	peaks (FE≥10)	33,477	26,549	17,873
	genes	27,174	22,271	16,158
	peaks	54,553	37,000	42,306
H3K9ac	peaks (FE≥10)	14,460	9,310	14,442
	genes	12,758	7,714	12,682

2.3.7 Annotation of the location of a given peak

With the software tool ChIPseeker (Yu et al., 2015) it is possible to visualize the location of a peak whether it is located in the promotor region, an exon, 5' UTR, 3'UTR, an intron or intergenic. The tool was executed on the Galaxy platform (Afgan et al., 2018) with the uploaded filtered and unfiltered peak files in bed format for every time point and modification.

For H3K9me2, around 97% of the peaks are located in the distal intergenic regions and 2-3% are located in the promotor region (Fig. 10A). For H3K4me3 and H3K9ac, between 33 and 67% of the unfiltered peaks are located in the distal intergenic regions, followed by the promotor region (27-40%) and exons (2-7%). Figure 10B presents the distribution of the peaks regarding the genomic features after the threshold of fold enrichment was set to ≥10. In general, the majority of peaks (82 to 89%) with higher fold enrichment are located in the promotor region. While for H3K4me3, D2 shows the highest number of peaks in the promotor region (89.52%), for H3K9ac, M0 and D2 show a similar number of peaks in the promotor (around 87%) and a lower number for M2 (82%). Around 10 to 15% of the peaks are located in the distal intergenic region and only very small portions of peaks are located in other exons and introns. These findings are in line with the general knowledge that euchromatic histone modifications are located in the TSS/ 5'/ Promotor region of a gene (Pfluger & Wagner, 2007).
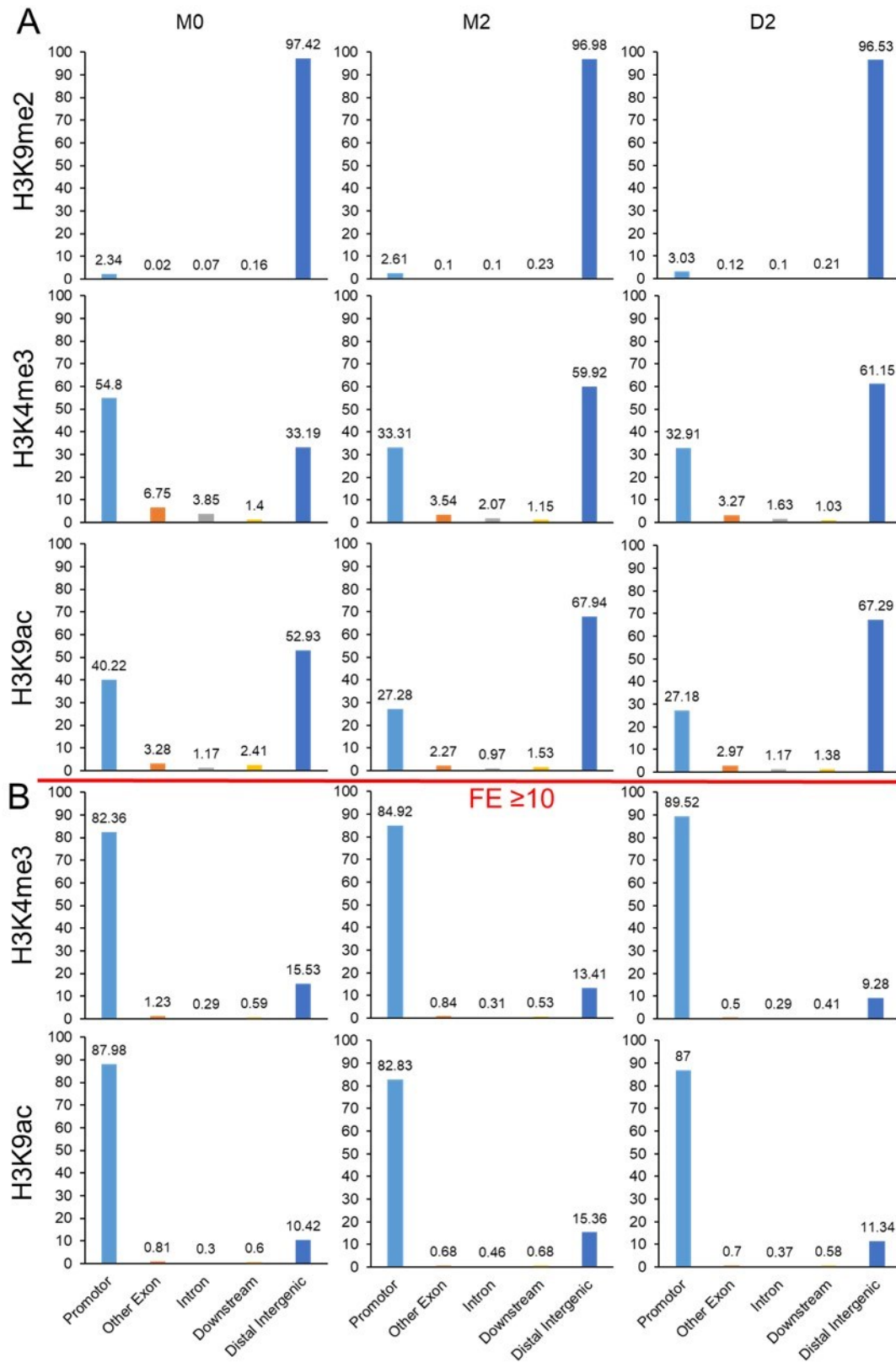
Figure 10. Distribution of the location of the peaks (**A**) unfiltered samples and (**B**) filtered samples (Fold Enrichment (FE) ≥ 10). The y-axis depicts the percentage of peaks (%).

2.4 Genes differentially labeled with H3K9me2, H3K4me3 and/or H3K9ac (M0vsM2vsD2)

2.4.1 H3K9me2 (M0vsM2vsD2)

It should be noted that unlike for H3K4me3 and H3K9ac, no fold enrichment threshold to filter the peaks were set for H3K9me2. While the peak number under these settings for M0 is nearly 150,000, around 21,000 and 13,000 peaks were detected for M2 and D2, respectively (Fig. 11A). The mark H3K9me2 is found to be associated with heterochromatin and plays an important role in silencing transposable elements (TE) (Xu & Jiang, 2020; Zhang et al., 2018). Therefore, only a very small number of genes associated with H3K9me2 has been identified. In M0, 1618 genes are labelled with H3K9me2, in M2 292 genes and in D2 only 250 genes. Comparison between all three time points show a small overlap of 85 genes associated with the heterochromatic mark in all time points (Fig. 11B). For M0, 1466 genes are exclusively labelled in this control stage, 134 genes in M2 and 107 in D2. The number of peaks located in the promotor (PRO), start codon (ATG) or gene body (BODY) were compared (Fig. 11C). A big part of the peaks is spanned over the promotor, start codon and gene body region while 483 peaks in M0 are uniquely located in the promotor region (70 in M2 and 68 in D2) and 360 peaks in the gene body (96 in M2 and 89 in D2). Since the interest of this study are potential changes in the epigenome of drought-induced genes, the focus of the ongoing research is set on the euchromatic marks, H3K4me3 and H3K9ac.
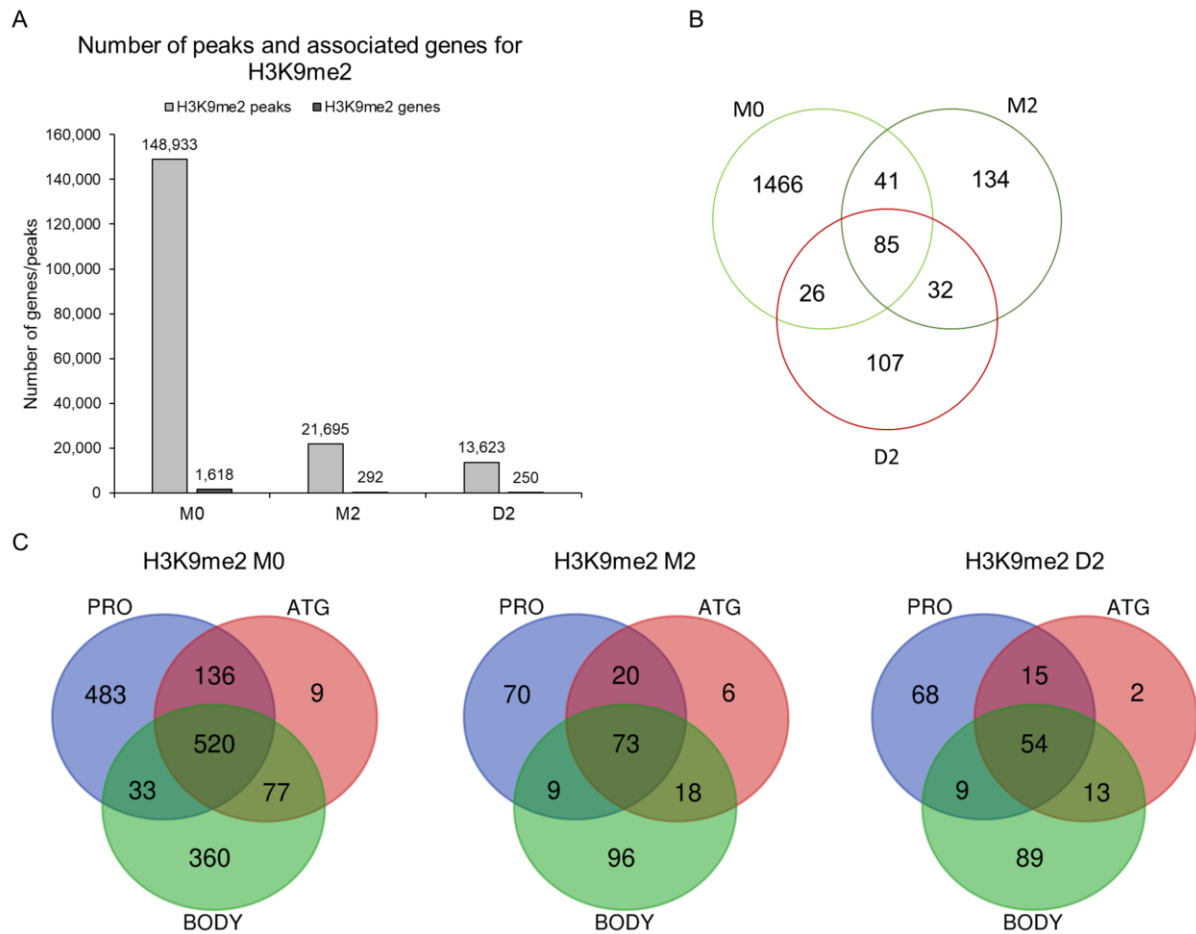
Figure 11. Comparison of genes associated with H3K9me2. (**A**) Number of peaks and genes associated with H3K9me2. (**B**) Venn diagram of the comparison of K9me2-labelled genes between all three time points (M0, M2 and D2). (**C**) Number of genes labelled with H3K9me2 in the promotor (PRO), start codon (ATG) and/or gene body (BODY) region.

2.4.2 H3K4me3 (M0vsM2vsD2)

The genes labelled with H3K4me3 in the control samples and in the drought stress sample were compared to detect similarities and differences between the distributions of the mark. Most of the peaks and corresponding genes are found in the M0 control sample (Fig. 12A), followed by M2. In D2 less genes are uniquely associated with H3K4me3. The comparison of all three time points (Fig. 12B) shows that more than half of the genes (~ 53%) with a H3K4me3 mark are shared between all three time points (15089). Nearly 16% of the genes (5347) are specific for M0, meaning that the histone mark exclusively appears in this control sample. Both of the control samples, M0 and M2, share 21.03% (5993) of the genes in comparison to 2.6% (745) between M0 and D2 and 0.68% (195) between M2 and D2. M2 contains 3.49% (994) of unique genes that are associated with H3K4me3. In D2 only 0.45% (129) of the genes are gaining the mark specifically during drought stress. The location of the peaks is presented in figure 12C. Like for H3K9me2, a majority of the peaks spans the promotor, the start codon and

the gene body region for every sample. There are slightly more peaks uniquely located in the promotor region than the gene body.
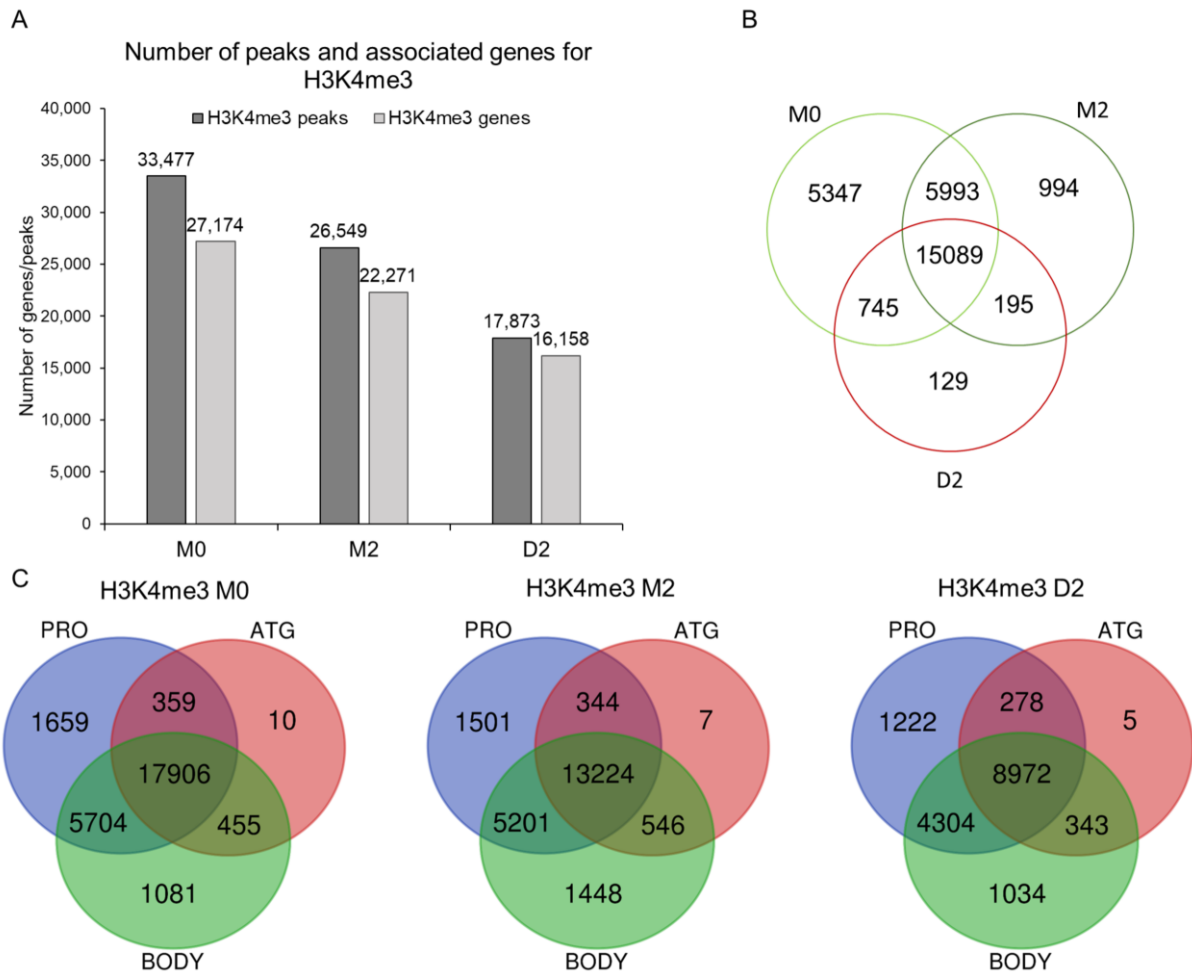
Figure 12. Comparison of genes associated with the H3K4me3 mark. (**A**) Number of peaks and genes associated with H3K4me3. (**B**) Venn diagram of the comparison of the genes associated with H3K4me3 between all three time points. (**C**) Number of genes labelled with H3K4me3 in the promotor (PRO), start codon (ATG) and/or gene body (BODY) region.

2.4.2.1 H3K4me3- two-time point comparison (M2vsD2)

The comparison between two time points (Fig. 13A) showed that the two control samples share more than 74% (21082) of the genes, 21.5% (6092) are unique for M0 and 4.2% (1189) are specific for M2. In contrast, M0 and D2 share 57.6% (15834) of the genes associated with H3K4me3 and 41.2% (11340) are unique in M0 and 1.1% (324) are specific for D2 (Fig. 13B). The comparison of the genes between M2 and D2 revealed that 66.1% (15284) are shared between both samples, 30.2% (6987) are specifically in M2 and only 3.8% (874) in D2 (Fig. 13C).
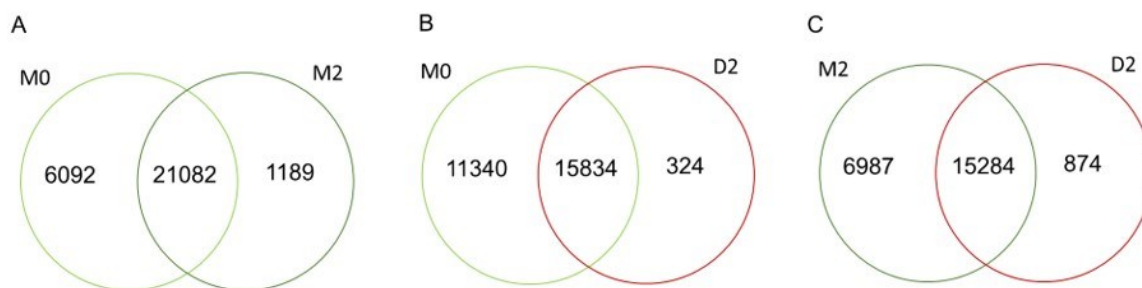
Figure 13. Comparison of genes enriched in H3K4me3 between two time points. (**A**) M0vsM2 (**B**) M0vsD2 and (**C**) M2vsD2.

2.4.3   H3K9ac (M0vsM2vsD2)

Figure 14 presents the results from the comparison of the genes enriched in H3K9ac between the three time points. M0 and D2 have nearly the same number of peaks and corresponding genes in comparison to M2 (Fig. 14A). The comparison between the three time points shows that 39.7% (6174) of the H3K9ac-enriched genes are common between all the time points (Fig. 14B). For M0, 11.9% (1862) are unique, 1.6% (260) for M2 and 12.9% (2008) show the mark only in D2. Interestingly, M0 and M2 only share 4.8% (751) of the genes whereas M0 and D2 share 25.5% (3971) of the genes. M2 and D2 share 3.4% (529) of the genes. Most of the peaks are extended over the promotor, the start codon and the gene body region (Fig. 14C). While for H3K9me2- and H3K4me3-labelled genes, the number of peaks uniquely resides in the promotor or gene body region are similar, there are nearly twice as much peaks located exclusively in the promotor region than in the gene body for H3K9ac-labelled genes.
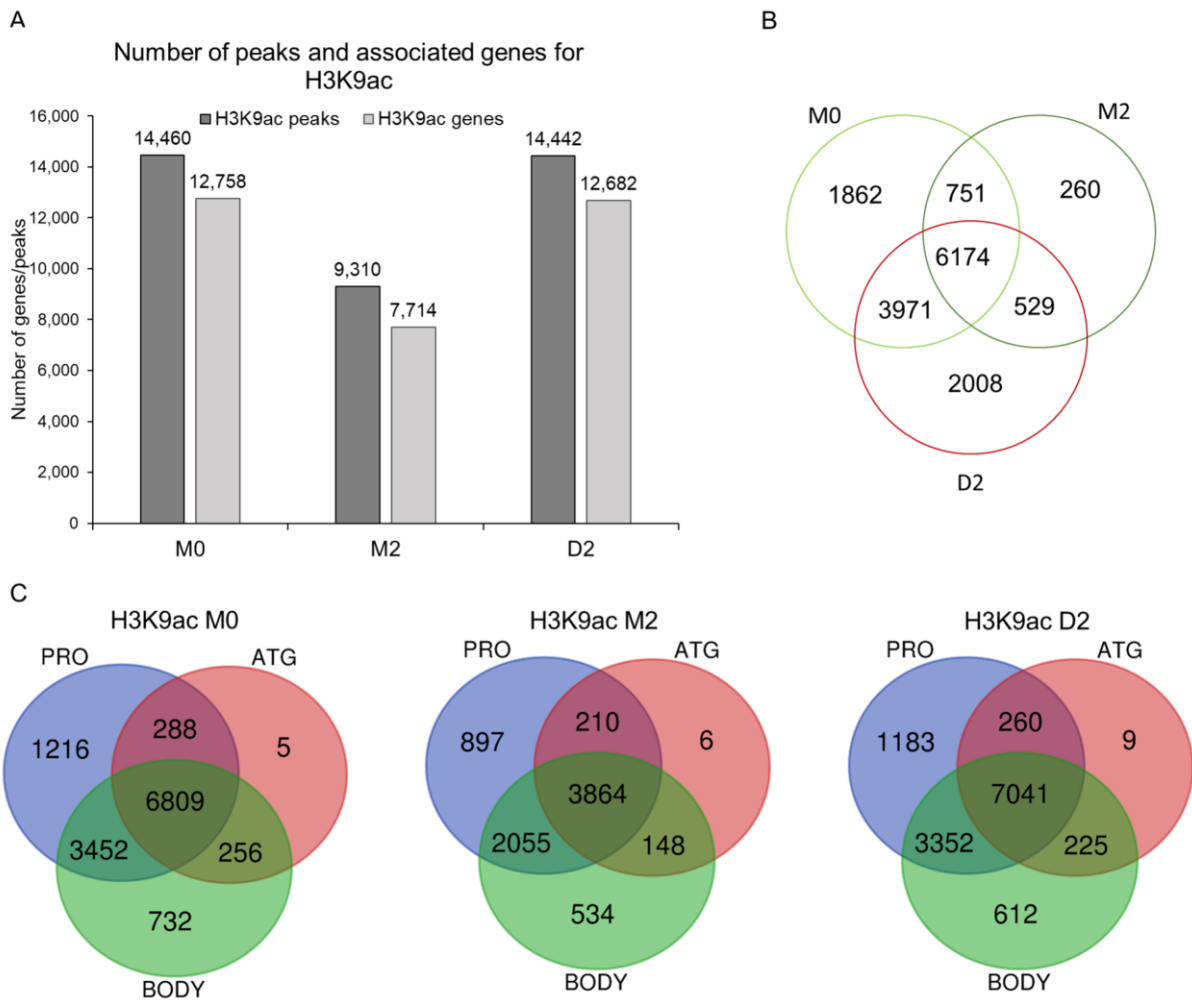
Figure 14. Comparison of genes that are associated with the H3K9ac mark. (**A**) Detected peaks and associated genes. (**B**) Venn diagram comparison of H3K9ac enriched genes for every time point. (**C**) Number of genes labelled with H3K9ac in the promotor (PRO), start codon (ATG) and/or gene body (BODY) region.

2.4.3.1 H3K9ac- two-time point comparison (M2vsD2)

M0 and D2 share 66.3% (10145) of the detected histone-modified genes whereas for M2vsM0 and D2vsM2 it is 51.2% (6925) and 49% (6703), respectively (Fig. 15). In M2, only 5.8% (789) and 7.4% (1011) of the genes appear exclusively at this time point in comparison to M0 and D2. M0 depicts 43% (5833) of the histone-modified genes compared to M2 and 17.1% (2613) compared to D2. In comparison to M2, 43.6% (5979) of the genes show the mark only in D2 and 16.6% (2537) compared to M0.
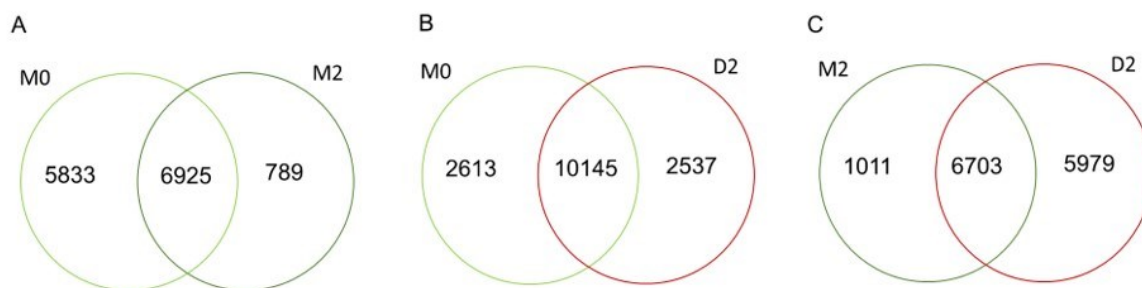
Figure 15. Comparison of genes enriched in H3K9ac between two time points. (**A**) M0vsM2 (**B**) M0vsD2 and (**C**) M2vsD2.

2.5 Gene ontology (GO) term enrichment

To get an overview about functional classes of genes differentially loaded with H3K4me3 and H3K9ac at the different conditions, GO enrichment analysis of genes associated with histone marks exclusively in M0, M2 or D2 were executed with the platform TRAPID (Bucchini et al., 2021). The program uses the Benjamini & Hochberg method for correcting and the maximum q-value was set to 0.05. With these settings, enrichment analysis was executed for the H3K4me3-marked genes in M0 and the H3K9ac-marked genes in M0 and D2. There was no significant enrichment for M2 and D2 (H3K4me3) and M2 (H3K9ac). Genes playing a role in the 'drug catabolic process' are the most overrepresented for H3K4me3 marked genes in M0 (Fig. 16A), followed by 'antibiotic catabolic process'. Terms belonging to the redox homeostasis like 'hydrogen peroxide catabolic process', 'oxidation-reduction process' and 'response to oxidative stress' show an enrichment as well as cell wall related processes ('cell wall organization or biogenesis'). H3K9ac-labeled genes in M0 (Fig. 16B) show an enrichment in the organitrogen compound metabolic process, cell wall related processes ('cell wall pectin biosynthesis process', 'rhamnogalacturonan II biosynthetic process'), 'response to stimulus', 'chemical homeostasis' and 'peptide biosynthetic process' amongst other enriched terms. In comparison, both marks exhibit genes belonging to cell wall related processes are overrepresented in M0. For GO term analysis of the H3K9ac-marked genes in D2, see chapter 2.6.
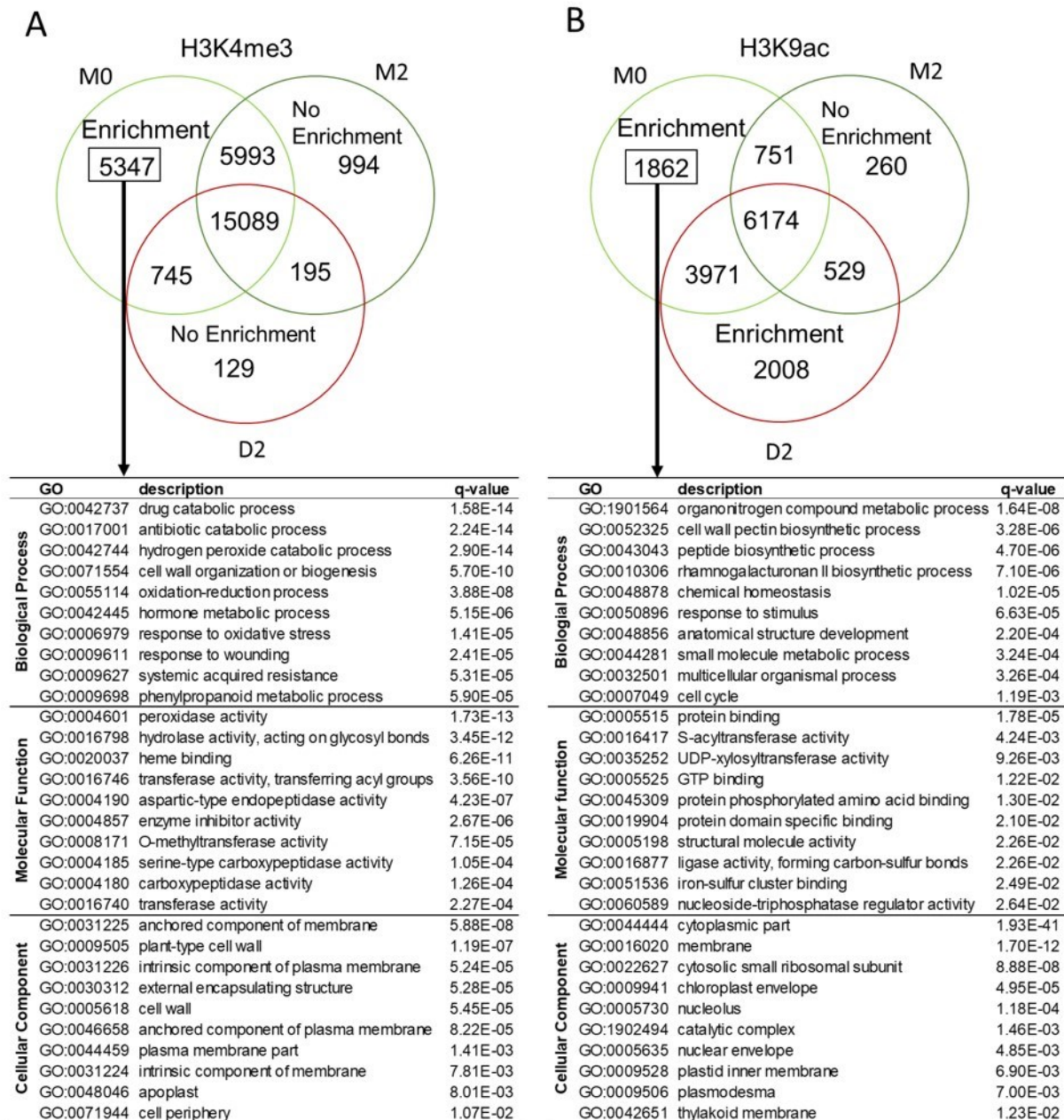
Figure 16. GO enrichment analysis of the genes labeled with (A) H3K4me3 and (B) H3K9ac in M0. Shown are the top ten enriched GO terms sorted by the lowest q-value for Biological Process, Molecular function and Cellular Component.

2.6 A detailed analysis of the genes associated with H3K9ac and/or H3K4me3 only in D2 (M0vsM2vsD2)

Comparing set of genes associated with the marks between all three time points revealed 129 genes associated with H3K4me3 and 2008 genes marked with H3K9ac specifically in D2 (see full list in Ost et al. (2023), Table S8, S9). The set of genes was functionally clustered and enrichment analysis were performed with TRAPID. While no significant enriched GO terms could be detected for the low number of H3K4me3-marked genes, this analysis allowed identifying specific functional classes of genes, which are marked with H3K9ac in response to

drought stress. Figure 17 shows the top ten enriched GO terms for the biological process (BP) and the molecular function (MF) for the 2008 genes associated exclusively with H3K9ac in D2 (see full GO term list in Appendix, Table 11). These genes have functions in several metabolic processes, involving small molecule metabolism, organophosphate metabolism, lipid metabolism and endopeptidase function. In addition, genes were found that are involved in plastid organization, embryo- and epidermis development and protein binding. The most striking set of genes with the highest q-value is involved in response to abiotic stimulus. This set of 193 genes, specifically loaded in response to drought with the euchromatic mark H3K9ac, is functionally connected to different abiotic stress responses, including drought/osmotic stress, light stimulus, salt stress, temperature stress, cold stress and external stimulus. Figure 34 (Appendix) shows increase in H3K9ac-loading for 10 well-known stress-related genes from the list: a 9-cis-epoxycarotenoid dioxygenase (central enzyme of ABA-biosynthesis), two Cytochrome P450 genes (known to act in biotic and abiotic stress pathways), two ethylene-responsive transcription factors (stress-response), a flowering locus T gene (regulates flowering time, also in response to environmental changes), two genes coding for HVA22-like proteins (involved in abiotic stress responses), a Zinc-finger protein and a LEA-family protein (both involved in abiotic stress responses).
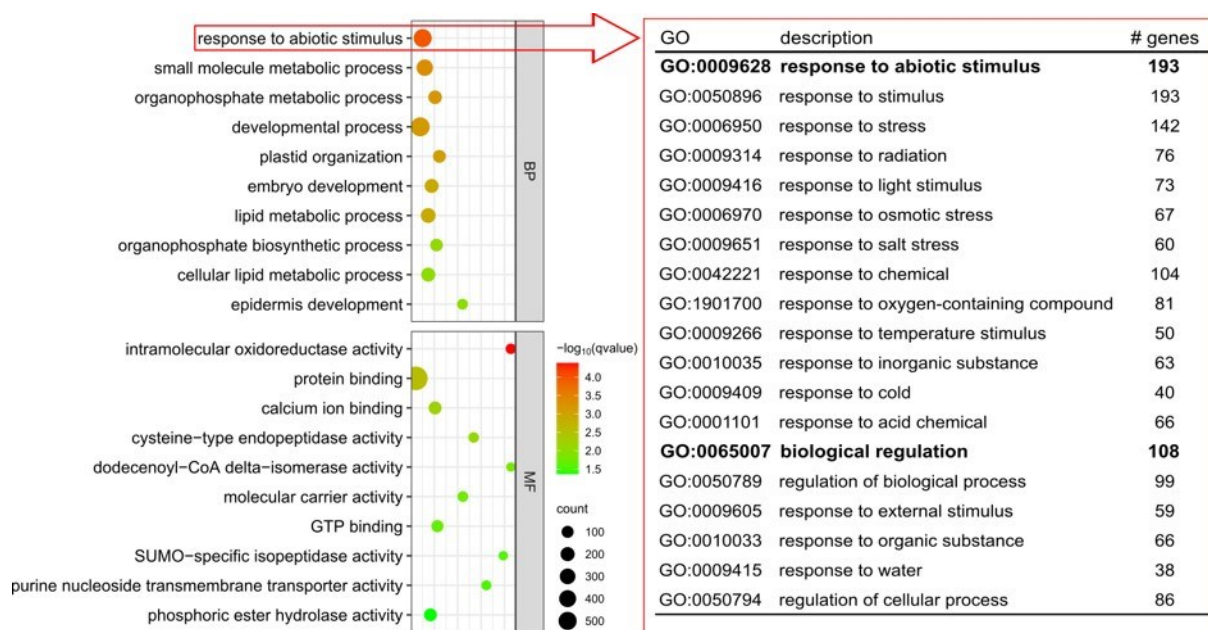
Figure 17. GO enrichment analysis of genes associated with H3K9ac in D2 in comparison to M0 and M2. The top ten GO terms for biological process (BP) and molecular function (MF) were chosen based on the q-value. Subset enrichment analysis were conducted for the over-represented term "response to abiotic stimulus", and the first two terms with corresponding subterms (in red) are shown, including the number (#) of genes in the subset terms.

Comparison between the 129 genes associated with H3K4me3 and the 2008 genes labeled with H3K9ac show 22 overlapping genes, including two sugar transporters, one Cytochrome P450, two transcription factors and a *PP2C* gene (Table 5).

Table 5. Genes labeled with H3K4me3 and H3K9ac in D2 (M0vsM2vsD2).

gene id	annotation
HORVU.MOREX.r2.2HG0145130	Aldo/keto reductase family oxidoreductase
HORVU.MOREX.r2.5HG0355750	Bidirectional sugar transporter SWEET
HORVU.MOREX.r2.5HG0384420	Calmodulin binding protein-like protein
HORVU.MOREX.r2.6HG0480100	Cytochrome P450
HORVU.MOREX.r2.4HG0331430	DCD (Development and cell death) domain protein
HORVU.MOREX.r2.1HG0047430	Diacylglycerol kinase
HORVU.MOREX.r2.2HG0085370	Flavin-containing monooxygenase
HORVU.MOREX.r2.1HG0072380	Glutaredoxin, putative
HORVU.MOREX.r2.2HG0172360	Heterogeneous nuclear ribonucleoprotein U-like protein 1
HORVU.MOREX.r2.1HG0074930	histone deacetylase-like protein
HORVU.MOREX.r2.UnG0635980	P-loop containing nucleoside triphosphate hydrolases superfamily protein
HORVU.MOREX.r2.7HG0620580	Protein kinase family protein
HORVU.MOREX.r2.5HG0392330	Protein phosphatase 2C
HORVU.MOREX.r2.4HG0294210	Protein TOC75-3, chloroplastic
HORVU.MOREX.r2.4HG0294200	Protein TOC75-3, chloroplastic
HORVU.MOREX.r2.1HG0022320	RING/U-box protein with C6HC-type zinc finger domain-containing protein
HORVU.MOREX.r2.6HG0480850	RNA-directed DNA polymerase (reverse transcriptase)-related family protein
HORVU.MOREX.r2.5HG0432710	Sec14p-like phosphatidylinositol transfer family protein
HORVU.MOREX.r2.6HG0516930	Sugar transporter, putative
HORVU.MOREX.r2.4HG0281420	Threonine dehydratase
HORVU.MOREX.r2.3HG0249890	Transcription factor
HORVU.MOREX.r2.3HG0219550	Transcription factor

2.6.1 Validation of the annotated peaks

To confirm the results from the ChIP-Seq, five genes associated with peaks were selected and corresponding primers were designed. Following genes were chosen: a gene encoding for an ABA receptor, the bidirectional sugar transporter SWEET (*SWEET*), a Heat shock transcription factor (*HS TF*), a Protein Phosphatase 2C (*PP2C*) and a bZIP Transcription factor (*bZIP TF*). Quantitative real-time PCR were performed and the percent input method was used for data normalization (Solomon et al., 2021). With this method, it is possible to calculate the ratio of the Ct values from the immunoprecipitated (IP) samples and the adjusted Ct value of the Input (IN). Figure 18 presents the calculated percentage of the input and the signal tracks of the selected genes marked with the PCR-amplified regions for control (M2) and drought stress (D2). The qRT-PCR confirmed the enrichment in the histone modifications at the specific loci. This analysis revealed a significant enhancement in both marks in drought stressed samples, with PP2C showing the strongest enrichment in both euchromatic marks.
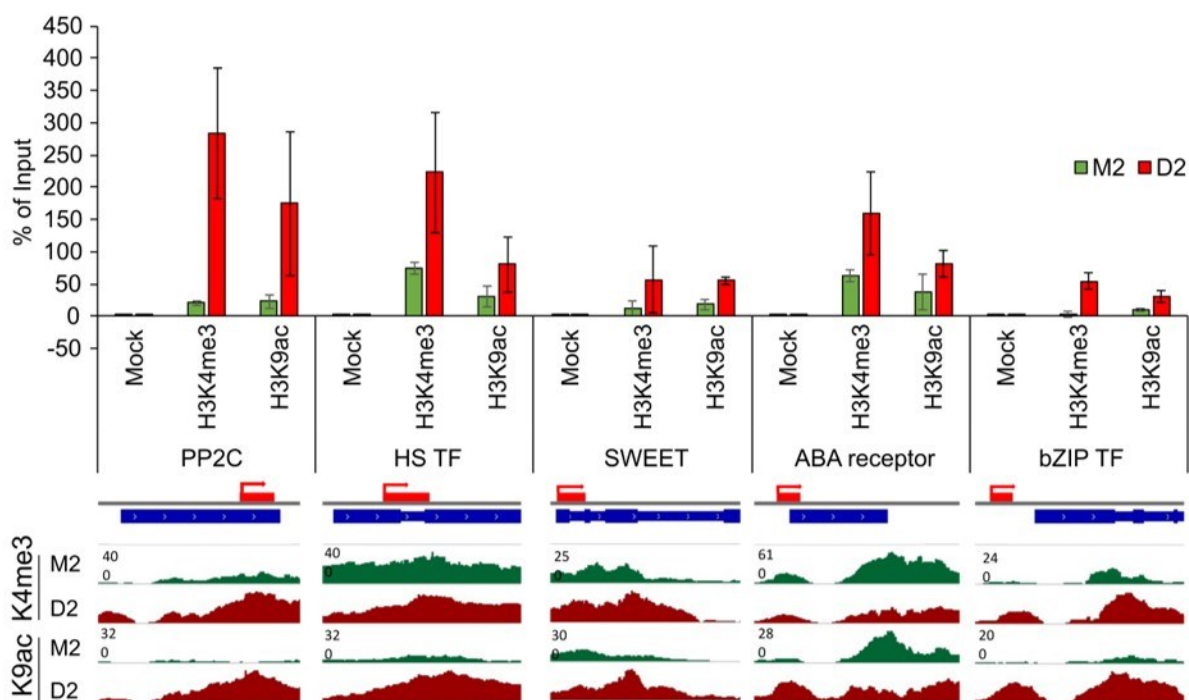
Figure 18. Validation of the ChIP-Seq results. The percentage of input was calculated for a protein phosphatase 2C (*PP2C*) gene, a heat shock transcription factor (*HS TF*), a bidirectional SWEET transporter (*SWEET*), a gene encoding for an ABA receptor and a bZIP transcription factor (*bZIP TF*) (n = 3). The red bands mark the PCR amplicon. In addition, signal tracks of histone 3 loading with K4me3 or K9ac of promoter and TSS regions of these genes are shown for M2 (green) and D2 (red).

As a conclusion it can be noted, that the heterochromatic mark H3K9me2 is associated with only a small number of genes in all time points. While the euchromatic mark H3K4me3 shows the highest abundance over the genome, H3K9ac revealed a more dynamic and specific distribution in response to the onset of drought.

2.7 Changes in the transcriptome during drought stress-induced senescence

To study the transcriptomic changes during drought stress, RNA-Seq was performed with the total genomic RNA from the samples of time points M0, M2 and D2. The RNA libraries were constructed and sequenced at IPK Gatersleben. The sequence data was analyzed and the differentially expressed genes were detected. The three selected time points open several possibilities to compare the differences in gene expression (M2 vs. M0, D2 vs. M0, D2 vs. M2) in control and during drought stress.

2.7.1 Mapping statistics

For the time point M0 three replicates were sequenced and for M2 and D2 four replicates. Table 6 presents the number of reads (processed, pseudoaligned and unique reads) and the corresponding percentage. The number of processed reads ranges between ~ 10 million to 29 million. The overall percentage of uniquely mapped reads ranges between 80 and 85%, indicating a good library quality to work with.

Table 6. Mapping statistics for the four replicates for M0, M2 and D2.

	Rep	Processed Reads	Pseudoaligned Reads	Unique	PA (%)	Unique (%)
	1	x	x	x	x	x
M0	2	13,119,218	10,840,077	10,492,457	82.6	80
	3	25,492,866	21,921,276	21,494,392	86	84.3
	4	21,678,819	18,140,558	17,718,441	83.7	81.7
	1	20,945,007	18,091,847	17,798,530	86.4	85
M2	2	25,946,606	22,565,645	22,109,727	87	85.2
	3	23,543,291	20,438,094	20,076,763	86.8	85.3
	4	18,048,888	15,137,859	14,888,759	83.9	82.5
	1	31,628,062	27,304,396	26,984,061	86.3	85.3
D2	2	23,347,962	20,012,144	19,797,276	85.7	84.8
	3	29,090,330	24,799,023	24,493,989	85.2	84.2
	4	21,296,845	18,044,835	17,762,480	84.7	83.4

After pseudo alignment with kallisto (Bray et al., 2016), as described in Material and Methods, the TPM (Transcripts per Kilobase Million) values and the read counts for every sample were calculated. The results were imported into R for statistical analysis. With the software package voom (variance modeling at the observation level) function (Law et al., 2014) the mean-variance relationship of the RNA-Seq data (log-)counts were calculated (Fig. 19A). The standard deviation first decreases and then increases at a relatively high level, which is described for higher biological variation. The multidimensional scaling (MDS) plot presents the similarity by distance between the drought stress samples (DS1-4) and the control samples (CT1-4) for D2vsM2 (Fig. 19B). The resulting list of differentially expressed genes (DEGs) as an output from the analysis were filtered based on the p-value and the logarithmic fold change. All genes with an adjusted p-value greater or equal to 0.05 were cut off from further results.

Genes with a logFC ≥ |1| were determined as differentially expressed. In Figure 19C the number of up- and downregulated genes between the different comparisons are presented. In M2vsM0, using the above mentioned strict criteria, no genes are significantly up- or downregulated. In the drought stress sample D2, 117 genes are upregulated during drought stress in comparison to M2 and 103 are downregulated (full list in Appendix, Table 12 and 13). In comparison to M0, 322 genes are upregulated in D2 and 303 genes are downregulated during drought stress.
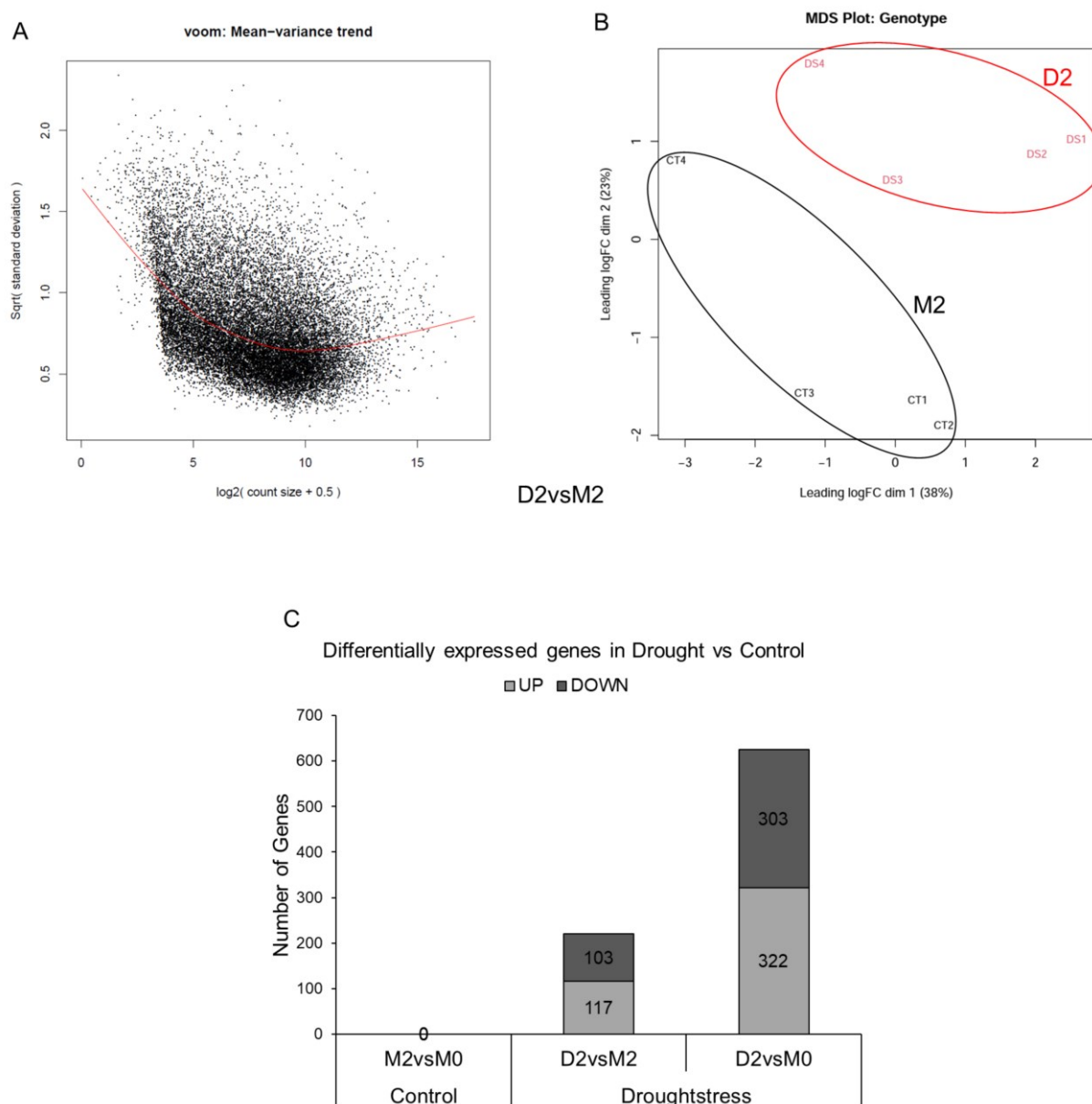
Figure 19. RNA-Seq results. (**A**) Voom plot. Shown are the mean-variance relationships for the data of D2vsM2. The x-axis presents the log2 counts per million reads (CPM) and the y-axis shows the sqrt (residual standard deviation). (**B**) Multidimensional scaling (MDS) plot of the drought (DS1-4) and the control (CT1-4) samples. (**C**). Number of up- and downregulated genes for the different time points for M2vsM0, D2vsM2 and D2vsM0 with a logFC ≥ |1| and an adjusted p-value ≤ 0.05.

2.7.2 Gene Ontology (GO) enrichment analysis with the DEG lists

Gene ontology (GO) enrichment analysis for the differentially expressed genes was executed with TRAPID with a maximum q-value set to 0.05. The top ten enriched GO terms for biological process (BP) and molecular function (MF) for up- and downregulated genes were chosen (Fig. 20). Starting with the upregulated genes, the most enriched GO terms belong to cell wall related processes (plant-type secondary cell wall biogenesis, lignin catabolic process and cellulose microfibril organization), stress responses (response to osmotic stress, response to water deprivation and response to cold), oxidation-reduction processes and the phenylpropanoid metabolic process. For the molecular function, genes showing, amongst other terms, an overrepresentation for hydroquinone:oxygen oxidoreductase activity, pyrroline-5-carboxylate reductase activity and succinate-semialdehyde dehydrogenase (NAD+) activity. For the downregulated genes, GO terms belonging to cell redox homeostasis, protein phosphorylation, reproduction and the red light signaling pathway are enriched. For the cellular component, no GO terms were significantly enriched.
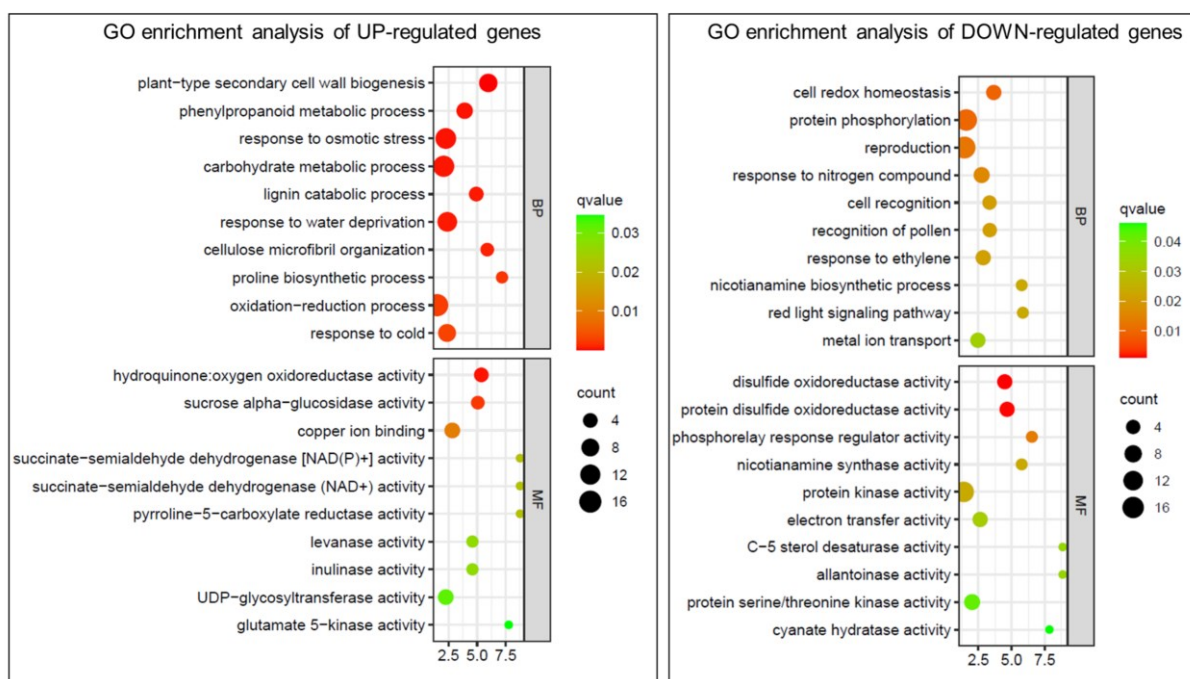
Figure 20. GO enrichment analysis of up- and downregulated genes during drought. Shown are the top ten overrepresented GO terms for Biological Process (BP) and Molecular Function (MF).

2.7.3 Validation of RNA-Seq

To validate the results of the RNA-Seq, six genes were selected: a Flavonoid O-methyltransferase (*FOMT*), a MYB transcription factor (*MYB TF*), a Cytochrome P450 (*CYP*) and three Protein Phosphatases 2C (*PP2Cs*) genes (Table 7). The genes are significantly upregulated and their logFC ranges from 1.99 to 7.48.

Table 7. Selected genes for RNA-Seq validation and their corresponding expression (logFC).

gene id	annotation	logFC	adj. P-val
HORVU.MOREX.r2.3HG0274970	O-methyltransferase	7.48	2.17E-02
HORVU.MOREX.r2.3HG0234850	MYB transcription factor	4.60	2.63E-02
HORVU.MOREX.r2.7HG0545260	Cytochrome P450	3.89	1.89E-02
HORVU.MOREX.r2.3HG0236180	Protein phosphatase 2C	3.54	9.33E-03
HORVU.MOREX.r2.1HG0066210	Protein phosphatase 2C	2.13	9.33E-03
HORVU.MOREX.r2.3HG0221890	Protein phosphatase 2C (HvABI1)	1.99	1.25E-02

Samples of the control (M2) and drought-stressed leaves (D2) were used for the qRT-PCR. As described before, the relative expression levels were calculated with the program REST. The *FOMT* depicts the highest expression in the RNA-Seq and it is significantly upregulated in D2 in comparison to M2 in the PCR analysis (Fig. 21). The *MYB TF* and the *CYP* gene are also significantly induced in drought in comparison to M2. The *PP2Cs* are also significantly induced in D2, but less strong than the other genes. Taken together, the qRT-PCR results confirm the RNA-Seq data.
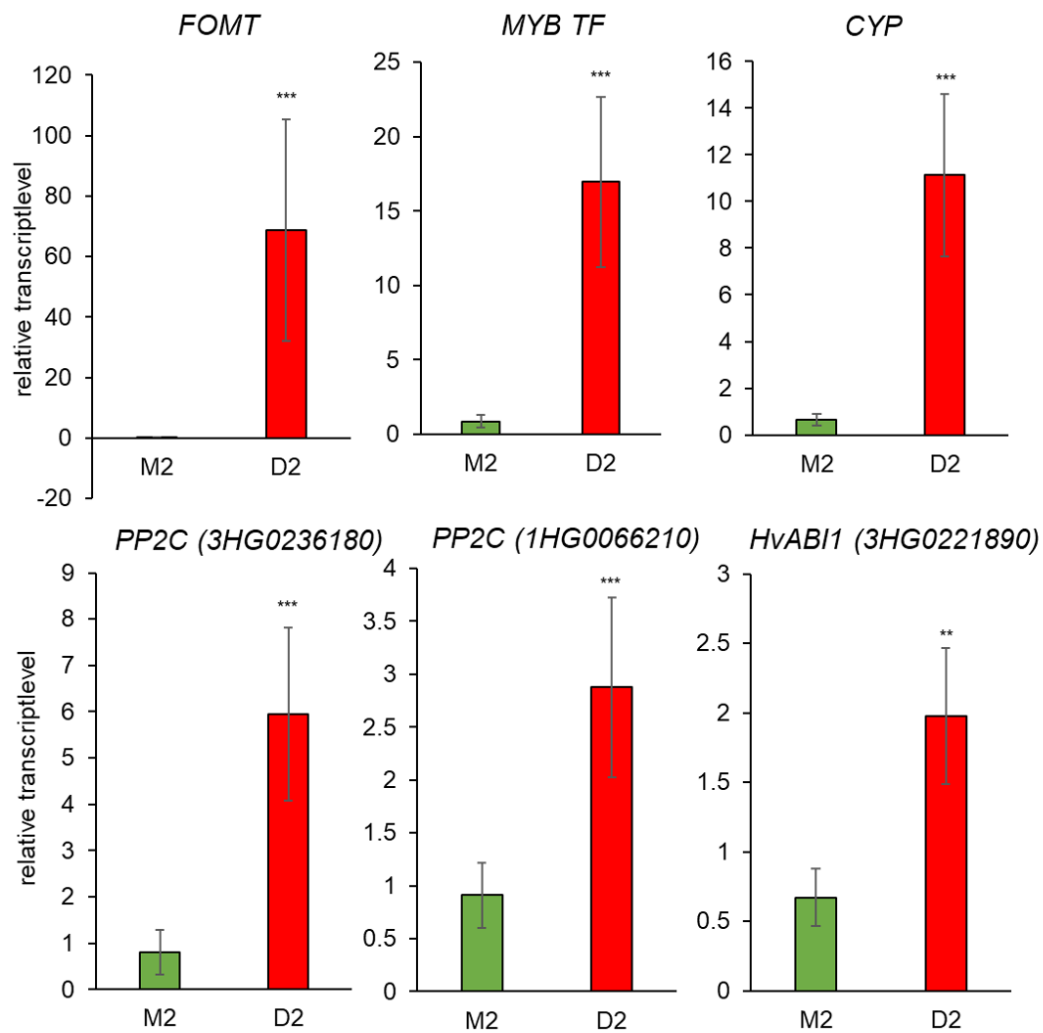
Figure 21. RNA-Seq validation via qRT-PCR with six selected genes. A Flavonoid O-methyltransferase (*FOMT*); a MYB transcription factor (*MYB TF*); a Cytochrome P450 (*CYP*) and three Protein phosphatase 2Cs (*PP2C*) were choosen. Shown are the mean relative transcript levels and standard errors calculated by the program REST (n=4). Asterisks indicate significantly differences in the transcript level (* p-val<0.05, ** p-val< 0.01, *** p-val<0.001).

It was shown that in the early phase of drought stress a set of genes is specifically up- or downregulated. Gene ontology analysis revealed that many of these genes are involved in cell wall related processes and in response to water stress.

2.7.4 Genic regions of euchromatic histone modifications at differentially expressed genes

Based on the transcriptomic analysis via RNA sequencing, the genes compared between M2 and D2 and associated with a peak exclusively in each condition, were sorted on their corresponding TPM (Transcripts Per Kilobase Million) values into mid/high-, low- and zero expression classes. Afterwards the genes were plotted against the signal tracks of the alignment files for M2 and D2 for both histone modifications (Fig. 22). Similarly, as described before, highest loading with H3K4me3 and H3K9ac at these genes is around TSS and adjoining gene body, positively correlating with the expression level, especially for H3K9ac.
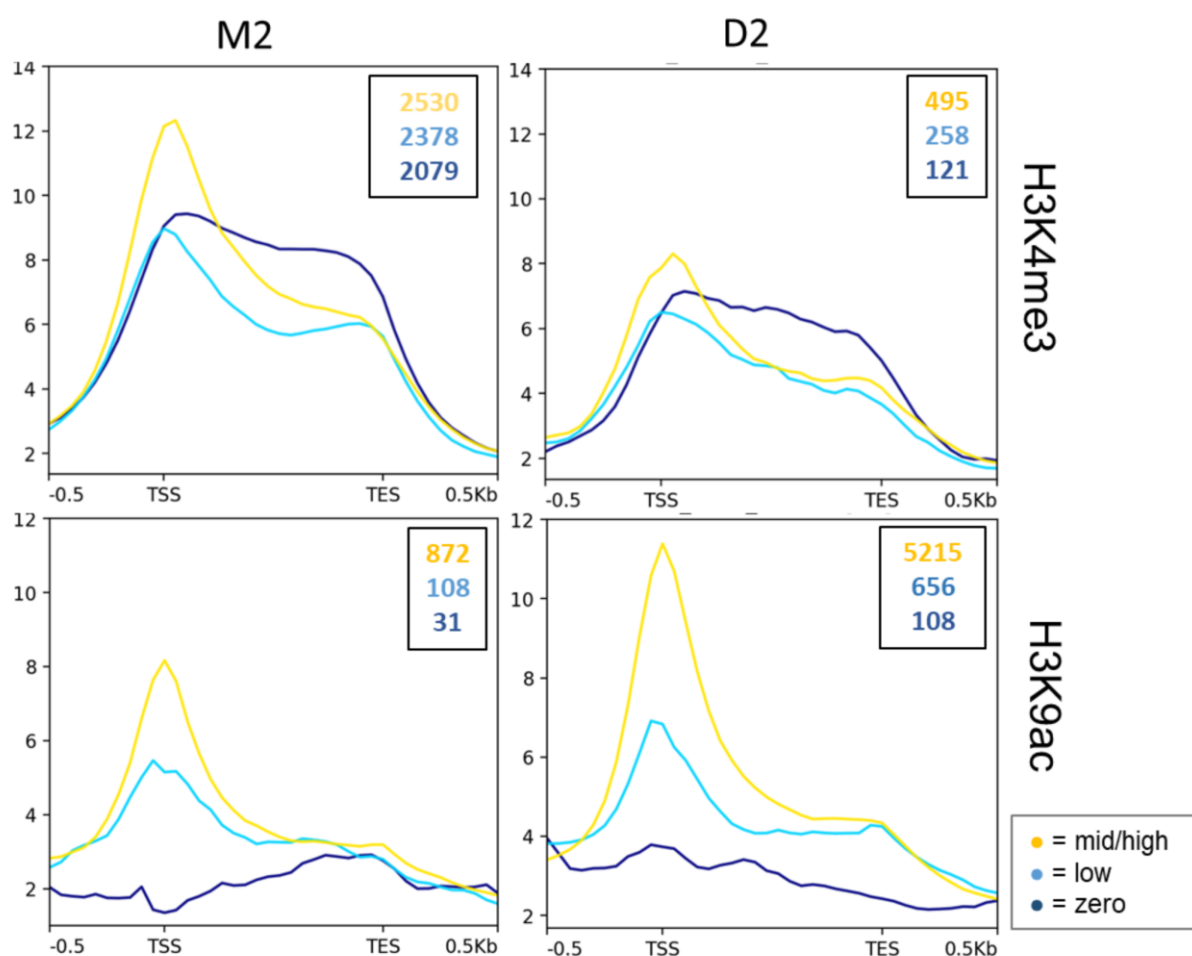
Figure 22. Distribution of genes associated with a histone mark. Genes associated with a peak were sorted into three expression levels (mid/high, low and zero expression) based on their TPM values and plotted over bigwig-files containing the signal tracks of M2 and D2 for each histone modification. The y-axis shows the fold enrichment and the x-axis the genic regions. Total number of genes belonging to the different expression groups are presented in the boxes.

2.8 Genes specifically labeled with H3K4me3 or H3K9ac AND being upregulated during development and drought stress

Via genome-wide ChIP-Seq, genes could be identified where loading with euchromatic marks H3K4me3 and H3K9ac is changed during development (M2vsM0) and in response to drought stress (D2vsM2). Using genome-wide RNA-Seq approach, parallel changes in transcriptional activity of barley genes during development and drought stress were additionally identified. To detect those genes, that are loaded with transcriptionally active H3K4me3 or H3K9ac after drought stress (D2vsM2), and are upregulated during drought stress, the corresponding ChIP-Seq data were intersected with the RNA-Seq data. Using stringent conditions, a small number of genes could be identified that are upregulated during drought stress and in parallel loaded with H3K4me3 (10 genes) or H3K9ac (12 genes). Since the main interest of this work is to detect potential changes in histone modifications during early drought stress events, the focus was put on the histone mark and gene expression changes in the drought stress sample D2.

2.8.1 Genes upregulated in early drought stress (D2vsM2) and labeled with H3K4me3 and/or H3K9ac

The genes loaded with the euchromatic marks H3K4me3 and/or H3K9ac during early drought stress (D2vsM2) were compared with those genes, that are also transcriptionally upregulated in this early phase of drought stress (Fig. 23A).
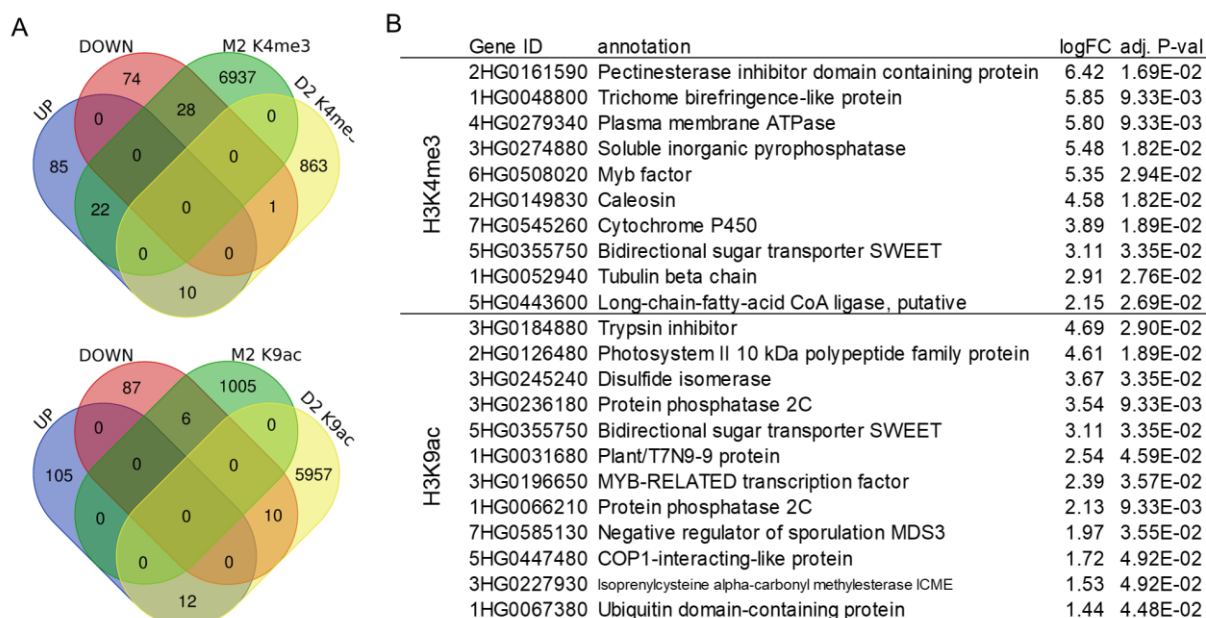
Figure 23. Comparison of the DEGs with the ChIP-Seq data. (A) Venn diagrams of H3K4me3 and H3K9ac labeled genes (M2vsD2) compared with up- and downregulated genes during drought. (B) List of genes upregulated at D2 and associated with H3K4me3 and H3K9ac.

In M2, 22 genes that are specifically associated with H3K4me3 are upregulated during drought stress and 28 genes are downregulated. For D2, 10 genes are upregulated during drought

stress and one is downregulated. For H3K9ac, six genes labeled with H3K9ac in M2 are downregulated and zero are upregulated. For D2, 12 are upregulated and 10 are downregulated. Figure 23B presents the genes upregulated in D2 and marked with the euchromatic histone modifications. The signal tracks of the fold enrichment for the histone marks were generated for these genes and visualized in IGV (Tables 8 and 9). Many of these genes are involved in abiotic stress responses, e.g., MYB-related transcription factors, cytochrome P450 and the bidirectional sugar transporter SWEET. Interestingly, two members of the PP2C family were loaded with H3K9ac and upregulated early during drought stress.

Table 8. Signal tracks of genes upregulated in D2 (D2vsM2) and labeled with H3K4me3.
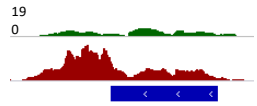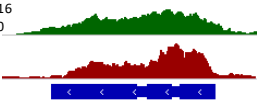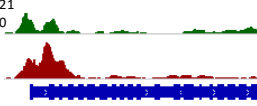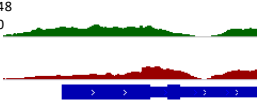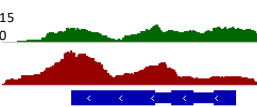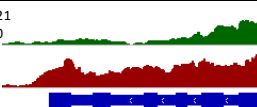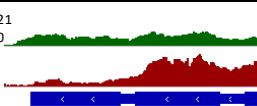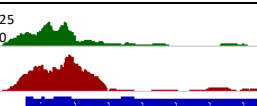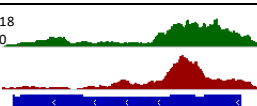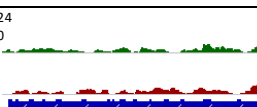
Gene ID	annotation	logFC	adj. P-val	signal track of histone enrichment
2HG0161590	Pectinesterase inhibitor domain containing protein	6.42	1.69E-02	
1HG0048800	Trichome birefringence-like protein	5.85	9.33E-03	
4HG0279340	Plasma membrane ATPase	5.80	9.33E-03	
3HG0274880	Soluble inorganic pyrophosphatase	5.48	1.82E-02	
6HG0508020	Myb factor	5.35	2.94E-02	
2HG0149830	Caleosin	4.58	1.82E-02	
7HG0545260	Cytochrome P450	3.89	1.89E-02	
5HG0355750	Bidirectional sugar transporter SWEET	3.11	3.35E-02	
1HG0052940	Tubulin beta chain	2.91	2.76E-02	
5HG0443600	Long-chain-fatty-acid CoA ligase, putative	2.15	2.69E-02	

46

Table 9. Signal tracks of genes upregulated in D2 (D2vsM2) and associated with H3K9ac.

Gene ID	annotation	logFC	adj. P-val	signal track of histone mark
3HG0184880	Trypsin inhibitor	4.69	2.90E-02	
2HG0126480	Photosystem II 10 kDa polypeptide family protein	4.61	1.89E-02	
3HG0245240	Disulfide isomerase	3.67	3.35E-02	
3HG0236180	Protein phosphatase 2C	3.54	9.33E-03	
5HG0355750	Bidirectional sugar transporter SWEET	3.11	3.35E-02	
1HG0031680	Plant/T7N9-9 protein	2.54	4.59E-02	
3HG0196650	MYB-RELATED transcription factor	2.39	3.57E-02	
1HG0066210	Protein phosphatase 2C	2.13	9.33E-03	
7HG0585130	Negative regulator of sporulation MDS3	1.97	3.55E-02	
5HG0447480	COP1-interacting-like protein	1.72	4.92E-02	
3HG0227930	Isoprenylcysteine alpha-carbonyl methylesterase ICME	1.53	4.92E-02	
1HG0067380	Ubiquitin domain-containing protein	1.44	4.48E-02	

2.8.2 Upregulation of Protein Phosphatase 2C (PP2C) during drought stress

The protein phosphatases 2C (PP2Cs) which play a central role in the ABA signaling module were analyzed in more detail. They function as a negative regulatory switch at the center of the ABA signaling network tuning the ABA response and integrating it with other developmental and stress-related pathways (Jung et al., 2020). In *A. thaliana*, 76 PP2Cs were identified and grouped into ten clades (A-J) and it was shown, that six of nine PP2Cs belonging to the clade A are involved in ABA signaling (Schweighofer et al., 2004). It was shown that the expression of some of these genes is under epigenetic control by altering their chromatin state (Jung et al., 2020). In *H. vulgare* cv. Morex, 85 PP2Cs were recently identified (Wu, 2022). Interestingly, in the present study, 26 PP2Cs, including six putative and six family protein PP2Cs, are gaining an acetylation of K9 during drought (Appendix, Table 14, signal tracks in Table 15). To quantify the signal strength of the acetylation of K9, deeptools BigwigSummary (Ramírez et al., 2014) and the program Diffbind (Stark & Brown, 2011) were used (Appendix, Table 14). Diffbind calculates the fold of the mean read concentration of peaks between two conditions, in this case M2 versus D2. The transcript abundance was presented as the ratio of D2/M2 of the mean TPM. For many of these barley *PP2C* genes, there is a clear correlation between the TPM ratio and the signal strength values, which means that transcript abundance of the *PP2C* genes in D2 correlates with their H3K9ac-loading (Fig. 24A). Blast analysis in combination with the recent PP2C phylogenetic studies in hulless barley (Liang et al., 2022) revealed, that six of the top seven K9ac-enriched PP2Cs are belonging to the clade A. Validation via qRT-PCR for three selected *PP2Cs* confirmed the results and continued expression analyses for later, more severe drought stress stages D3 and D4 clearly showed an increasing relative transcript level for all three *PP2Cs* (Fig. 24B).
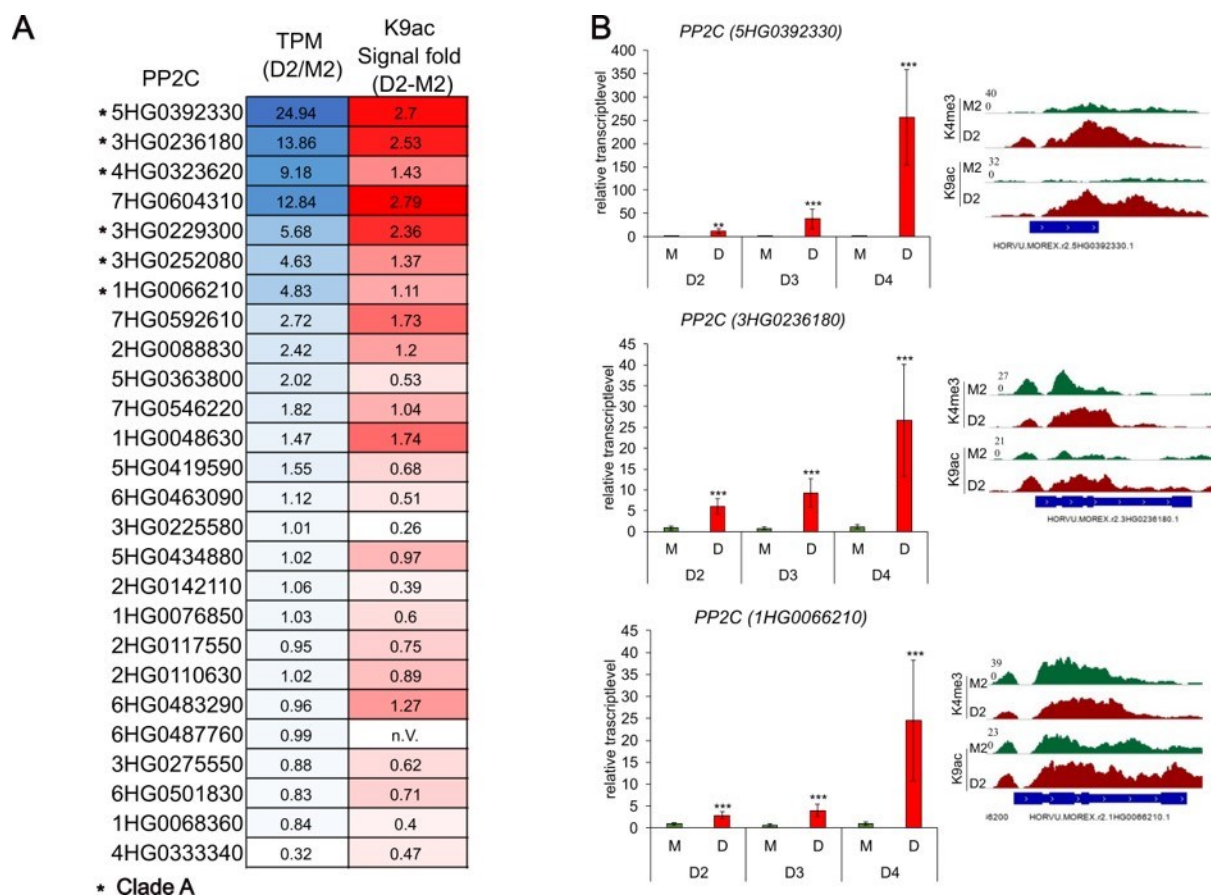
Figure 24. Correlation between drought stress-induced transcriptional up-regulation and loading with H3K9ac of *Hordeum PP2Cs*. (**A**) Heatmap of the 26 *PP2Cs* labelled with H3K9ac in D2. Shown are the color-coded values for the TPM (Transcript per Kilobase Million) ratio (D2/M2) in blue and the signal of H3K9ac enrichment (signal fold D2-M2) in red. Darker colors indicate higher values; asterisks mark the *PP2Cs* that are belonging to clade A. (**B**) Validation of three selected *PP2Cs* via qRT-PCR. Shown are the relative transcript level calculated with the Ct-values from the qRT-PCR for the stages D2, D3 and D4 with the corresponding histone mark signal tracks for D2.

However, not all identified *PP2Cs* show this correlation. For example, the upregulated *PP2C 3HG0221890* (Fig. 25), despite being clearly upregulated, does not show a change in the acetylation level of K9 and BLAST analysis revealed that this gene encodes *abscisic acid-insensitive 1* (*ABI1*) which is involved in stomatal regulation and ABA mediated responses as a negative regulator (Pinheiro & Chaves, 2011).
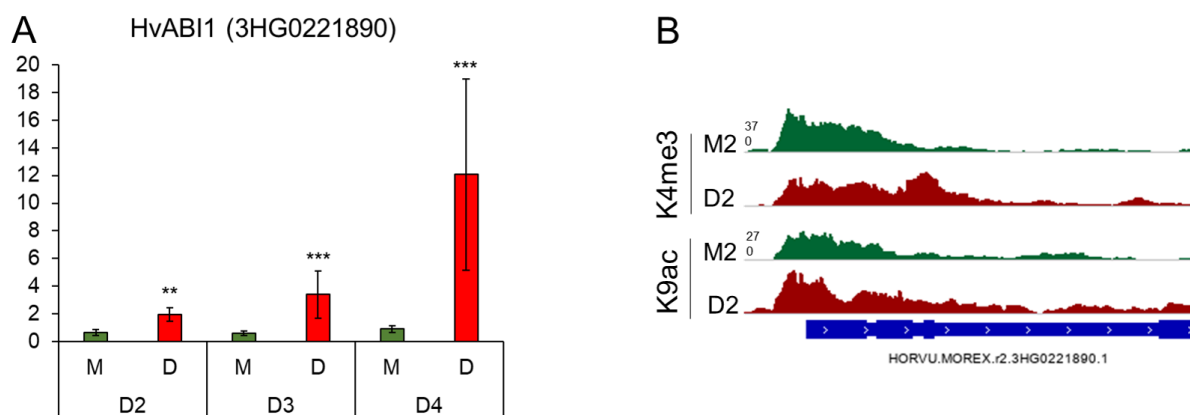
Figure 25. Upregulated *HvABI1* during drought stress (D2vsM2). Shown are the relative transcript level for stage D2, D3 and D4 calculated with the REST program from qRT-PCR data. On the right, the corresponding signal track of histone mark enrichment for H3K4me3 and H3K9ac is presented.

A small set of genes is upregulated during drought and simultaneously associated with H3K9ac and/or H3K4me3. Notably, a majority of these histone-modified genes are involved in the abiotic stress response. Especially, a set of PP2Cs show a correlation between upregulation and being acetylated during drought.

2.9 Whole-genome bisulfite sequencing (WGBS)

To investigate potential changes in the methylome, e.g., global DNA methylation during early drought stress, a whole-genome bisulfite sequencing (WGBS) was performed. The same samples and time points as used for the ChIP- and RNA-Seq were investigated (M2vsD2). Three independent biological replicates were sequenced multiple times. Before sequencing, the samples were treated with bisulfite, which converts cytosine residues to uracil whereas methylated cytosines are not changed.

To analyze the output of the WGBS, several pipelines were used. Starting with Methylstar (Shahryary et al., 2020) which combines Trimmomatic (Bolger et al., 2014) for read trimming, Bismark (Krueger & Andrews, 2011) for alignment, FastQC (Andrews, 2010) for quality control and BEDTools (Quinlan & Hall, 2010) and followed by MethylC (Lu et al., 2023), the sequence data were processed and differentially methylated regions (DMRs) could be identified.

2.9.1 Mapping statistics

Bismark is implemented into the Methylstar pipeline and is executed for read alignment in which bisulfite converted reads are mapped to the converted reference genome. For both time points (M2 and D2), three replicates were processed. Table 10 presents the mapping statistics. The mapping efficiency ranges between 50 and 54.9% for the different replicates. The average sequencing depth is between 2.3 and 6.5 and the coverage is between 75.9 and 92.2%.

Table 10. Mapping statistics. Mapping efficiency (in %), average sequencing depth and the coverage (in %) are presented for both time points and their corresponding replicates.

		sequence pairs	unique paired-end alignments	Mapping efficiency (%)	Average sequencing depth (X)	Coverage %
M2	Rep1	157,653,677	86,102,527	54.6	4.2	88.1
	Rep2	91,058,949	50,015,786	54.9	2.3	75.9
	Rep3	129,664,779	68,040,518	52.5	3.1	82.7
D2	Rep1	139,682,553	70,913,242	50.8	3.2	82.3
	Rep2	185,746,089	100,256,012	54	4.5	89.1
	Rep3	281,284,174	151,312,577	53.8	6.5	92.2

2.9.2 Global distribution of methylation levels

With the recently developed software MethylC-analyzer (Lu et al., 2023), the WGBS data could be processed. As described before, the raw reads were quality checked, trimmed and Bismark executed the alignment to the converted Morex V2 reference genome. Bismark generates report files, which contain the methylation status for every cytosine in the genome and can be used as an input for the MethylC-analyzer.

To observe differences and similarities between the replicates, principal component analysis (PCA) of the M2- and D2 replicates for every chromosome and context were executed (data not shown). An exemplary PCA for chromosome 1 (CG context) for M2 and D2 shows a similarity between four of the replicates (M2: Rep1 and Rep3, D2: Rep2 and Rep3), whereas M2_Rep2 and D2_Rep1 are more distinct to the other samples (Fig. 26A). Furthermore, a hierarchical cluster heatmap of the methylation levels for every replicate was generated (Fig. 26B). No obvious difference between the replicates of M2 and D2 could be observed.
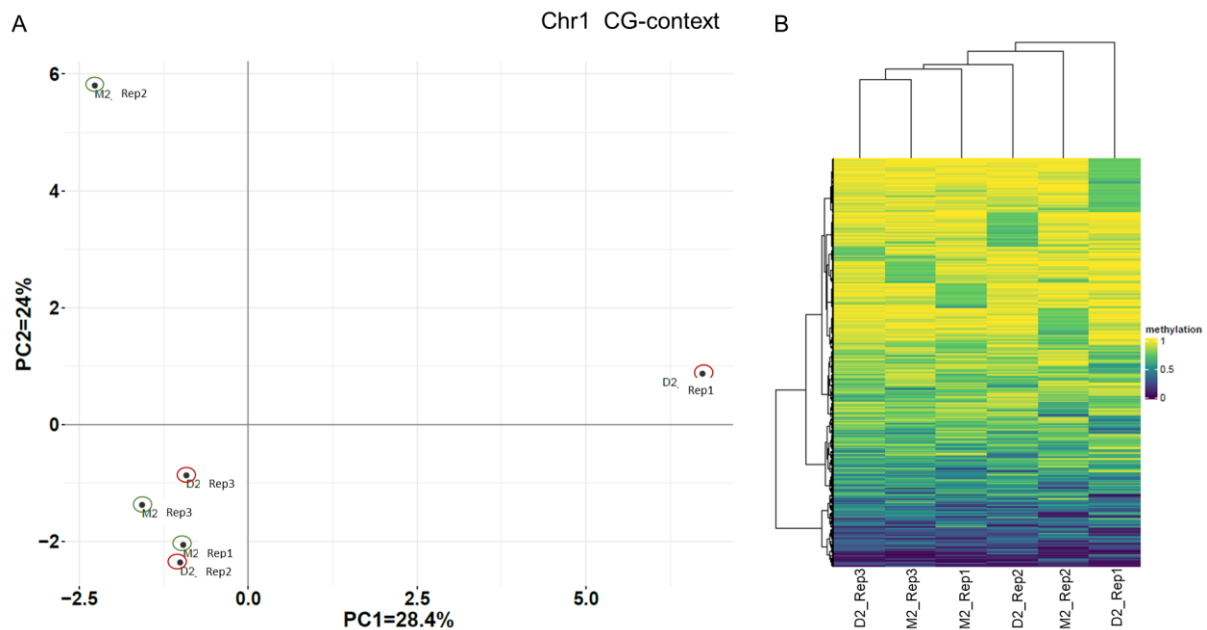
Figure 26. Comparison of the replicates for Chromosome 1 (CG context). (**A**) Principal component analysis (PCA) of the two samples (M2 and D2) and their corresponding replicates. M2 (Rep1-3) represents the control and D2 (Rep1-3) the drought stress sample. (**B**) Heat map of the methylation levels of the different replicates.

MethylC calculates the global, average methylation levels (in %) for all contexts (CG, CHG and CHH) and all chromosomes (Fig. 27). The average CG methylation shows a high value of around 88-92% for every chromosome. For CHG, it is around 60-62% and for CHH around 6%. There is no obvious difference in the global methylation levels for M2 and D2 and between the chromosomes, except chromosome 4 showing higher levels in CG (92,2%) and CHG (65,5%) context. Similar numbers were detected in a recently published study in hulless barley. PEG-6000-treated roots and leaves revealed an average genome-wide cytosine methylation of 91.71% for CG, 67.36% for CHG and 3.14% for CHH (Jiabu et al., 2023). These first results indicate that there is no measurable change in the overall methylation levels between control and drought stressed samples.
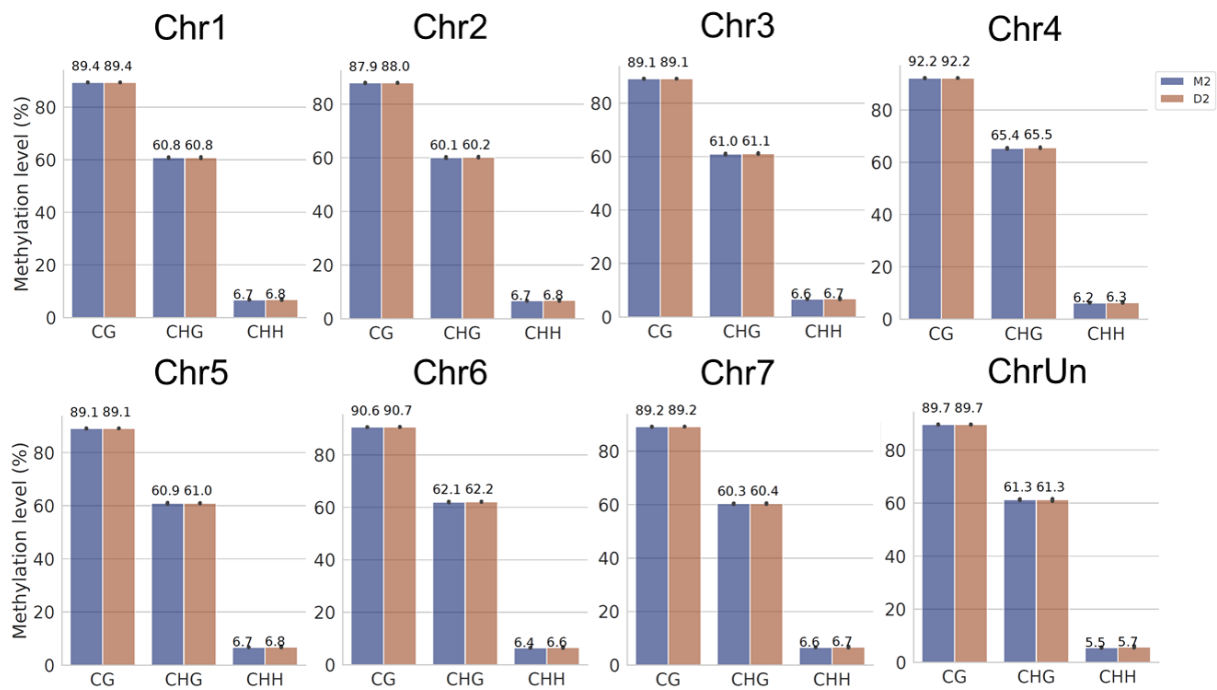
Figure 27. Global, average methylation levels (%) for CG, CHG and CHH. The seven barley chromosomes and the uncharacterized chromosome (ChrUn) are presented. The control is marked with blue and the drought sample is marked with orange.

In a next step, metagene plots were generated that present the methylation levels (in %) over the genomic region (Fig. 28). For CHG and CHH, methylation levels rise upstream to the TSS and downstream to the TES, while for CG, the methylation levels in the gene body depicts the same level as upstream TSS and downstream TES. Methylation levels for all contexts are the lowest at the TSS and TES. This distribution could be detected for every chromosome and could be also shown for spring barley cultivars, in populus, mungbeans and rice (Liang et al., 2014; Garg et al., 2015; Malinowska et al., 2020; Zhao et al., 2022).
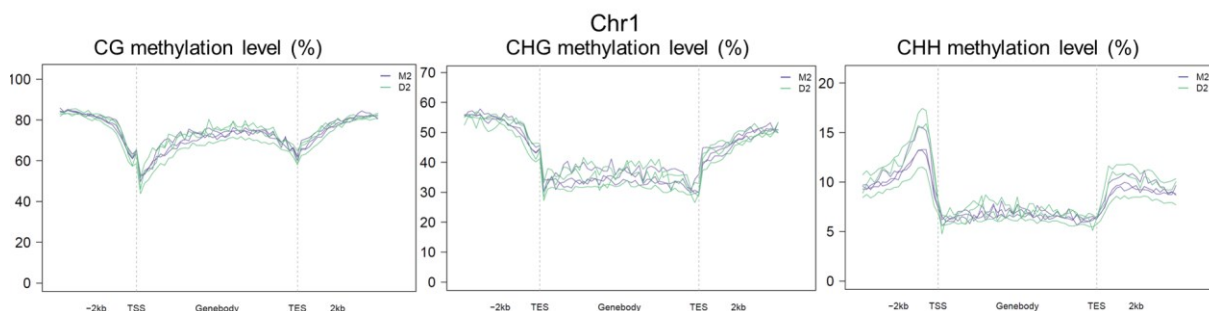
Figure 28. Average methylation level in percentage. Methylation levels over Transcription start site (TSS), genebody and Transcription ending site (TES) on chromosome 1 for CG, CHG and CHH are presented. The blue lines represent the three M2 replicates and the purple line are the three D2 replicates.

2.9.3 Identification of differentially methylated regions (DMRs) and associated genes (DMGs)

Differentially methylated regions (DMR) in the drought stress sample D2 in comparison to the control were identified by methylC. A total number of 9140 DMRs in D2 were identified, of which 7767 are located in transposable elements (TE) and 736 in genes (Fig. 29A). The remaining 637 DMRs were not annotated. Furthermore, 4350 of the DMRs were hypo- and 4790 DMRs hypermethylated in response to drought stress, with the majority in the CHG context with 2934 hypo- and 3236 hypermethylated DMRs (Fig. 29B). Genes overlapping with the DMRs were considered as differentially methylated regions- associated genes (DMGs, Fig. 29C), resulting in total 339 hypo- and 376 hypermethylated DMGs. Of these, the majority is found in the CHG- and CHH context.
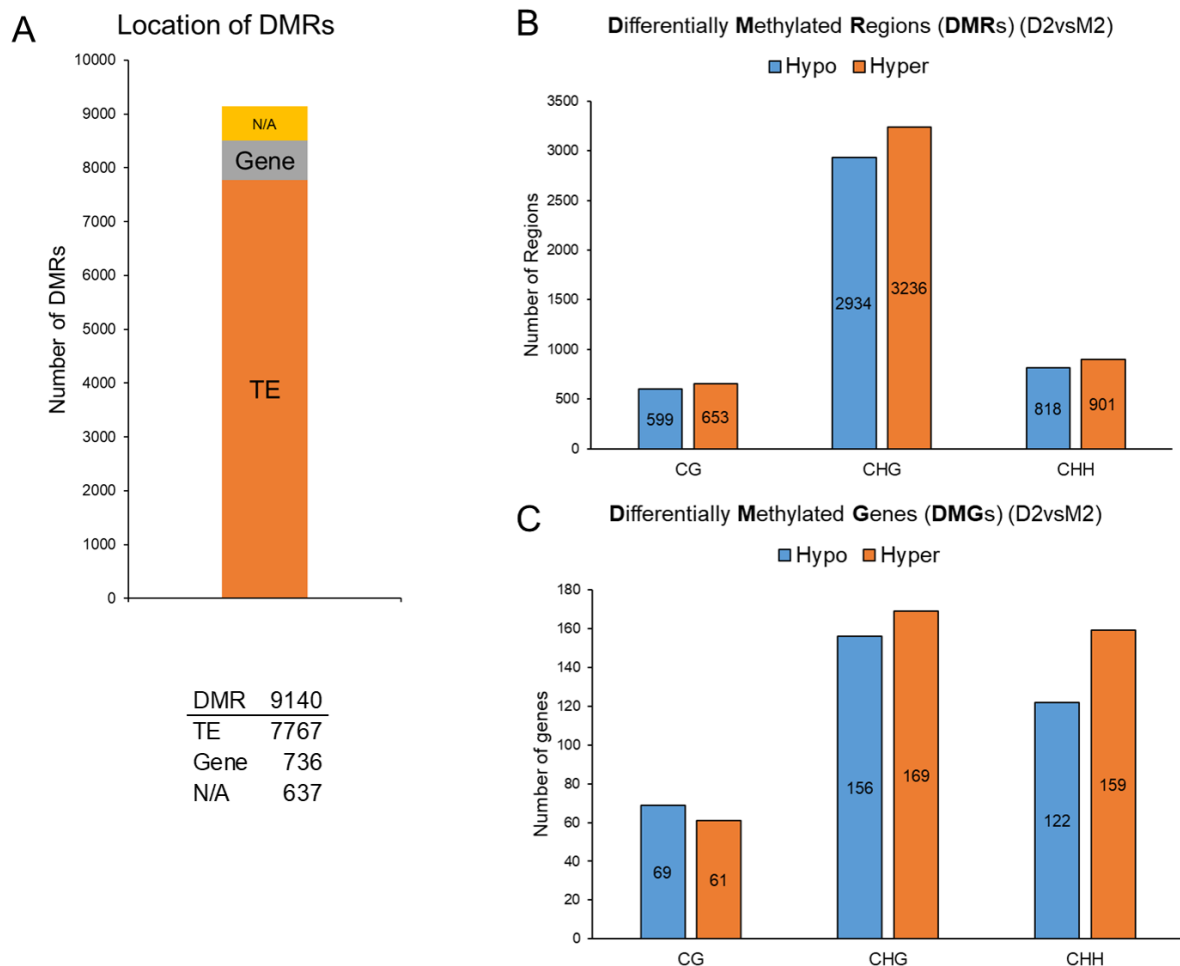
Figure 29. Differentially methylated regions (DMRs) and genes (DMGs). Presented for all chromosomes and all three contexts (CG, CHG and CHH). (**A**) Location of the differentially methylated regions. Number of hyper- and hypomethylated DMRs (**B**) and DMGs (**C**) in all three contexts.

The distribution of the DMRs were visualized in IGV together with the peak distribution of the histone marks (Fig. 30). Interestingly, the density of the DMRs is high at the centromeres (red

rectangle) and pericentromeric region. This distribution was already described for *A. thaliana* (Zhang et al., 2006; Zilberman et al., 2007).
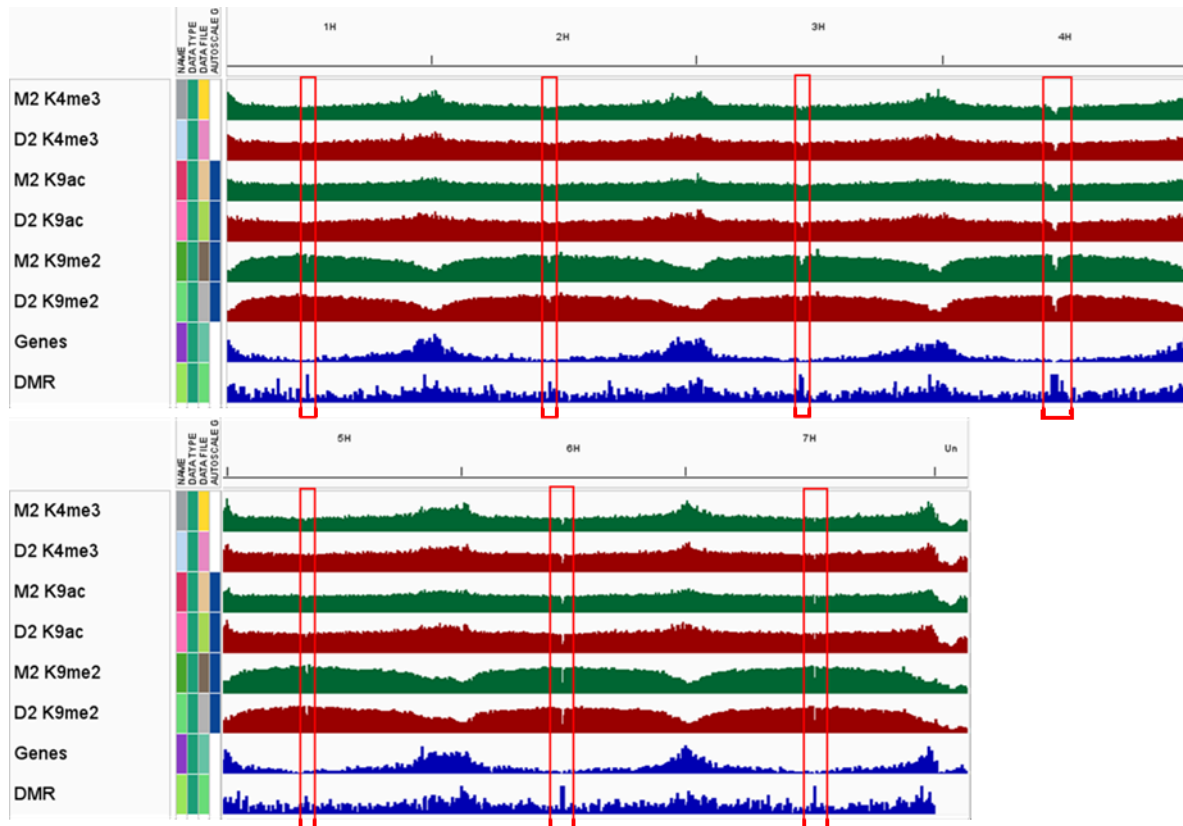
Figure 30. Distribution of differentially methylated regions (DMRs). The red rectangle marks the centromeres. The signal tracks of the histone marks are presented as well, in green for M2 and red for D2.

The distribution of the location of the hyper- and hypomethylated regions in genes is presented in Figure 31A. Much more methylated sites are located in the promotor region of genes and this could be observed for every methylation context, e.g., 147 genes show CHH hypermethylation in the promotor in comparison to 16 genes exhibiting a CHH hypermethylation in the gene body.

Comparison of the mean length of genes associated with DNA methylation in the promotor or gene body region revealed that genes with body methylation are longer in average than genes with promotor methylation (Fig. 31B). It has been shown before that genes exhibiting gene body methylation are generally longer in comparison to unmethylated genes and are constitutively expressed (Zhang et al., 2006; Takuno & Gaut, 2013; Niederhuth et al., 2016; Zhang et al., 2018).
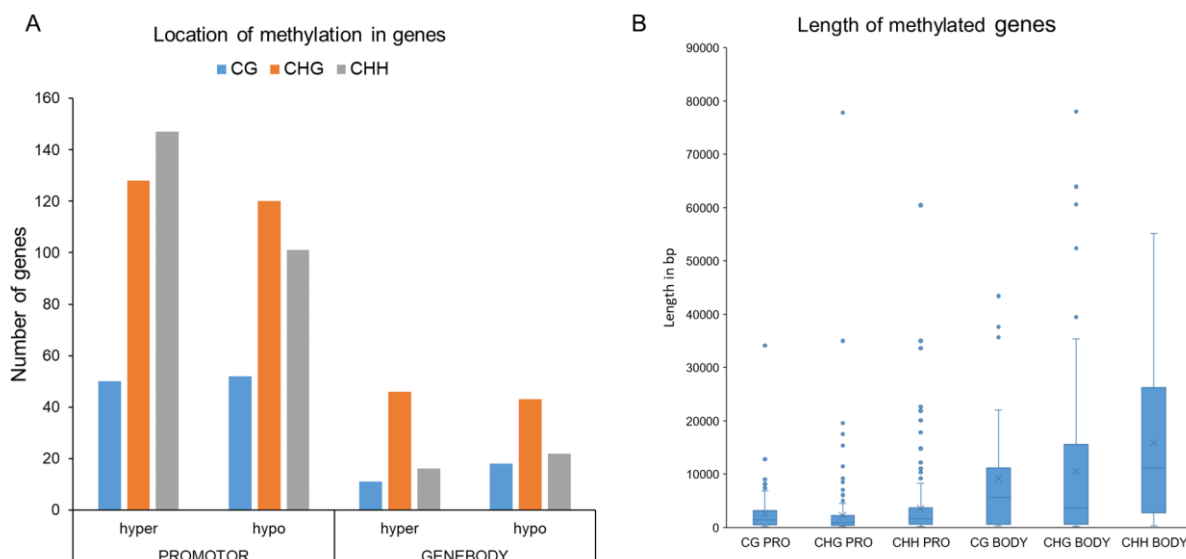
Figure 31. Profile of methylated genes. (**A**) Number of hyper- or hypomethylated genes located in the promotor or genebody region in CG, CHG and CHH context. (**B**) Average length (in bp) of genes differentially methylated in promotor (PRO) or gene body (BODY) in CG, CHG and CHH context.

Go enrichment analysis for the hypermethylated DMGs showed no significant enriched GO terms. For the 330 hypomethylated genes, a small set of GO terms are overrepresented (Fig. 32A). The GO term 'carbohydrate phosphorylation' belonging to the biological process (BP) is enriched. Interestingly, genes, belonging to the ribonucleoprotein complex, the ribosome and the structural constituent of ribosome are overrepresented. Comparison of genes labelled with H3K4me3 or H3K9ac in D2 with the hypo- and hypermethylated DMGs revealed only a small number of genes associated with H3K4me3 and/or H3K9ac and being hyper- or hypo-methylated (Fig. 32B). Comparison of DMGs with the list of DEGs showed that only one gene is shared, a *Trypsin Inhibitor* (Fig. 32C). The gene is also upregulated (logFC=4.7) and associated with H3K9ac in D2. The hypomethylation in the CHH context in D2 is located in the promotor region of the gene (red rectangle) (Fig. 32D).

A

	GO	description	log2	q-value
BP	GO:0046835	carbohydrate phosphorylation	6.70	1.66E-02
CC	GO:1990904	ribonucleoprotein complex	1.83	5.68E-06
	GO:0005840	ribosome	1.85	2.09E-05
	GO:0032991	protein-containing complex	1.09	2.61E-04
	GO:0043228	non-membrane-bounded organelle	1.19	5.33E-04
	GO:0043232	intracellular non-membrane-bounded organelle	1.19	5.33E-04
MF	GO:0003735	structural constituent of ribosome	2.12	1.19E-06
	GO:0005198	structural molecule activity	1.98	4.09E-06
	GO:0004335	galactokinase activity	6.70	1.66E-02
	GO:0005534	galactose binding	5.96	4.65E-02

B

C

D

Figure 32. Analysis of the methylated genes. (**A**) GO enrichment analysis of the 330 hypo-methylated DMGs. Shown are the enriched GO terms for Biological Process (BP), Cellular Component (CC) and Molecular Function (MF). (**B**) Venn diagram of genes labelled with H3K4me3 or H3K9ac and showing hyper- or hypo-methylation. (**C**) Venn diagram of shared genes between DMGs and DEGS. (**D**) Signal tracks and location of the hypo methylation (red rectangle) for the Trypsin inhibitor.

To summarize, the WGBS revealed an overall stable barley methylome at the onset of drought stress. A small amount of differentially methylated genes could be observed but no significant changes in the genome-wide DNA methylation could be detected between control and drought stressed samples. Furthermore, no apparent relation between the histone modification patterns or the transcriptome changes and the DNA methylation pattern were found.

3 Discussion

The experimental set-up of this study allowed a slow decrease of the relative soil water content, after withholding the water at day 11, simulating a more natural drought stress. While a majority of studies concentrated on proceeded drought stress in barley (Talamè et al., 2007; Samarah et al., 2009; Zhao et al., 2010; Wehner et al., 2016), the focus of this research laid on transcriptomic and epigenetic responses in the early phase of drought stress in barley plants. Therefore, time points for sampling were chosen at an early stage, when only 10-15% of the chlorophyll and only 5-10% of the photosynthetic performance was lost. Whereas no phenotypic differences could be observed in the primary leaves between control and early drought stressed plants, transcriptomic analysis via qRT-PCR already showed that at this time point, some marker genes of drought stress are either induced or repressed (Fig.4).

3.1 Challenges of ChIP-derived NGS data analyses

Besides its benefits to the determination of genome-wide reprogramming of gene expression and distribution of histone modifications via RNA-Seq and ChIP-Seq approaches, analysis of NGS data comes along with some challenges (Park, 2009). Given a fairly big genome size of ~5.1 Gb for barley (Doležel et al., 1998; International Barley Genome Sequencing Consortium et al., 2012; Mascher et al., 2017), a certain sequencing depth has to be obtained to gain a sufficient coverage of the genome (Sims et al., 2014). Furthermore, around 80% of the barley genome derived from transposable elements (Mascher et al., 2017). This complicates the sufficient sequencing, covering and mapping of NGS-derived data although ChIP-Seq is much more improved in comparison to older ChIP methods (e.g. ChIP-Chip) regarding covering repetitive DNA (Park, 2009). The downstream analysis of NGS data relies on an efficient and precise alignment of the reads to the reference genome (mapping). The ENCODE consortium suggests a minimum of 20 million reads uniquely mapped to the genome for mammalian broad-source histone marks (Landt et al., 2012) but no guidelines for plant material could be found. Regarding the present ChIP-Seq, around 7 to 32 million reads mapped uniquely to the reference genome with mapping rates between 82.94 and 99.31%, indicating a good library to work with.

As mentioned before, the sampling time occurred at the onset of drought stress with only slight differences between the control and the drought stress samples. PCA eventually confirmed these assumptions by depicting similarities between control and drought conditions. Nevertheless, a PCA of all samples, time points and histone modifications pointed out similarities and differences between conditions and histone marks. Despite no prominent physiological differences between the control and drought stressed samples in this work, it was possible to obtain a reasonable number of peaks with MACS2. The decision to use the

pooled peak calling instead of separately identifying peaks was based on the observation that the associated genes overlap majorly between pooled and separately called peaks. Furthermore, pooled peak calling detected some more peaks. To enhance the quality of the detected peaks, one replicate was discarded from the analysis due to its weak signal in every time point. In addition, to get reliable data, the q-value for peak calling was set to <0.05 and only peaks with a fold enrichment ≥10 were used for further analysis. Chipseeker output revealed that filtering the peaks disposed a huge number of peaks located in the distal intergenic region.

3.2 Early response to drought involves upregulation of specific stress-related genes in barley

RNA-Seq analysis allowed identifying a number of genes already differentially expressed in barley plants in the early phase of drought stress. GO enrichment analysis of these upregulated genes showed an overrepresentation for cell wall related processes, the phenylpropanoid metabolic process, proline biosynthetic process, oxidation-reduction process and response to water deprivation and osmotic stress. As outlined below, these are processes, which are known to be related to abiotic stress responses.

In more detail, a significant amount of the upregulated genes plays a role in cell wall-related processes, including three cellulose synthase genes, four laccases, three COBRA-like proteins and a fasciclin-like arabinogalactan protein. Plants under water deprivation react by re-structuring their cell wall, e.g. by loosening or tightening cell walls in a tissue-specific manner (Wu & Cosgrove, 2000; Moore et al., 2008). This maintains the ability of certain cells to grow, whereas non-necessary tissue will be stiffened. Clauw et al. (2015) observed the downregulation of genes involved in cell wall strengthening and the upregulation of cell wall loosening expansins, pectin lyases and pectin methylesterases in *A. thaliana* leaves under mild drought stress. These findings lead to the conclusion that the cells of the leaf tissue are staying in a so-called "growth-ready state", allowing them to expand when environmental conditions get back to normal. GO analysis in the present work revealed that genes involved in plant-type secondary cell wall biogenesis, lignin catabolic process and cell wall thickening are overrepresented, suggesting a stress-induced expression of genes involved in limiting cell wall extensibility, as was also described in Lu & Neumann (1998). In addition, the overrepresented phenylpropanoid pathway is also known to play a role in abiotic stress response, regulating an increase in protective compounds, e.g., phenolics, flavonoids or anthocyanins (Yaqoob et al., 2022). Furthermore, two upregulated genes were identified that play an important role in the proline biosynthetic process: the delta-1-pyrroline-5-carboxylate synthase (*P5CS*) and the delta-pyrroline-5-carboxylate reductase (*P5CR*) (Appendix, Table

12). P5CS catalyzes the conversion of glutamate to glutamic-5-semialdehyde that in turn is able to convert to the intermediate delta-pyrroline-5-carboxylate (P5C). P5C is then converted to proline by P5CR (Verslues & Sharma, 2010). It has been shown, that proline accumulates in water stressed plants and seems to be important for the osmoregulation (Verslues & Sharma, 2010).

3.3 Early response to drought stress includes global re-orientation of histone modifications H3K9ac and H3K4me3

With the aid of the ChIP method followed by deep sequencing, drought-responsive changes in global distribution of the histone modifications H3K4me3 and H3K9ac could be detected. Both euchromatic marks, in contrast to heterochromatic mark H3K9me2, were associated with areas of active gene transcription, which in crop plants as barley are located at the ends of all seven chromosomes. A spatial distribution of these marks at open and transcriptionally active chromatin areas was already reported before for different plant species (Probst & Mittelsten Scheid, 2015). In general, H3K4me3 was found at twice as much genes as H3K9ac, which was also reported before for *A. thaliana* during developmental leaf senescence and in *Paulownia fortunei* (Brusslan et al., 2015; Yan et al., 2020). In addition, the majority of genes marked with H3K9ac (98, 4%) were simultaneously marked with H3K4me3 (see Ost et al. (2023), Fig. 3A). The strong coincidence of these both marks was also observed in *A. thaliana* (Roudier et al., 2011; Malapeira et al., 2012; Brusslan et al., 2015). However, the loading with H3K9ac was much more flexible and in contrast to the loading with H3K4me3, sensitively responded to development and to onset of stress. While comparison of the three samples (M0, M2 and D2) revealed that there is no major difference in the distribution of H3K4me3 in response to onset of drought, distribution of H3K9ac was clearly altered. This indicates that trimethylation of H3K4 is on one hand a widespread epigenetic mark in barley, but that on the other hand acetylation of H3K9, at least under the investigated early drought conditions, is a much more dynamic histone modification, sensitively reacting to environmental cues. Kim et al. (2008) showed that the acetylation of K9 at the drought-inducible gene related to Apetala2 (*RAP2.4*) occurred strongly already after 1 hour of drought treatment, whereas the trimethylation of H3 only accumulated later gradually. Based on their data on leaf senescence in *A. thaliana*, Brusslan et al. (2015) suggested that the H3K9ac mark appears before the trimethylation of K4, postulating a possible role for H3K9ac as a template for the H3K4me3 mark. In their review, Ueda and Seki (2020) discuss that a fast response to environmental stress via acetylation and a slower longer term response of methylation regarding flowering or stress memory could be beneficial.

The genes which specifically gain euchromatic H3K9ac marks in early drought stress comprise, besides genes involved in several metabolic processes, many stress-related genes, including genes involved in response to cold, light, salt and drought with several of them being involved in ABA-related stress-responses. This indicates that the early response to drought in the model crop plant *H. vulgare* involves higher-order regulation of expression of genes involved in abiotic stress responses via differential histone modifications. These findings are supported by the results of a genome-wide ChIP-sequencing in *B. distachyon*, where they could show that after onset of stress, the level of H3K9ac is increased at drought-responsive genes (Song et al., 2020). For barley, it could be shown, that the levels of H3K4me3 are increased at the Heat shock protein 17 (*HSP17*) whereas H3K9me2 is reduced (Temel et al., 2017). Recently it was shown that overexpression of the WHIRLY1 protein in drought-stressed barley lead to a decrease in H3K9ac and H3K4me3 levels at the ABA-related genes *HvNCED1* and *HvS40* which revealed its possible regulatory role towards drought stress responses by interacting with epigenetic regulators (Manh et al., 2023).

3.4 Genes loaded with euchromatic H3K9ac AND induced at early drought stress

ChIP-Seq analyses revealed that specific sets of genes were loaded with euchromatic mark H3K9ac already at the early stages of drought stress. To avoid the secondary effects of prolonged drought treatment, this work aimed to detect early responses to drought. An interesting set of genes was identified, loaded with euchromatic histone modifications in early drought conditions, corresponding to their respective upregulation. To identify these genes, RNA-Seq was performed with the same samples used for ChIP-Seq, comparing the transcriptome of drought-stressed plants with that of control plants. As expected under these early and mild drought stress conditions, RNA-Seq revealed a relative small number of DEGs. This result is not surprising, since barley is quite tolerant towards a dry environment comparatively to other crops (Tommasini et al., 2008; Cai et al., 2020). Intersection of the ChIP-Seq- and these RNA-Seq data revealed an interesting overlap of a small number of genes (Fig. 23). Intersection of epigenome and trancriptome data displayed that around 11% of the early upregulated genes were loaded with H3K9ac in response to onset of drought. A relative small overlap between RNA-Seq and ChIP-Seq data was also reported before. This could be also seen in drought-stressed maize, where only 25-30% of the genes labeled with increased H3K4me3 or H3K9ac were also upregulated (Forestan et al., 2020). ChIP-Seq and qRT-PCR analysis of PEG-6000 treated *B. distachyon* revealed 40 genes with increased H3K9ac level of which 23 depict elevated transcription levels (Song et al., 2020). Similar results could be seen in rice (Zong et al., 2013). In senescing *A. thaliana* leaves, 22% of the genes, that are upregulated during senescence are also gaining a trimethylation of K4 and only 2% of these genes show elevated H3K9ac marks (Brusslan et al., 2015).

Interestingly, about half of these genes loaded with euchromatic marks and being upregulated during the drought stress encode proteins involved in stress responses and ABA signaling. This indicates an epigenetic control level of a part of drought stress-induced reprogramming of gene expression via establishment of euchromatic marks. For example the Trypsin inhibitor (Bowman-Birk type, Plant protease inhibitor) was shown to play a role mainly in host defense, but newer results indicate also a possible role in drought tolerance (Zhang et al., 2008; Vaseva et al., 2016; Malefo et al., 2020; Herwade et al., 2021). Cytochrome P450 (CYP), which shows a clear enrichment in H3K4me3 (Table 8), is an oxidoreductase enzyme which catalyzes NADPH- and/or O2-dependant hydroxylation reactions (reviewed in Pandian et al., 2020). Although, CYPs represent around 1% of the protein coding sequences, little is known about the biological functions of most of the CYPs (Tamiru et al., 2015). So far, it is known, that ABA 8'-hydroxylases belonging to the CYP707A family control the ABA concentration during stress, which could be shown for barley (Millar et al., 2006), soybean (Zheng et al., 2012) and other plants. Recently, it was revealed that a complex of Histone Deacetylase 9 (HDA9), the protein Powerdress (PWR) and ABA INSENSITIVE 4 (ABI4) regulates the expression of *CYP707A1* and *CYP707A2* genes epigenetically through histone deacetylation (Ali & Yun, 2020; Baek et al., 2020; Khan et al., 2020).

During drought, five genes belonging to the MYB family are significantly upregulated (logFC= 2.3-5.3) and two of them are associated with changes in histone modifications during drought: a MYB factor and a MYB related transcription factor. The MYB gene family presents a large group of genes that mainly act as transcription factors with a diverse set of functions (reviewed in Baldoni et al., 2015; Roy, 2016). Regarding drought, the gene *NbPHAN*, a transcription factor with a MYB domain from *Nicotiana benthamiana,* is involved in leaf development and plays a putative role in ABA-independent drought tolerance pathways (Huang et al., 2013). In case of epigenetic regulation of MYB transcription factors, little is known so far, but it could be shown that one MYB transcription factor in soybean (*Glyma11g02400*) is associated with H3K4me3 in upcoming salinity stress (Song et al., 2012).

The trimethylation of H3K4 at the MYB factor is more enriched at the gene body than at the promotor region. Overall, the breadth of the H3K4 trimethylation mark seems to be broader than the breadth of the H3K9ac mark (Fig. 9 and 22). It could be shown in mammalian cells, that broad-spreaded H3K4me3 often marks genes that are important for cell identity and function (Benayoun et al., 2014). Genome-wide studies of H3K9ac and H3K4me3 during developmental senescence in *A. thaliana* revealed that H3K4me3 marks covered nearly two times the gene area than H3K9ac marks. The genes with the broadest H3K4me3 coverage were assigned to the GO term photosynthesis (Brusslan et al., 2015). Van Dijk et al. (2010)

discovered atypically broader H3K4me3 distribution profiles at dehydration and ABA- inducible genes in a genome-wide ChIP-seq study in *A. thaliana*.

Two more genes, which were described as positive regulators in ABA signaling are the COP1-interacting-like protein (Ren et al., 2016) and the Isoprenylcysteine alpha-carbonyl methylesterase (ICME) (Huizinga et al., 2008). Both of these genes depict enhanced acetylation in drought, especially at the ATG region of the gene.

3.5   PP2Cs are associated with H3K9ac in drought

As described in the last chapter, about half of the genes loaded already during early stress response with euchromatic marks and being upregulated during the drought stress encode proteins involved in stress responses and ABA signaling. Among them are two MYB or MYB-related transcription factors, cytochrome P450, the sugar transporter SWEET and the PP2Cs involved in drought stress signaling (Millar et al., 2006; Baldoni et al., 2015; Gong & Yang, 2022). Interestingly, two members of the PP2C family, involved in the central ABA signaling module (Soon et al., 2012), were also already significantly upregulated and loaded with H3K9ac.

The regulation of PP2C genes was further investigated, including the later stages of drought stress. Among the 26 annotated PP2C genes associated with H3K9ac in drought, seven were upregulated, with two of them showing significant upregulation at early phases, indicating that several PP2Cs, being central regulators in ABA signaling after the onset of drought, are loaded with euchromatic marks and thus upregulated. Moreover, comparison of the TPM expression values and the signal enrichment of H3K9ac revealed a correlation between the expression and the acetylation of several *PP2C* genes. *PP2Cs* with higher transcript levels in D2 depict also a stronger acetylation in D2, emphasizing the activating role of K9ac in gene expression (Brownell & Allis, 1996; Tian et al., 2005; Zhou et al., 2010). Interestingly, six of the seven top K9ac-enriched *PP2Cs* are belonging to the clade A. Recent phylogenetic and transcriptomic studies in Tibetan hulless barley revealed, that most of the upregulated *PP2Cs* during dehydration stress belong to the clade A or F (Liang et al., 2022). Similar results were seen in maize, where a majority of the tested clade A *ZmPP2Cs* are induced either under drought or ABA treatment (Xiang et al., 2017; He et al., 2019). Upregulation of the PP2C-As *ABI1* and *ABI2* during stress conditions (salt-, drought-, osmotic stress) and downregulation of the ABA receptors *RCAR3* and *RCAR10* in *A. thaliana* leads to the suggestion, that higher PP2C levels desensitize the plant to high ABA levels in a negative feedback loop mechanism (Szostkiewicz et al., 2010; Fuchs et al., 2013; Singh et al., 2016). In confirmative experiments it was concluded, that an increased PP2C:PYR/PYL ratio is important for the activation of the

downstream ABA signaling cascade (Chan, 2012). Similar results could be also shown in barley (Seiler et al., 2014).

Earlier, it has been shown in barley, that several members of the *PP2C* and *SnRK2* gene family are upregulated during stress, whereas six members of the *PYR/PYL* gene family either show no expression under short-term stress or even a downregulation in prolonged water stress in wild type barley (Seiler et al., 2014). Bashkara et al. (2012) observed that the clade A PP2C, *Highly ABA-induced1 (HAI1),* was strongly induced under low water potential and in parallel showed limited binding interaction to the PYL receptors resulting in HAI1 remaining active. Recently, it could be shown, that the *PP2C* gene transcription is repressed by the MYB transcription factor AtMYB44 which recruits histone deacetylases by building a complex with other repressors (Nguyen et al., 2019; Jung et al., 2020). Under salt stress conditions, AtMYB44 vanishes from the promotor and acetylation of H3K9 and trimethylation of H3K4 increase, resulting in the transcription of the *PP2C* gene.

RNA-Seq analyzes of the *PP2C (5HG0392330)* shows a not significant upregulation (logFC= 4.9, padj=0.07) in drought whereas qRT-PCR analysis could confirm an upregulation in D2 and an increasing gene expression in the ongoing drought stress (D3 and D4). Similar to the other *PP2Cs* being upregulated during stress and showing enhanced acetylation in D2, the *PP2C* gene shows a strong enrichment of H3K9ac but also H3K4me3 at the promotor region and the gene body in D2. BLAST analysis revealed a homology to the rice PP2C *OsPP108/OsPP2C68*, which is highly upregulated under ABA, salt and drought stress and overexpression of this PP2C in rice leads to ABA insensitivity and elevated tolerance to drought, salt and mannitol stress (Singh et al., 2015).

3.6 The barley methylome appears to be relatively unaffected during early drought stress events

To obtain a sufficient coverage of the barley genome, multiple sequencing is necessary for usable results. In this work, every replicate has been sequenced three times, resulting in a sufficient number of reads (Table 10). The mapping rates range between 50.8 and 54.9% and the average sequencing depth of the genome comprises 2x and 6x coverage. Experiments with human brain cells lead to the conclusion, that a sequencing depth of 5x-15x of the genome is sufficient for the analysis of differential methylated regions (DMRs) (Ziller et al., 2015). The fairly low mapping rates and coverage of the barley genome leads to a more complicated analysis and the informative value of the results should be handled and interpreted with caution. PCA depicts a high similarity between two M2 and two D2 samples, while two other samples, D2_Rep1 and M2_Rep2, are more distant to the others. A heatmap of the methylation showed no obvious difference in general methylome between drought stress and

control. The methylation levels between M2 and D2 for all three contexts depict no major differences, resulting in an only small number of DMRs and associated DMGs. These results lead to the conclusion that the methylome of barley remains rather stable at the early phase of drought stress, showing no significant changes in the CG, CHG and CHH methylation context. The distribution of the methylation levels of CG, CHG and CHH context over the genes is similar to the methylation level distribution in other plants, e.g., populus, rice and mungbean (Liang et al., 2014; Garg et al., 2015; Zhao et al., 2022). Comparison with the transcriptome data revealed only one overlapping gene, a Trypsin inhibitor. Two studies in *A. thaliana*, one with mild- and the other with slow-onset of drought stress revealed no robust/significant correlation between drought-mediated changes in differentially methylated regions and drought-induced changes in the gene expression (Ganguly et al., 2017; Van Dooren et al., 2020). Although, the studies mainly examined transgenerational effects of drought stress on DNA methylation, the changes in DNA methylation in one generation were not that prominent. Furthermore, for mild-stressed *A. thaliana* plants no global change in the methylation levels for CG, CHG and CHH context could be observed between control and drought. On the other hand, multiple studies report methylome changes due to drought stress. Garg et al. (2015) showed that there are prominent differences in the methylation status between three different rice cultivars in response to stress. Interestingly, despite finding a significant enrichment of differentially expressed genes that are linked to hyper- or hypo-methylated DMRs, the majority of identified DEGs showed no correlation. These findings are supported by the research of Wang et al. (2016), who detected that only a small number of DMGs between two rice genotypes in drought shows different expression levels. Furthermore, one of the rice genotypes, which is drought-tolerant, depicts much less DMRs in comparison to the drought-sensitive cultivar, suggesting a more stable methylome for drought-tolerant rice genotypes. Similar result could be shown in maize with two drought-sensitive and two drought-tolerant lines (Wang et al., 2021). It has to be noted that methylome changes during drought detected in these studies are between different lines or cultivars. In the present work, the comparison is in between the same cultivar leading to less profound differences in DNA methylation.

As mentioned earlier, around 5% of the *A. thaliana* genes are methylated in the promotor region and nearly one third exhibit gene body methylation (Zhang et al., 2006; Zilberman et al., 2007; Zhang et al., 2018). As a result of the small number of promotor methylations, it is suggested that DNA methylation regulates only a small portion of *A. thaliana* genes (Matzke & Mosher, 2014; Zhang et al., 2018). Plants with a larger genome, especially crops, tend to have more repetitive DNA (Flavell et al., 1974; SanMiguel et al., 1996). By shotgun sequencing BAC clones, Mascher et al. (2017) generated a map-based reference sequence for the barley genome. For the annotation of repetitive elements, a Triticeae-specific repeat library was used

(Wicker et al., 2002) and 3.7 Gb (80.8%) of the genome were classified as transposable elements. A global drought stress study in barley leaves and roots, using the methylation-sensitive amplification polymorphism (MSAP) method followed by sequencing, revealed that changes in the DNA methylation pattern due to the stress treatment were 65% related to the gene body and only 35% in the promotor region independent of root or leave tissue (Chwialkowska et al., 2016). These findings are contrary to this research. The reason might be that barley plants in both investigations had different levels of drought stress. Of all 754 identified differentially methylated genes, 598 genes (79.3%) are methylated in the promotor region and only 156 (20.7%) in the gene body.

3.7 Conclusion

Barley has developed complex mechanisms to adapt to drought stress. One of these mechanisms involves histone modifications, particularly H3K9 acetylation, that leads to the up-regulation of specific genes (Fig. 33). It is shown, that already in the early phase of drought stress, when chloroplasts are still active, a specific set of genes is loaded with H3K9ac and upregulated. Among these genes are ABA-related genes, e.g., genes encoding *PP2Cs* involved in the central regulatory unit of ABA action. These results indicate that in response to drought the H3K9ac mark works in a more flexible manner in comparison to the trimethylation of H3K4, suggesting a potential role of H3K9 acetylation in the short-stress memory of plants, as discussed by Ding et al. (2012), Kim et al. (2012), Lämke et al. (2016) and Asensi-Fabado et al. (2017). Furthermore, our results support the findings of Brusslan et al. (2015), which propose that H3K9ac can act as a template for the trimethylation of H3K4. On the other hand, the barley methylome appears to be relatively stable under the onset of drought stress and no apparent linkage between histone modification patterns, transcriptomic changes and the DNA methylation pattern has been observed.
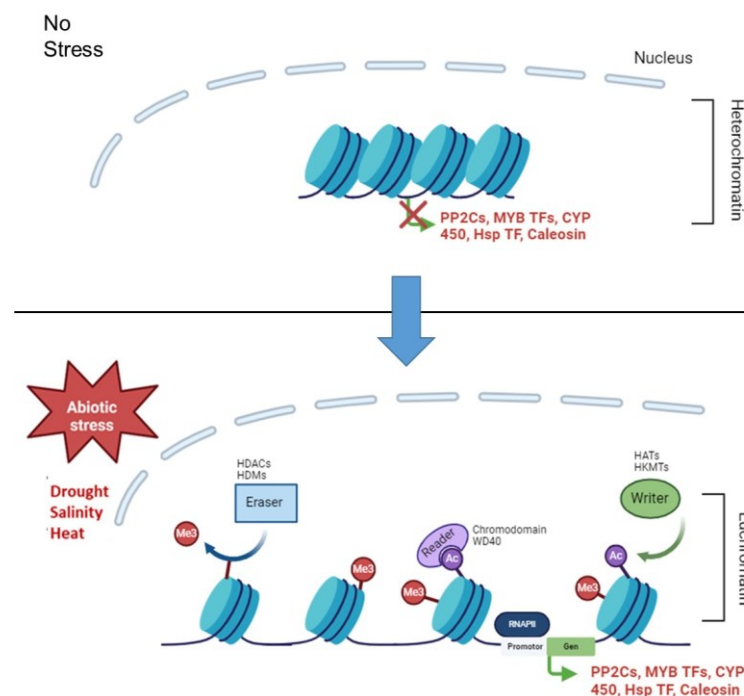
Figure 33. Working model of the changes in histone modifications and chromatin structure during abiotic stress. Shown are the histones modified with H3K4me3 (green circles with "Me3") and H3K9ac (blue circles with "Ac") in the nucleus. Due to an abiotic stimulus (e.g., drought, salinity or heat), enhanced trimethylation of H3K4 and acetylation of H3K9 occur at the histones, resulting in an open chromatin structure. In this state, RNA polymerase II (RNAPII) gains access to the DNA at the promotor region, enabling the transcription of abiotic stress response genes, including PP2Cs (protein phosphatase 2C), MYB TFs (MYB-related transcription factors), CYPs (cytochrome P450) and Heat shock TF (heat shock transcription factor). Created with BioRender.com

4 Material and Methods

4.1 Chemicals

The used chemicals were obtained from following companies: AppliChem GmbH (Darmstadt, Germany), Biozym Diagnostics GmbH (Hessisch Oldendorf, Germany), Calbiochem®, Carl Roth GmbH & Co. KG (Karlsruhe, Germany), Duchefa Biochemie B.V. (Haarlem, Netherlands), MBI Fermentas, Merck Eurolab HmBH, Roche Diagnostics GmbH (Mannheim, Germany), Sigma-Aldrich GmbH (owned by MerckKGaA, Darmstadt, Germany), Th. Geyer GmbH & Co. KG (Renningen, Germany), Qiagen GmbH (Hilden, Germany). All buffers and solutions were made with demineralised and autoclaved water (TKA GenPure; Thermo Electron LED).

4.1.1 Kits

For the purification of the DNA of the chromatin immune precipitation the Nucleospin-Extract II-Kit of Macherey & Nagel (Düren, Germany) was used. For the isolation of the RNA for the RNA sequencing the RNeasy Plant Mini Kit from Qiagen (Hilden, Germany) was used. The isolation of the DNA was carried out with the DNeasy Plant Mini Kit of Qiagen (Hilden, Germany). The transcription of the RNA into cDNA occurred with the RevertAid RT Reverse Transcription Kit from Thermo Fischer Scientific (Massachusetts, USA). The antibodies were distributed from Abcam (Cambridge, UK).

Antigen (primary)	Host	Clonality	Producer
H3K9me2	mouse	monoclonal	Abcam (ab1220)
H3K9ac	rabbit	polyclonal	Abcam (ab10812)
H3K9me3	rabbit	polyclonal	Abcam (ab8580)

4.1.2 DNA-Ladder

The DNA-Ladder from Fermentas (Thermo Fisher Scientific, Massachusetts, USA) was used.

4.1.3 Oligonucleotides

The used primers were provided by Eurofins Genomics (Ebersberg, Germany). The Primer were designed with the Primer3web v4.1.0 software (Kõressaar & Remm, 2007; Untergasser et al., 2012; Kõressaar et al., 2018), the NCBI primer blast tool (Ye et al., 2012) and checked with the IPK Galaxy Blast Suite on the Galaxy platform (Jalili et al., 2021). The primers and their corresponding sequences are listed in the Appendix, Table 16.

4.2 Plant material and growth under drought stress conditions

Barley (*H. vulgare* cv. Morex) seeds, obtained from IPK Gatersleben (OT Gatersleben, Seeland, Germany), were incubated for 72 h at 4 °C in darkness, followed by 24 h at room

temperature on wet tissue paper. Germinated seedlings were sown as described by Temel et al. [58] with slight modifications. Fifty Mitscherlich pots, each containing 12 seedlings and 1.5 kg ED73 soil (Einheitserdewerke Werkverband e.V., Sinntal-Altengronau, Germany), were placed in a greenhouse cabinet and grown under long-day conditions (16 h light, 23° C/8 h dark, 18 °C, light intensity 100 µmol m^{-2} s^{-1} and 45–50% relative humidity). On the twelfth day after sowing (das), the water for half of the pots was withheld to induce drought stress, while the other half served as the control group and was watered. Every two days, the pots were rotated around the cabinet, weighed to calculate the soil water content, and physiological parameters were measured. The experiment was performed eight times. For RNA expression analysis, RNA-sequencing and Bisulfite-treatment, primary leaves were harvested, frozen in liquid nitrogen and stored at −80 °C. For the Chromatin immunoprecipitation (ChIP), 1 g of primary leaves was harvested and fixed with formaldehyde before being frozen in liquid nitrogen and stored at −80 °C.

4.3 Documentation on the physiological parameters

To examine the process of the developmental and drought stress induced leaf senescence the relative chlorophyll content and the PSII efficiency were measured every second day.

4.3.1 Measurement of the relative chlorophyll content

The relative chlorophyll content and the PSII efficiency were measured every second day between 7 and 47 das. The relative chlorophyll content was measured using the SPAD (Soil Plant Analysis Development) tool from Minolta (Konica Minolta Sensing Europe B.V., Munich, Germany). The relative chlorophyll content of 20 primary leaves from 20 plants was measured at the top, middle and bottom of the leave, and the mean value was calculated. Each data point represents the mean of at least five biological replicates.

4.3.2 Measuring of the chlorophyll fluorescence as dimension for the PSII efficiency

The chlorophyll fluorescence is the difference between the maximum (Fm) and minimum (F0) fluorescence and is called variable fluorescence (Fv). The PSII efficiency was calculated using the following formula: (Fm − Fo)/Fm = Fv/Fm. Leaves were dark adapted for 10 min, and PSII efficiency was measured using the MINI-PAM fluorometer (Walz GmbH, Effeltrich, Germany).

4.3.3 Definition of the developmental stages

For the comparison of the different approaches, stages of development based on the relative chlorophyll content were defined. M0 as the control stage with the maximum relative chlorophyll content were set as 100%. S1/D1 marked the stage with 5% less chlorophyll content in which **S**1 corresponds to the time point of developmental **s**enescence and **D**1 the time point in the **d**rought stress plants. At the S2/D2 stage the chlorophyll content is 10% less,

at this stage, the sample for the RNA- and ChIP-Seq were taken. S3/D3 have a chlorophyll content of 75%, S4/D4 of 50%. In the last stage (S5/D5) the chlorophyll content is 25%.

4.4 Sampling

For the isolation of total RNA and DNA, 5-7 primary leaves were taken starting at 7 das in two-day intervals and flash frozen at -80 °C until usage. For the ChIP, samples were taken at the M0, M2 and D2 stages, crosslinked with formaldehyde and frozen at -80 °C until usage.

4.5 Isolation of nucleic acids

4.5.1 Trizol method

The primary leaves which were frozen in liquid nitrogen were pestled in a mortar to fine powder. Around 100 mg of the powder were mixed with 1 ml heated TRIzol (60 °C), vortexed and incubated for 5 min at 60 °C. After a ten-minute centrifugation step at 4 °C and 13000 rpm the supernatant was transferred into a new tube and mixed with 200 µl chloroform. The mixture was vortexed strongly for 1 min and incubated at room temperature for 5 min. After the centrifugation step (15 min, 13000 rpm, 4 °C), the aqueous upper layer was carefully taken to a new tube and mixed with 250 µl 0,8 M Na-Citrate/ 1,2 M NaCl-solution and 250 µl Isopropanol. After 10 minutes of incubation at room temperature, the mixture was centrifugated 10 minutes at 13000 rpm and 4 °C. The supernatant was discarded and the pellet was washed with 70% ethanol for 5 min at 13000 rpm. The pellet was dried for 2 min at 60 °C and resuspended for 10 minutes at 60 °C in 100 µl DEPC-H_2O. For an optimal purification of the RNA a second precipitation with 10 µl 4M NaCL solution and 220 µl pure Ethanol was carried out. After a 10-minute incubation at room temperature and 10 min centrifugation the pellet was washed and dried and resuspended in 20-50 µl DEPC- H_2O depending on the size of the pellet. The concentration was measured with the NanoDrop (Thermo Fisher Scientific, Massachusetts, USA).

4.5.2 Isolation of genomic RNA

For the isolation of RNA for the sequencing the RNeasy Plant Mini Kit from Qiagen (Hilden, Germany) was used with minor changes. At the beginning of the isolation the TRIzol method was used until the separating of the phases with the aid of chloroform. The upper aqueous layer was taken and mixed with 0.5 volume Ethanol and afterwards given on the pink column of the Rneasy Kit and followed the protocol steps.

4.5.3 Isolation of genomic DNA

For the DNA isolation the DNeasy Plant Mini Kit from Qiagen (Hilden, Germany) was used according to the manufacturers guidelines.

4.6 Chromatin immunoprecipitation (ChIP)

The Chromatin Immunoprecipitation (ChIP) was carried out after Ay et al. (2015) with some minor modifications.

4.6.1 Sampling and crosslinking

For every time point (M0, M2, D2), 4 g of barley primary leave material were harvested. The leaves were mixed with crosslinking-buffer (0.4 M saccharose, 10 mM Tris-HCl pH 8, 1 mM EDTA, 1 mM PMSF) and 1% formaldehyde and the samples were put under pressure (18-20 mmHg) for 10 minutes in the vacuum dryer filled with ice. The reaction was stopped by giving 0,1 M glycine solution to the samples and putting again a pressure of 18-20 mmHg for 5 minutes on the samples. The reactions were made on ice and during the pressure treatment, the samples were shaken. Afterwards the samples were washed and frozen at -80 °C until usage.

4.6.2 Chromatin isolation and fragmentation

One gram of leave material was grinded and mixed with an extraction buffer (0.4 M saccharose, 10 mM Tris-HCl pH 8, 10 mM $MgCl_2$,5 mM ß-Mercaptoethanol, 0.05 mM PMSF, protease-inhibitor-cocktail). After filtering through Miracloth® (Merck Millipore, Massachusets, USA) the mixture was centrifuged for 20 minutes at 4 °C and 13000 rpm. After discarding the supernatant, the pellet was resuspended in 1 ml of extraction buffer (0.25 M saccharose, 10 mM Tris-HCl pH 8, 10 mM $MgCl_2$, 1% TritoX-100, 5 mM ß-Mercaptoethanol, 0.1 mM PMSF and proteinase-inhibitor-cocktail) and centrifuged for 10 min at 4 °C and 13000 rpm. The resulting pellet were resuspendend in 300 µl extraction buffer (1.7 M saccharose, 10 mM Tris-HCl pH 8, 2 mM $MgCl_2$, 0.15% Triton X-100, 5 mM ß-Mercaptoethanol, 0.1 mM PMSF, protease-inhibitor-cocktail) and layered in a new eppendorf tube on 300 µl of the same buffer, followed by a 1-hour centrifugation step at 4 °C and 13000 rpm. After discarding the supernatant, the pellet was resuspended in 500 µl cold cell nuclei lysis buffer (50 mM Tris-HCl pH 8, 10 mM EDTA, 1% SDS, 0.1 mM PMSF). The sonication of the chromatin was conducted with a Covaris Sonicator M220 for 5 min (W 10; PP 50; C/B 200; T 6 °C). After sonication the samples were frozen at -80 °C until usage.

4.6.3 Pre-clearing and immune precipitation

134 µl of protein G sepharose beads were pipetted into a 15 ml falcon and washed three times with 3,35 ml ChIP dilution buffer. Inbetween they were centrifuged for 30 seconds at 4500 rpm and 4 °C to pellet down the beads. The chromatin solution was given to the beads in volume ration of 1:10 and incubated for 1 hour on a rotating wheel. After a one-minute centrifugation step at 4 °C and 45000 rpm the supernatant was split into several samples with a volume

around 600 µl. 10 µg of antibodies were given to each aliquot except for the input samples. The incubation was over night at 4 °C at the spinning wheel.

4.6.4 Collection, washing and elution of the immune complexes

For each sample 45 µl Protein G Sepharose Beads were three times equilibrated with ChIP dilution buffer (1.1% Triton X-100, 1.2 mM EDTA, 16.7 mM Tris-HCl pH 8, 167 mM NaCl). After every washing step the beads were pelleted for 30 seconds at 4 °C and 5000 rpm. After putting the chromatin solution to the beads, except for the input samples, the samples rotated for 3 hours at the rotator. Afterwards the sample were centrifuged for 30 seconds at 2500 rpm and the supernatant was discarded. In the following order 1 ml of washing solution was given to the beads, rotated for 10 minutes and centrifuged for 30 seconds at 4 °C and 2500 rpm: low salt buffer (150 mM NaCl, 0.1% SDS, 1% Triton X-100, 2 mM EDTA, 20 mM Tris-HCl pH 8), high salt buffer (500 mM NaCl, 0.1% SDS, 1% Trition X-100, 2 mM EDTA, 20 mM Tris-HCl pH 8), LiCl washing buffer (0.25 M LiCl, 1% Nonident P-40, 1% Desoxycholate sodium salt, 1 mM EDTA, 10 mM Tris-HCl pH 8) and twice TE buffer (10 mM Tris-HCl pH 8, 1 mM EDTA). For elution of the immune complexes, hot (65 °C) elution buffer (1% SDS, 0.1 M $NaHCO_3$) was given to the samples and the mixtures were vortexed for 15 minutes at 65 °C. Afterwards the samples were centrifuged for 30 seconds at 13000 rpm. This procedure was conducted two times and the eluates were combined.

4.6.5 Reverse Crosslinking

For reverse crosslinking 20 µl of 5 M NaCl was given to the samples (including the inputs) and shaken overnight at 65 °C.

4.6.6 Proteinase K-digestion and DNA clean-up

50 µl 0, 1 M EDTA-solution, 10 µl 2 M Tris-HCl buffer (pH 6,5) and 1 µl Proteinase K (20 mg/ml) were given to the samples and incubated for 3 hours at 45 °c while slightly shaking. Afterwards the DNA was purified with the Nucleospin extraction II kit from Macherey & Nagel (Düren, Germany). Instead of NT buffer NTB buffer was used. Furthermore, the elution was repeated twice with 77 µl of elution buffer. The DNA concentration were measured with a Qubit.

4.6.7 Precipitation of the DNA samples

In order to concentrate the samples, the DNA samples were split up in two samples each 600 µl and 1/10 volume of 3 M sodium acetate (pH 5.2) and 2 volumes of cold ethanol (100%) were added to the DNA samples. The samples were incubated 20 minutes on ice and then centrifuged for 20 minutes at 4°C and 14000 rpm, followed by a five-minute washing step with 150 µl ethanol (80%). After drying the pellet, the DNA was resuspended in 27 µl of elution

buffer (EB) from the Nucleospin extraction II kit from Macherey & Nagel (Düren, Germany). The two samples were combined to an end volume of 54 µl.

4.7 Library preparation and sequencing

The preparation of the libraries and the sequencing for the ChIP-, the RNA- and the Bisulfite-sequencing was done at IPK Gatersleben (OT Gatersleben, Seeland, Germany). All the leaf material for the three different sample preparations was taken at the same time points and from the same pots. The samples for the RNA- and Bisulfite-Sequencing were from the same leaf material.

4.7.1 Preparing the libraries for sequencing

The ChIP DNA (three independent replicates) samples were processed with the Illumina TruSeq ChIP Library Preparation Kit (Illumina Inc., San Diego, CA, USA). Library preparation for the RNA-Seq (three independent replicates) was undertaken with the Illumina TruSeq RNA Library Preparation Kit (Illumina Inc., San Diego, CA, USA). The DNA samples for Bisulfite sequencing (three independent replicates) were denatured and bisulfite converted with the EZ DNA Methylation-Gold Kit from ZymoResearch (California, USA). The libraries for sequencing were prepared with the ACCEL-NGS® METHYL-SEQ DNA LIBRARY KIT (Swift Biosciences, IDT, Iowa, USA). All the library preparations were conducted according to the manufacturer guidelines.

4.7.2 Next Generation Sequencing

The libraries resulting from the ChIP- and RNA experiments were sequenced (paired-end, 2 x 101 cycles) on the Illumina HiSeq2500 device (Illumina Inc., San Diego, CA, USA). The bisulfite samples were sequenced with the NovaSeq 6000 (Illumina Inc., San Diego, CA, USA).

4.8 cDNA-Synthesis and quantitative Real-Time PCR

With the RevertAid™ H Minus First Strand cDNA Synthesis Kit (Thermo Fisher Scientific, Waltham, MA, USA), 1 µg of total RNA was transcribed into cDNA following the manufacturer's instructions. For qRT-PCR, 2 µL of cDNA template was mixed with 5 µl of KAPA SYBR fast qPCR Mastermix (KAPA Biosystems, Inc., Wilmington, Massachusetts), 2.2 µl DEPC-treated water and 0.4 µl of the gene-specific primers (Appendix, Table 16). To exclude the amplification of unspecific products, a no RT (reverse transcriptase) control was additionally run. Quantitative RT-PCR was performed using the CFX Connect Real-Time PCR Detection System from Bio Rad (Bio-Rad Laboratories Inc., Göttingen, Germany). For each sample, three dilution series (1:4, 1:16, 1:64) were used. For the determination of the relative gene expression, the REST-384 ©2006 software v2 (Pfaffl, 2002) was used with genes *HvActin*,

HvPP2A and *HvGCN2* (constant expression under control and drought conditions*)* as reference genes for normalization.

4.9 Measuring of the concentrations

In general, all DNA and RNA concentrations were measured using a nanospectrophotometer (NanoPhotometer® NP80, Implen, Munich, Germany). Samples for sequencing were additionally measured with the Bioanalyzer2100 system (Agilent Technologies, Santa Clara, CA, USA) using the RNA 6000 pico kit and the HS DNA kit (Agilent Technologies, Santa Clara, CA, USA) and with a Qubit 4 Fluorometer (Thermo Fischer Scientific, Waltham, MA, USA).

4.10 Validation of RNA-Seq and ChIP-Seq results

To validate the detected peaks, quantitative real-time PCR of the ChIPed-DNA was performed with five different gene-specific primer sets (Appendix, Table 16). To normalize the ChIP-qPCR data, the percent input method was used as described in Solomon et al., 2021. The adjusted input was calculated from the log2 of the 10% starting chromatin which was used as the input for the ChIP. The Ct values of three independent qRT-PCR were used. For the validation of the RNA-Seq, six different genes were chosen from the DEG list and qRT-PCR were performed as described in 4.8.

4.11 Bioinformatic analysis and Data Bank Research

4.11.1 Bioinformatic analysis of the Chromatin Immunprecipitation followed by sequencing (ChIP-seq)

The output of the paired-end sequenced DNA and RNA samples were provided in a compressed FASTQ format (fq.gz). The analysis of the sequenced data was accomplished in cooperation with the IPK Gatersleben who provided a specific workflow.

4.11.2 Read alignment

In a first step, the Illumina adapters, which were fused to the DNA fragments beforehand, were trimmed with the tool cutadapt v1.12 (Martin, 2011) with reads shorter than minlen=30 after trimming were discarded. Subsequently, the trimmed reads were aligned to the reference Morex genome V2 (Mascher, 2019; Monat et al., 2019) with BWA-MEM v0.7.15 (Li & Durbin, 2010; Li, 2013), using the default parameters. The output files in SAM (Sequence Alignment/Map) format were converted into BAM format with SAMtools v1.3 (Li et al., 2009) and the files were sorted. PCR and optical duplicates were removed by the tool Novosort (http://www.novocraft.com/documentation/Novosort-2/, V3.06.05). The complete command run in parallel (Tange, 2011).

4.11.3 Peak calling with MACS2

To quantify the regions that are enriched in reads, the software MACS (Zhang et al., 2008) were used, to be more specific, the advanced release MACS2 v2.1.1. MACS2 expects inputs in BED, BAM/SAM or BEDPE/BAMPE format. For the analysis, the BED format was choosen as an input. With BEDTools v2.26.0 (Quinlan & Hall, 2010) the BAM files were converted to BED files, while reads with a mapping quality below minqual=20 were discarded. In order to use the MACS2 command callpeak, in a first step the d- or fragment size from the alignment for the immunoprecipitated sample (IP) and the Input has to be calculated. The mean value of both values were taken and set as --extsize. The mappable genome size of barley is g = 4833791107. Following parameters were set in the command: -p: 1e-2, --shift 0, --keep-dup all, --seed 12345. For the histone modification H3K9me2, the additional argument -- broad were set.

4.11.4 Pooled peak calling with MACS2 and stricter parameter setting

For the pooled peak calling all the BED files from every replicate for each time point were taken with the corresponding input files and the peaks were identified. The –extsize was set as the mean from all calculated fragment sizes of the single files. After discarding replicate 4, BAM-files were used for pooled peak calling using the q-value set to 0.05. The resulting peaks were filtered by cutting off all peaks with a fold enrichment smaller or equal to 10.

4.11.5 Gene annotation

One of the MACS2 output files is an excel tabular file with the called peaks and contains information about chromosome name, start/end position of peak, length of peak et cetera. This peak list was converted into a BED file. With the tool BEDTools v2.29.0 and the intersect command, overlaps between the ChIP-Seq peak region lists and the gene region lists were generated. The gene region lists contain the gene body list, which is the genomic sequence between start and stop codons of high-confidence (HC) genes; the ATG list, which contains the 250 bp upstream and downstream regions of start codons and the PROMOTOR list, which contains the 1000 bp upstream regions of start codons. Text files as outputs were generated.

4.11.6 Generating bigWig files with deepTools

The sorted BAM files, resulting from the read alignment in 4.11.2, were filtered with the SAMtools view command. In a next step, the sorted, filtered bam files were indexed in CSI format using SAMtools index. With the software deepTools (Ramírez et al., 2014) and the argument bamcompare, bigWig tracks were generated using the default settings.

4.11.7 Building signal tracks of the histone modification enrichment levels of the MACS2 output file

Signal tracks of the histone modification fold enrichment were generated with the MACS2 bdgcmp command with following settings: –m FE and –p 0.0001. As inputs, the treatment pileup signal file and the lambda control file, resulting from the MACS2 callpeak-command, were used to create a bedGraph file containing the fold enrichment.

4.11.8 Generation bigWig files with UCSC bedGraphToBigWig

The bedGraph files were uploaded on the Galaxy web platform (Afgan et al., 2018). Files in the bedGraph format can be converted into a bigWig track with the bedGraphToBigWig converter of the UCSC genome browser, which is imbedded on the Galaxy platform. The converted tracks were downloaded and visualized in IGV (Integrative Genomics Viewer) (Robinson et al., 2011).

4.11.9 Peak distribution around the genes with deepTools scale-regions and plot heatmap

To plot the peak distribution over the signal track profiles of the genes in combination with their expression level, the software deepTools (Ramírez et al., 2014) were used. Based on the transcriptomic analysis via RNA sequencing, the genes associated with a peak were sorted on their corresponding TPM values into mid/high-, low- and zero expression classes. The resulting list of genes were converted into a count matrix followed by creating a density plot of the reads around the transcription start site (TSS)/start codon and the transcription end site (TES) with the deepTools commands scale-regions and plotProfile with a window size of 500 bp before the TSS and after the TES and a region body length of 1000 bp.

4.12 GO enrichment analysis with TRAPID

The GO term enrichment analysis was executed using the TRAPID software v2.0 (Bucchini et al., 2021), and the maximum q-value was set to 0.05. The enrichment bubble plots were plotted using http://www.bioinformatics.com.cn/srplot (accessed on 1 April 2023), an online platform for data analysis and visualization.

4.13 Bioinformatic analysis of RNA-Seq

The workflow for the analysis of the RNA-Seq data were provided by IPK Gatersleben. The raw RNA-Seq output files were handed out in compressed FASTQ format (paired-end).

4.13.1 Quantifying transcript abundance with kallisto

First, a list of all sample directories were generated. Before using kallisto v0.45.0 (Bray et al., 2016) for pseudo alignment, it is important to create an index for the reference sequence (FASTA format). The kallisto command were executed with the default parameters, except for

bootstrap-samples, which was set to 40. The TPM values and read counts for every gene in every sample were calculated by the kallisto software (abundance data).

4.13.2 Setting up a sample information table

The information about the samples (sample ID, stage, treatment, replicate number, sample name) were put together in a table, which was saved in Excel and R format.

4.13.3 Importing and analyzing the kallisto results in R

The resulting abundance data from the kallisto pseudoalignment were imported into R v3.5.1 (R core Team, 2014) for statistical analysis. Therefore, packages from R were used for further analyzes including data.table (https://cran.r-project.org/web/packages/data.table/), parallel and openxlsx (Schauberger et al., 2020) (https://CRAN.R-project.org/package=openxlsx).

4.13.4 Normalization with edgeR and limma

The synthetic ERCC spike-ins (Jiang et al., 2011), which were used for the RNA-Seq samples, were dismissed as well as genes with less than 5 counts across all samples. The following steps for data normalization were executed by the R packages edgeR (McCarthy et al., 2012; Robinson et al., 2010) and limma (Ritchie et al., 2015), both available from the Bioconductor project (Gentleman et al., 2004). After formatting the expression matrix, the matrix was converted to edgeR DGEList object and normalization factors regarding differences in the total read count between the samples were calculated with calcNormFactors. Subsequently, an experimental design matrix was set up with the factor 'treatment'. With the aid of the voom (variance modeling at the observational level) function (Law et al., 2014) from the limma package, the mean-variance relationship of the RNA-Seq data (log-)counts were calculated. The counts were joined at the gene and sample level.

4.13.5 Analysis of differential gene expression

The previous set up design matrix were fit to the voom-transformed count matrix using lmFit. A contrast matrix for comparing the drought stress samples with the control samples were set up with the aid of the makeContrasts function by limma. The genes that are differentially expressed between control and drought stress samples were identified. Genes were defined to be up regulated or down regulated, if the log2 fold change (logFC) was greater than 1 or less than -1, respectively. The adjusted q-value cut-off was set to <0.05.

4.14 Bioinformatic analysis of the WGBS data

4.14.1 Whole genome bisulfite sequencing

The samples were sequenced on a NovaSeq 6000. Every sample were sequenced three times in paired-end mode and in total three biological replicates of each sample (M2 and D2) were used for sequencing.

4.14.2 Data processing with MethylStar

For analyzing the sequence data, the software tool MethylStar (Shahryary et al., 2020) were used which combines several components (e.g. Trimmomatic, FastQC, Bismark) for the processing of WGBS-derived data. Each sample were sequenced three times and in a first step, the three paired-end files were concatenated into one. Subsequent, the paired-end reads were quality checked with FastQC (Andrews, 2010) and Trimmomatic (Bolger et al., 2014) to get rid of potential adapter contaminations and to trim the 3'- and 5'-ends of the reads.

4.14.3 Bismark read alignment and methylation calling

To map the WGBS reads and to identify methylation calls the bismark program (Krueger & Andrews, 2011), implemented in MethylStar, were used. Like the analyses before, the Morex genome V2 was used as the reference genome for genome indexing in the first step genome preparation. The paired-end reads were aligned to the bisulfite converted reference genome with Bowtie2 v2.3.5.1 (Langmead & Salzberg, 2012) with default parameters except for the output set to -- directional. The deduplicate_bismark command was run with the samples to remove multiple alignments to the genome with default parameters. Then, the methylation for every cytosine were called with the function bismark_methylation_extractor. For further analysis, the genome-wide cytosine (CX) report were generated for each sample. Due to the huge size of the generated data, the CX report were generated for every chromosome separately.

4.14.4 MethylC

The CX-report files were used as an input for further analysis with the recently developed MethylC program (Lu et al., 2023). The MethylC pipeline combines different tools to analyze and visualize the outcome of the WGBS. First, a principal component analysis (PCA) with the replicates of M2 and D2 were conducted as well as the generating of a hierarchical clustering heatmap. Besides the genome-wide methylation level (%) for the CG, CHG and CHH context, MethylC also detects the differentially methylated regions (DMRs) between M2 and D2 and the associated differentially methylated genes (DMGs). The location of the DMRs were detected by intersecting the lists of annotated genes and transposable elements (TEs) (Mascher, 2019) with the list of DMRs.

4.15 Data analysis software

For blasting barley genes, the IPK Barley Blast server on the Galaxy platform (https://galaxy-web.ipk-gatersleben.de/, accessed on April, 2021) were used. To compare the list of genes with each other, a web tool creating venn diagrams was used (https://bioinformatics.psb.ugent.be/webtools/Venn/, accessed on 1 March 2018). For calculating the differences in the signal tracks between M2 and D2, deepTools'

multiBigwigSummary (Ramírez et al., 2014) and the Diffbind package (Stark & Brown, 2011) were used.

5 References

Afgan, E., Baker, D., Batut, B., van den Beek, M., Bouvier, D., Čech, M., Chilton, J., Clements, D., Coraor, N., Grüning, B. A., Guerler, A., Hillman-Jackson, J., Hiltemann, S., Jalili, V., Rasche, H., Soranzo, N., Goecks, J., Taylor, J., Nekrutenko, A., & Blankenberg, D. (2018). The Galaxy platform for accessible, reproducible and collaborative biomedical analyses: 2018 update. *Nucleic Acids Research*, *46*(W1), W537–W544. https://doi.org/10.1093/nar/gky379

Agius, F., Kapoor, A., & Zhu, J. K. (2006). Role of the Arabidopsis DNA glycosylase/lyase ROS1 in active DNA demethylation. *Proceedings of the National Academy of Sciences of the United States of America*, *103*(31), 11796–11801. https://doi.org/10.1073/pnas.0603563103

Ali, A., & Yun, D.-J. (2020). Chromatin remodeling complex HDA9-PWR-ABI4 epigenetically regulates drought stress response in plants. *Plant Signaling & Behavior*, *15*(10), 1803568. https://doi.org/10.1080/15592324.2020.1803568

Allis, C. D., & Jenuwein, T. (2016). The molecular hallmarks of epigenetic control. *Nature Reviews Genetics*, *17*(8), 487–500. https://doi.org/10.1038/nrg.2016.59

An, C., Deng, L., Zhai, H., You, Y., Wu, F., Zhai, Q., Goossens, A., & Li, C. (2022). Regulation of jasmonate signaling by reversible acetylation of TOPLESS in Arabidopsis. *Molecular Plant*, *15*(8), 1329–1346. https://doi.org/10.1016/j.molp.2022.06.014

Andrews, S. (2010). *Babraham bioinformatics-FastQC: a quality control tool for high throughput sequence data. 2010.* http://www.bioinformatics.babraham.ac.uk/projects/fastqc/

Arya, G., & Schlick, T. (2009). A tale of tails: how histone tails mediate chromatin compaction in different salt and linker histone environments. *Journal of Physical Chemistry A*, *113*(16), 4045–4059. https://doi.org/10.1021/jp810375d

Asensi-Fabado, M.-A., Amtmann, A., & Perrella, G. (2017). Plant responses to abiotic stress: The chromatin context of transcriptional regulation. *Biochimica et Biophysica Acta (BBA) - Gene Regulatory Mechanisms*, *1860*(1), 106–122. https://doi.org/10.1016/j.bbagrm.2016.07.015

Ausín, I., Alonso-Blanco, C., Jarillo, J. A., Ruiz-García, L., & Martínez-Zapater, J. M. (2004). Regulation of flowering time by FVE, a retinoblastoma-associated protein. *Nature Genetics*, *36*(2), 162–166. https://doi.org/10.1038/ng1295

Avramova, Z. (2009). Evolution and pleiotropy of TRITHORAX function in Arabidopsis. *International Journal of Developmental Biology*, *53*(2–3), 371–381. https://doi.org/10.1387/ijdb.082664za

Ay, N., Janack, B., Fischer, A., Reuter, G., & Humbeck, K. (2015). Alterations of histone modifications at the senescence-associated gene HvS40 in barley during senescence. *Plant Molecular Biology*, *89*(1–2), 127–141. https://doi.org/10.1007/s11103-015-0358-2

Badr, A., Müller, K., Schäfer-Pregl, R., El Rabey, H., Effgen, S., Ibrahim, H. H., Pozzi, C., Rohde, W., &

Salamini, F. (2000). On the origin and domestication history of barley (Hordeum vulgare). *Molecular Biology and Evolution*, *17*(4), 499–510. https://doi.org/10.1093/oxfordjournals.molbev.a026330

Baek, D., Shin, G., Kim, M. C., Shen, M., Lee, S. Y., & Yun, D. J. (2020). Histone Deacetylase HDA9 With ABI4 Contributes to Abscisic Acid Homeostasis in Drought Stress Response. *Frontiers in Plant Science*, *11*, 1–12. https://doi.org/10.3389/fpls.2020.00143

Baker, K., Dhillon, T., Colas, I., Cook, N., Milne, I., Milne, L., Bayer, M., & Flavell, A. J. (2015). Chromatin state analysis of the barley epigenome reveals a higher-order structure defined by H3K27me1 and H3K27me3 abundance. *The Plant Journal*, *84*(1), 111–124. https://doi.org/10.1111/tpj.12963

Baldoni, E., Genga, A., & Cominelli, E. (2015). Plant MYB transcription factors: Their role in drought response mechanisms. *International Journal of Molecular Sciences*, *16*(7), 15811–15851. https://doi.org/10.3390/ijms160715811

Benayoun, B. A., Pollina, E. A., Ucar, D., Mahmoudi, S., Karra, K., Wong, E. D., Devarajan, K., Daugherty, A. C., Kundaje, A. B., Mancini, E., Hitz, B. C., Gupta, R., Rando, T. A., Baker, J. C., Snyder, M. P., Cherry, J. M., & Brunet, A. (2014). H3K4me3 breadth is linked to cell identity and transcriptional consistency. *Cell*, *158*(3), 673–688. https://doi.org/10.1016/j.cell.2014.06.027

Benhamed, M., Bertrand, C., Servet, C., & Zhou, D. X. (2006). Arabidopsis GCN5, HD1, and TAF1/HAF2 interact to regulate histone acetylation required for liqht-responsive gene expression. *Plant Cell*, *18*(11), 2893–2903. https://doi.org/10.1105/tpc.106.043489

Berger, S. L. (2007). The complex language of chromatin regulation during transcription. *Nature*, *447*(7143), 407–412. https://doi.org/10.1038/nature05915

Bernatavichute, Y. V., Zhang, X., Cokus, S., Pellegrini, M., & Jacobsen, S. E. (2008). Genome-Wide Association of Histone H3 Lysine Nine Methylation with CHG DNA Methylation in Arabidopsis thaliana. *PLoS ONE*, *3*(9), e3156. https://doi.org/10.1371/journal.pone.0003156

Bernstein, B. E., Humphrey, E. L., Erlich, R. L., Schneider, R., Bouman, P., Liu, J. S., Kouzarides, T., & Schreiber, S. L. (2002). Methylation of histone H3 Lys 4 in coding regions of active genes. *Proceedings of the National Academy of Sciences of the United States of America*, *99*(13), 8695–8700. https://doi.org/10.1073/pnas.082249499

Bernstein, B. E., Kamal, M., Lindblad-Toh, K., Bekiranov, S., Bailey, D. K., Huebert, D. J., McMahon, S., Karlsson, E. K., Kulbokas, E. J., Gingeras, T. R., Schreiber, S. L., & Lander, E. S. (2005). Genomic maps and comparative analysis of histone modifications in human and mouse. *Cell*, *120*(2), 169–181. https://doi.org/10.1016/j.cell.2005.01.001

Berr, A., Shafiq, S., & Shen, W.-H. (2011). Histone modifications in transcriptional activation during plant development. *Biochimica et Biophysica Acta (BBA) - Gene Regulatory Mechanisms*, *1809*(10), 567–576. https://doi.org/10.1016/j.bbagrm.2011.07.001

Black, J. C., Van Rechem, C., & Whetstine, J. R. (2012). Histone Lysine Methylation Dynamics: Establishment, Regulation, and Biological Impact. *Molecular Cell*, *48*(4), 491–507. https://doi.org/10.1016/j.molcel.2012.11.006

Bolger, A. M., Lohse, M., & Usadel, B. (2014). Trimmomatic: A flexible trimmer for Illumina sequence data. *Bioinformatics*, *30*(15), 2114–2120. https://doi.org/10.1093/bioinformatics/btu170

Bray, N. L., Pimentel, H., Melsted, P., & Pachter, L. (2016). Near-optimal probabilistic RNA-seq quantification. *Nature Biotechnology*, *34*(5), 525–527. https://doi.org/10.1038/nbt.3519

Brownell, J. E., & Allis, C. D. (1996). Special HATs for special occasions: linking histone acetylation to chromatin assembly and gene activation. *Current Opinion in Genetics & Development*, *6*(2), 176–184. https://doi.org/10.1016/S0959-437X(96)80048-7

Brunet, A., Sweeney, L. B., Sturgill, J. F., Chua, K. F., Greer, P. L., Lin, Y., Tran, H., Ross, S. E., Mostoslavsy, R., Cohen, H. Y., Hu, L. S., Cheng, H. L., Jedrychowski, M. P., Gygi, S. P., Sinclair, D. A., Alt, F. W., & Greenberg, M. E. (2004). Stress-Dependent Regulation of FOXO Transcription Factors by the SIRT1 Deacetylase. *Science*, *303*(5666), 2011–2015. https://doi.org/10.1126/science.1094637

Brusslan, J. A., Bonora, G., Rus-Canterbury, A. M., Tariq, F., Jaroszewicz, A., & Pellegrini, M. (2015). A genome-wide chronological study of gene expression and two histone modifications, H3K4me3 and H3K9ac, during developmental leaf senescence. *Plant Physiology*, *168*(4), 1246–1261. https://doi.org/10.1104/pp.114.252999

Bucchini, F., Del Cortona, A., Kreft, Ł., Botzki, A., Van Bel, M., & Vandepoele, K. (2021). TRAPID 2.0: A web application for taxonomic and functional analysis of de novo transcriptomes. *Nucleic Acids Research*, *49*(17), 1–17. https://doi.org/10.1093/nar/gkab565

Busk, P. K., & Pagès, M. (1998). Regulation of abscisic acid-induced transcription. *Plant Molecular Biology*, *37*(3), 425–435. https://doi.org/10.1023/A:1006058700720

Cai, K., Chen, X., Han, Z., Wu, X., Zhang, S., Li, Q., Nazir, M. M., Zhang, G., & Zeng, F. (2020). Screening of Worldwide Barley Collection for Drought Tolerance: The Assessment of Various Physiological Measures as the Selection Criteria. *Frontiers in Plant Science*, *11*, 1–16. https://doi.org/10.3389/fpls.2020.01159

Carchilan, M., Delgado, M., Ribeiro, T., Costa-Nunes, P., Caperta, A., Morais-Cecílio, L., Jones, R. N., Viegas, W., & Houbena, A. (2007). Transcriptionally active heterochromatin in rye B chromosomes. *Plant Cell*, *19*(6), 1738–1749. https://doi.org/10.1105/tpc.106.046946

Carrozza, M. J., Utley, R. T., Workman, J. L., & Côté, J. (2003). The diverse functions of histone acetyltransferase complexes. *Trends in Genetics*, *19*(6), 321–329. https://doi.org/10.1016/S0168-9525(03)00115-X

Chan, S. W. L., Henderson, I. R., & Jacobsen, S. E. (2005). Gardening the genome: DNA methylation

in Arabidopsis thaliana. *Nature Reviews Genetics*, *6*(5), 351–360. https://doi.org/10.1038/nrg1601

Chan, Z. (2012). Expression profiling of ABA pathway transcripts indicates crosstalk between abiotic and biotic stress responses in Arabidopsis. *Genomics*, *100*(2), 110–115. https://doi.org/10.1016/j.ygeno.2012.06.004

Charron, J.-B. F., He, H., Elling, A. A., & Deng, X. W. (2009). Dynamic Landscapes of Four Histone Modifications during Deetiolation in Arabidopsis. *The Plant Cell*, *21*(12), 3732–3748. https://doi.org/10.1105/tpc.109.066845

Chen, Y., Dubois, M., Vermeersch, M., Inzé, D., & Vanhaeren, H. (2021). Distinct cellular strategies determine sensitivity to mild drought of Arabidopsis natural accessions. *Plant Physiology*, *186*(2), 1171–1185. https://doi.org/10.1093/PLPHYS/KIAB115

Chen, Z. J., & Tian, L. (2007). Roles of dynamic and reversible histone acetylation in plant development and polyploidy. *Biochimica et Biophysica Acta - Gene Structure and Expression*, *1769*(5–6), 295–307. https://doi.org/10.1016/j.bbaexp.2007.04.007

Choi, Y., Gehring, M., Johnson, L., Hannon, M., Harada, J. J., Goldberg, R. B., Jacobsen, S. E., & Fischer, R. L. (2002). DEMETER, a DNA glycosylase domain protein, is required for endosperm gene imprinting and seed viability in Arabidopsis. *Cell*, *110*(1), 33–42. https://doi.org/10.1016/S0092-8674(02)00807-3

Chwialkowska, K., Nowakowska, U., Mroziewicz, A., Szarejko, I., & Kwasniewski, M. (2016). Water-deficiency conditions differently modulate the methylome of roots and leaves in barley (Hordeum vulgare L.). *Journal of Experimental Botany*, *67*(4), 1109–1121. https://doi.org/10.1093/jxb/erv552

Clauw, P., Coppens, F., De Beuf, K., Dhondt, S., Van Daele, T., Maleux, K., Storme, V., Clement, L., Gonzalez, N., Inzé, D., Beuf, K. De, Dhondt, S., Daele, T. Van, Maleux, K., Storme, V., Clement, L., Gonzalez, N., Inzé, D., & Systems, P. (2015). Leaf responses to mild drought stress in natural variants of Arabidopsis. *Plant Physiology*, *167*(3), 800–816. https://doi.org/10.1104/pp.114.254284

Cohen, P. T. W. (1997). Novel protein serine/threonine phosphatases: Variety is the spice of life. *Trends in Biochemical Sciences*, *22*(7), 245–251. https://doi.org/10.1016/S0968-0004(97)01060-8

Cokus, S. J., Feng, S., Zhang, X., Chen, Z., Merriman, B., Haudenschild, C. D., Pradhan, S., Nelson, S. F., Pellegrini, M., & Jacobsen, S. E. (2008). Shotgun bisulphite sequencing of the Arabidopsis genome reveals DNA methylation patterning. *Nature*, *452*(7184), 215–219. https://doi.org/10.1038/nature06745

Cominelli, E., Galbiati, M., Vavasseur, A., Conti, L., Sala, T., Vuylsteke, M., Leonhardt, N., Dellaporta, S. L., & Tonelli, C. (2005). A guard-cell-specific MYB transcription factor regulates stomatal movements and plant drought tolerance. *Current Biology*, *15*(13), 1196–1200. https://doi.org/10.1016/j.cub.2005.05.048

Cutler, S. R., Rodriguez, P. L., Finkelstein, R. R., & Abrams, S. R. (2010). Abscisic Acid: Emergence of

a Core Signaling Network. *Annual Review of Plant Biology*, *61*(1), 651–679. https://doi.org/10.1146/annurev-arplant-042809-112122

Dar, N. A., Amin, I., Wani, W., Wani, S. A., Shikari, A. B., Wani, S. H., & Masoodi, K. Z. (2017). Abscisic acid: A key regulator of abiotic stress tolerance in plants. *Plant Gene*, *11*, 106–111. https://doi.org/10.1016/j.plgene.2017.07.003

De Nadal, E., Zapater, M., Alepuz, P. M., Sumoy, L., Mas, G., & Posas, F. (2004). The MAPK Hog1 recruits Rpd3 histone deacetylase to activate osmoresponsive genes. *Nature*, *427*(6972), 370–374. https://doi.org/10.1038/nature02258

Dietz, K.-J., Zörb, C., & Geilfus, C.-M. (2021). Drought and crop yield. *Plant Biology*, *23*(6), 881–893. https://doi.org/10.1111/plb.13304

Ding, Y., Avramova, Z., & Fromm, M. (2011a). The Arabidopsis trithorax-like factor ATX1 functions in dehydration stress responses via ABA-dependent and ABA-independent pathways. *The Plant Journal*, *66*(5), 735–744. https://doi.org/10.1111/j.1365-313X.2011.04534.x

Ding, Y., Avramova, Z., & Fromm, M. (2011b). Two Distinct Roles of ARABIDOPSIS HOMOLOG OF TRITHORAX1 (ATX1) at Promoters and within Transcribed Regions of ATX1-Regulated Genes. *The Plant Cell*, *23*(1), 350–363. https://doi.org/10.1105/tpc.110.080150

Ding, Y., Fromm, M., & Avramova, Z. (2012). Multiple exposures to drought "train" transcriptional responses in Arabidopsis. *Nature Communications*, *3*(1), 740. https://doi.org/10.1038/ncomms1732

Doležel, J., Greilhuber, J., Lucretti, S., Meister, A., Lysák, M. A., Nardi, L., & Obermayer, R. (1998). Plant Genome Size Estimation by Flow Cytometry: Inter-laboratory Comparison. *Annals of Botany*, *82*(suppl_1), 17–26. https://doi.org/10.1093/oxfordjournals.aob.a010312

Domcke, S., Bardet, A. F., Adrian Ginno, P., Hartl, D., Burger, L., & Schübeler, D. (2015). Competition between DNA methylation and transcription factors determines binding of NRF1. *Nature*, *528*(7583), 575–579. https://doi.org/10.1038/nature16462

Du, J., Zhong, X., Bernatavichute, Y. V., Stroud, H., Feng, S., Caro, E., Vashisht, A. A., Terragni, J., Chin, H. G., Tu, A., Hetzel, J., Wohlschlegel, J. A., Pradhan, S., Patel, D. J., & Jacobsen, S. E. (2012). Dual binding of chromomethylase domains to H3K9me2-containing nucleosomes directs DNA methylation in plants. *Cell*, *151*(1), 167–180. https://doi.org/10.1016/j.cell.2012.07.034

Ebbs, M. L., Bartee, L., & Bender, J. (2005). H3 Lysine 9 Methylation Is Maintained on a Transcribed Inverted Repeat by Combined Action of SUVH6 and SUVH4 Methyltransferases. *Molecular and Cellular Biology*, *25*(23), 10507–10515. https://doi.org/10.1128/mcb.25.23.10507-10515.2005

Ebbs, M. L., & Bender, J. (2006). Locus-specific control of DNA methylation by the Arabidopsis SUVH5 histone methyltransferase. *Plant Cell*, *18*(5), 1166–1176. https://doi.org/10.1105/tpc.106.041400

Eberharter, A., Lechner, T., Goralik-Schramel, M., & Loidl, P. (1996). Purification and characterization of the cytoplasmic histone acetyltransferase B of maize embryos. *FEBS Letters*, *386*(1), 75–81. https://doi.org/10.1016/0014-5793(96)00401-2

Eichten, S. R., & Springer, N. M. (2015). Minimal evidence for consistent changes in maize DNA methylation patterns following environmental stress. *Frontiers in Plant Science*, *6*, 1–10. https://doi.org/10.3389/fpls.2015.00308

Elhamamsy, A. R. (2016). DNA methylation dynamics in plants and mammals: overview of regulation and dysregulation. *Cell Biochemistry and Function*, *34*(5), 289–298. https://doi.org/10.1002/cbf.3183

Fang, H., Liu, X., Thorn, G., Duan, J., & Tian, L. (2014). Expression analysis of histone acetyltransferases in rice under drought stress. *Biochemical and Biophysical Research Communications*, *443*(2), 400–405. https://doi.org/10.1016/j.bbrc.2013.11.102

Ferchichi, S., Hessini, K., Dell'Aversana, E., D'Amelia, L., Woodrow, P., Ciarmiello, L. F., Fuggi, A., & Carillo, P. (2018). Hordeum vulgare and Hordeum maritimum respond to extended salinity stress displaying different temporal accumulation pattern of metabolites. *Functional Plant Biology*, *45*(11), 1096–1109. https://doi.org/10.1071/FP18046

Flavell, R. B., Bennett, M. D., Smith, J. B., & Smith, D. B. (1974). Genome Size and the Proportion of Repeated Nueleotide Sequence DNA in Plants. *Biochemical Genetics*, *12*(4), 257–269.

Forestan, C., Farinati, S., Zambelli, F., Pavesi, G., Rossi, V., & Varotto, S. (2020). Epigenetic signatures of stress adaptation and flowering regulation in response to extended drought and recovery in Zea mays. *Plant Cell and Environment*, *43*(1), 55–75. https://doi.org/10.1111/pce.13660

Foroozani, M., Vandal, M. P., & Smith, A. P. (2021). H3K4 trimethylation dynamics impact diverse developmental and environmental responses in plants. *Planta*, *253*(1), 1–17. https://doi.org/10.1007/s00425-020-03520-0

Fuchs, J., Demidov, D., Houben, A., & Schubert, I. (2006). Chromosomal histone modification patterns - from conservation to diversity. *Trends in Plant Science*, *11*(4), 199–208. https://doi.org/10.1016/j.tplants.2006.02.008

Fuchs, S., Grill, E., Meskiene, I., & Schweighofer, A. (2013). Type 2C protein phosphatases in plants. *FEBS Journal*, *280*(2), 681–693. https://doi.org/10.1111/j.1742-4658.2012.08670.x

Fujita, Y., Fujita, M., Satoh, R., Maruyama, K., Parvez, M. M., Seki, M., Hiratsu, K., Ohme-Takagi, M., Shinozaki, K., & Yamaguchi-Shinozaki, K. (2005). AREB1 is a transcription activator of novel ABRE-dependent ABA signaling that enhances drought stress tolerance in Arabidopsis. *Plant Cell*, *17*(12), 3470–3488. https://doi.org/10.1105/tpc.105.035659

Fujita, Y., Fujita, M., Shinozaki, K., & Yamaguchi-Shinozaki, K. (2011). ABA-mediated transcriptional regulation in response to osmotic stress in plants. *Journal of Plant Research*, *124*(4), 509–525.

https://doi.org/10.1007/s10265-011-0412-3

Fujita, Y., Nakashima, K., Yoshida, T., Katagiri, T., Kidokoro, S., Kanamori, N., Umezawa, T., Fujita, M., Maruyama, K., Ishiyama, K., Kobayashi, M., Nakasone, S., Yamada, K., Ito, T., Shinozaki, K., & Yamaguchi-Shinozaki, K. (2009). Three SnRK2 protein kinases are the main positive regulators of abscisic acid signaling in response to water stress in arabidopsis. *Plant and Cell Physiology*, *50*(12), 2123–2132. https://doi.org/10.1093/pcp/pcp147

Fujita, Y., Yoshida, T., & Yamaguchi-Shinozaki, K. (2013). Pivotal role of the AREB/ABF-SnRK2 pathway in ABRE-mediated transcription in response to osmotic stress in plants. *Physiologia Plantarum*, *147*(1), 15–27. https://doi.org/10.1111/j.1399-3054.2012.01635.x

Furihata, T., Maruyama, K., Fujita, Y., Umezawa, T., Yoshida, R., Shinozaki, K., & Yamaguchi-Shinozaki, K. (2006). Abscisic acid-dependent multisite phosphorylation regulates the activity of a transcription activator AREB1. *Proceedings of the National Academy of Sciences of the United States of America*, *103*(6), 1988–1993. https://doi.org/10.1073/pnas.0505667103

Ganguly, D. R., Crisp, P. A., Eichten, S. R., & Pogson, B. J. (2017). The arabidopsis DNA methylome is stable under transgenerational drought stress. *Plant Physiology*, *175*(4), 1893–1912. https://doi.org/10.1104/pp.17.00744

Garg, R., Narayana Chevala, V., Shankar, R., & Jain, M. (2015). Divergent DNA methylation patterns associated with gene expression in rice cultivars with contrasting drought and salinity stress response. *Scientific Reports*, *5*(1), 14922. https://doi.org/10.1038/srep14922

Gehring, M., Huh, J. H., Hsieh, T. F., Penterman, J., Choi, Y., Harada, J. J., Goldberg, R. B., & Fischer, R. L. (2006). DEMETER DNA glycosylase establishes MEDEA polycomb gene self-imprinting by allele-specific demethylation. *Cell*, *124*(3), 495–506. https://doi.org/10.1016/j.cell.2005.12.034

Geiger, D., Scherzer, S., Mumm, P., Stange, A., Marten, I., Bauer, H., Ache, P., Matschi, S., Liese, A., Al-Rasheid, K. A. S., Romeis, T., & Hedrich, R. (2009). Activity of guard cell anion channel SLAC1 is controlled by drought-stress signaling kinase-phosphatase pair. *Proceedings of the National Academy of Sciences of the United States of America*, *106*(50), 21425–21430. https://doi.org/10.1073/pnas.0912021106

Gentleman, R. C., Carey, V. J., Bates, D. M., Bolstad, B., Dettling, M., Dudoit, S., Ellis, B., Gautier, L., Ge, Y., Gentry, J., Hornik, K., Hothorn, T., Huber, W., Iacus, S., Irizarry, R., Leisch, F., Li, C., Maechler, M., Rossini, A. J., Sawitzki, G., Smith, C., Smyth, G., Tierney, L., Yang, J. Y., & Zhang, J. (2004). Open Access Bioconductor: open software development for computational biology and bioinformatics. *Genome Biology*, *5*(10), 1–16. https://doi.org/https://doi.org/10.1186/gb-2004-5-10-r80

Gong, Z., Xiong, L., Shi, H., Yang, S., Herrera-Estrella, L. R., Xu, G., Chao, D. Y., Li, J., Wang, P. Y., Qin, F., Li, J., Ding, Y., Shi, Y., Wang, Y., Yang, Y., Guo, Y., & Zhu, J. K. (2020). Plant abiotic stress response and nutrient use efficiency. *Science China Life Sciences*, *63*(5), 635–674.

https://doi.org/10.1007/s11427-020-1683-x

Gong, Z., & Yang, S. (2022). Drought meets SWEET. *Nature Plants*, *8*(1), 25–26. https://doi.org/10.1038/s41477-021-01032-7

Gosti, F., Beaudoin, N., Serizet, C., Webb, A. A. R., Vartanian, N., & Giraudat, J. (1999). ABI1 protein phosphatase 2C is a negative regulator of abscisic acid signaling. *Plant Cell*, *11*(10), 1897–1909. https://doi.org/10.1105/tpc.11.10.1897

Guo, L., Yu, Y., Law, J. A., & Zhang, X. (2010). Set domain group2 is the major histone H3 lysine 4 trimethyltransferase in Arabidopsis. *Proceedings of the National Academy of Sciences of the United States of America*, *107*(43), 18557–18562. https://doi.org/10.1073/pnas.1010478107

Guo, P., Baum, M., Grando, S., Ceccarelli, S., Bai, G., Li, R., Von Korff, M., Varshney, R. K., Graner, A., & Valkoun, J. (2009). Differentially expressed genes between drought-tolerant and drought-sensitive barley genotypes in response to drought stress during the reproductive stage. *Journal of Experimental Botany*, *60*(12), 3531–3544. https://doi.org/10.1093/jxb/erp194

Halder, K., Chaudhuri, A., Abdin, M. Z., Majee, M., & Datta, A. (2022). Chromatin-Based Transcriptional Reprogramming in Plants under Abiotic Stresses. *Plants*, *11*(11), 1–19. https://doi.org/10.3390/plants11111449

Harb, A., Krishnan, A., Ambavaram, M. M. R., & Pereira, A. (2010). Molecular and physiological analysis of drought stress in arabidopsis reveals early responses leading to acclimation in plant growth. *Plant Physiology*, *154*(3), 1254–1271. https://doi.org/10.1104/pp.110.161752

Harwood, W. A. (2019). An Introduction to Barley: The Crop and the Model. In *Methods in Molecular Biology* (Vol. 1900, pp. 1–5). https://doi.org/10.1007/978-1-4939-8944-7_1

He, G., Elling, A. A., & Deng, X. W. (2011). The Epigenome and Plant Development. *Annu. Rev. Plant Biol*, *62*, 411–435. https://doi.org/10.1146/annurev-arplant-042110-103806

He, Y., Michaels, S. D., & Amasino, R. M. (2003). Regulation of Flowering Time by Histone Acetylation in Arabidopsis. *Science*, *302*(5651), 1751–1754. https://doi.org/10.1126/science.1091109

He, Z., Wu, J., Sun, X., & Dai, M. (2019). The Maize Clade A PP2C Phosphatases Play Critical Roles in Multiple Abiotic Stress Responses. *International Journal of Molecular Sciences*, *20*(14), 3573. https://doi.org/10.3390/ijms20143573

Henderson, I. R., & Jacobsen, S. E. (2007). Epigenetic inheritance in plants. *Nature*, *447*(7143), 418–424. https://doi.org/10.1038/nature05917

Herwade, A. P., Kasar, S. S., Rane, N. R., Ahmed, S., Maras, J. S., & Pawar, P. K. (2021). Characterization of a Bowman–Birk type trypsin inhibitor purified from seeds of Solanum surattense. *Scientific Reports*, *11*(1), 1–10. https://doi.org/10.1038/s41598-021-87980-8

Hong, B., Uknes, S. J., & Ho, T. hua D. (1988). Cloning and characterization of a cDNA encoding a

mRNA rapidly-induced by ABA in barley aleurone layers. *Plant Molecular Biology*, *11*(4), 495–506. https://doi.org/10.1007/BF00039030

Houben, A., Demidov, D., Gernand, D., Meister, A., Leach, C. R., & Schubert, I. (2003). Methylation of histone H3 in euchromatin of plant chromosomes depends on basic nuclear DNA content. *Plant Journal*, *33*(6), 967–973. https://doi.org/10.1046/j.1365-313X.2003.01681.x

Hsu, P. K., Dubeaux, G., Takahashi, Y., & Schroeder, J. I. (2021). Signaling mechanisms in abscisic acid-mediated stomatal closure. *Plant Journal*, *105*(2), 307–321. https://doi.org/10.1111/tpj.15067

Hu, C. A., Delauney, A. J., & Verma, D. P. (1992). A bifunctional enzyme (delta 1-pyrroline-5-carboxylate synthetase) catalyzes the first two steps in proline biosynthesis in plants. *Proceedings of the National Academy of Sciences*, *89*(19), 9354–9358. https://doi.org/10.1073/pnas.89.19.9354

Hu, G., Huang, B., Wang, K., Frasse, P., Maza, E., Djari, A., Benhamed, M., Gallusci, P., Li, Z., Zouine, M., & Bouzayen, M. (2021). Histone posttranslational modifications rather than DNA methylation underlie gene reprogramming in pollination-dependent and pollination-independent fruit set in tomato. *New Phytologist*, *229*(2), 902–919. https://doi.org/10.1111/nph.16902

Hu, Y., Lu, Y., Zhao, Y., & Zhou, D.-X. (2019). Histone Acetylation Dynamics Integrates Metabolic Activity to Regulate Plant Response to Stress. *Frontiers in Plant Science*, *10*, 1236. https://doi.org/10.3389/fpls.2019.01236

Huang, C., Hu, G., Li, F., Li, Y., Wu, J., & Zhou, X. (2013). NbPHAN, a MYB transcriptional factor, regulates leaf development and affects drought tolerance in Nicotiana benthamiana. *Physiologia Plantarum*, *149*(3), 297–309. https://doi.org/10.1111/ppl.12031

Huizinga, D. H., Omosegbon, O., Omery, B., & Crowell, D. N. (2008). Isoprenylcysteine methylation and demethylation regulate abscisic acid signaling in Arabidopsis. *Plant Cell*, *20*(10), 2714–2728. https://doi.org/10.1105/tpc.107.053389

Imai, S., Armstrong, C. M., Kaeberlein, M., & Guarente, L. (2000). Transcriptional silencing and longevity protein Sir2 is an NAD-dependent histone deacetylase. *Nature*, *403*(6771), 795–800. https://doi.org/10.1038/35001622

Imhof, A., & Wolffe, A. P. (1998). Transcription: Gene control by targeted histone acetylation. *Current Biology*, *8*(12), R422–R424. https://doi.org/10.1016/S0960-9822(98)70268-4

International Barley Genome Sequencing Consortium, T., Mayer, K. F. X., Waugh, R., Langridge, P., Close, T. J., Wise, R. P., Graner, A., Matsumoto, T., Sato, K., Schulman, A., Ariyadasa, R., Schulte, D., Poursarebani, N., Zhou, R., Steuernagel, B., Mascher, M., Scholz, U., Shi, B., Madishetty, K., Svensson, J. T., … Stein, N. (2012). A physical, genetic and functional sequence assembly of the barley genome. *Nature*, *491*(7426), 711–716. https://doi.org/10.1038/nature11543

Jackson, J. P., Johnson, L., Jasencakova, Z., Zhang, X., PerezBurgos, L., Singh, P. B., Cheng, X., Schubert, I., Jenuwein, T., & Jacobsen, S. E. (2004). Dimethylation of histone H3 lysine 9 is a

critical mark for DNA methylation and gene silencing in Arabidopsis thaliana. *Chromosoma*, *112*(6), 308–315. https://doi.org/10.1007/s00412-004-0275-7

Jackson, J. P., Lindroth, A. M., Cao, X., & Jacobsen, S. E. (2002). Control of CpNpG DNA methylation by the KRYPTONITE histone H3 methyltransferase. *Nature*, *416*(6880), 556–560. https://doi.org/10.1038/nature731

Jalili, V., Afgan, E., Gu, Q., Clements, D., Blankenberg, D., Goecks, J., Taylor, J., & Nekrutenko, A. (2021). The Galaxy platform for accessible, reproducible and collaborative biomedical analyses: 2020 update. *Nucleic Acids Research*, *48*(W1), W395–W402. https://doi.org/10.1093/NAR/GKAA434

Janack, B., Sosoi, P., Krupinska, K., & Humbeck, K. (2016). Knockdown of WHIRLY1 Affects Drought Stress-Induced Leaf Senescence and Histone Modifications of the Senescence-Associated Gene HvS40. *Plants*, *5*(3), 37. https://doi.org/10.3390/plants5030037

Jasencakova, Z., Soppe, W. J. J., Meister, A., Gernand, D., Turner, B. M., & Schubert, I. (2003). Histone modifications in Arabidopsis - High methylation of H3 lysine 9 is dispensable for constitutive heterochromatin. *Plant Journal*, *33*(3), 471–480. https://doi.org/10.1046/j.1365-313X.2003.01638.x

Jenuwein, T., & Allis, C. D. (2001). Translating the Histone Code. *Science*, *293*(5532), 1074–1080. https://doi.org/10.1126/science.1063127

Jiabu, D., Yu, M., Xu, Q., Yang, H., Mu, W., & Basang, Y. (2023). Genome-Wide DNA Methylation Dynamics During Drought Responsiveness in Tibetan Hulless Barley. *Journal of Plant Growth Regulation*, *42*(7), 4391–4401. https://doi.org/10.1007/s00344-022-10903-y

Jiang, C., Mithani, A., Belfield, E. J., Mott, R., Hurst, L. D., & Harberd, N. P. (2014). Environmentally responsive genome-wide accumulation of de novo Arabidopsis thaliana mutations and epimutations. *Genome Research*, *24*(11), 1821–1829. https://doi.org/10.1101/gr.177659.114

Jiang, D., Kong, N. C., Gu, X., Li, Z., & He, Y. (2011). Arabidopsis COMPASS-Like Complexes Mediate Histone H3 Lysine-4 Trimethylation to Control Floral Transition and Plant Development. *PLoS Genetics*, *7*(3), e1001330. https://doi.org/10.1371/journal.pgen.1001330

Jiang, L., Schlesinger, F., Davis, C. A., Zhang, Y., Li, R., Salit, M., Gingeras, T. R., & Oliver, B. (2011). Synthetic spike-in standards for RNA-seq experiments. *Genome Research*, *21*(9), 1543–1551. https://doi.org/10.1101/gr.121095.111

Jones, L., Hamilton, A. J., Voinnet, O., Thomas, C. L., Maule, A. J., & Baulcombe, D. C. (1999). RNA-DNA interactions and DNA methylation in post-transcriptional gene silencing. *Plant Cell*, *11*(12), 2291–2301. https://doi.org/10.1105/tpc.11.12.2291

Jung, C., Nguyen, N. H., & Cheong, J.-J. (2020). Transcriptional Regulation of Protein Phosphatase 2C Genes to Modulate Abscisic Acid Signaling. *International Journal of Molecular Sciences*, *21*(24),

9517. https://doi.org/10.3390/ijms21249517

Kamachi, K., Yamaya, T., Mae, T., & Ojima, K. (1991). A role for glutamine synthetase in the remobilization of leaf nitrogen during natural senescence in rice leaves. *Plant Physiology*, *96*(2), 411–417. https://doi.org/10.1104/pp.96.2.411

Kerk, D., Bulgrien, J., Smith, D. W., Barsam, B., Veretnik, S., & Gribskov, M. (2002). The complement of protein phosphatase catalytic subunits encoded in the genome of Arabidopsis. *Plant Physiology*, *129*(2), 908–925. https://doi.org/10.1104/pp.004002

Khan, A. R., Enjalbert, J., Marsollier, A.-C., Rousselet, A., Goldringer, I., & Vitte, C. (2013). Vernalization treatment induces site-specific DNA hypermethylation at the VERNALIZATION-A1 (VRN-A1) locus in hexaploid winter wheat. *BMC Plant Biology*, *13*(1), 209. https://doi.org/10.1186/1471-2229-13-209

Khan, I. U., Ali, A., Khan, H. A., Baek, D., Park, J., Lim, C. J., Zareen, S., Jan, M., Lee, S. Y., Pardo, J. M., Kim, W. Y., & Yun, D. J. (2020). PWR/HDA9/ABI4 Complex Epigenetically Regulates ABA Dependent Drought Stress Tolerance in Arabidopsis. *Frontiers in Plant Science*, *11*, 1–13. https://doi.org/10.3389/fpls.2020.00623

Kim, H. J., Hyun, Y., Park, J. Y., Park, M. J., Park, M. K., Kim, M. D., Kim, H. J., Lee, M. H., Moon, J., Lee, I., & Kim, J. (2004). A genetic link between cold responses and flowering time through FVE in Arabidopsis thaliana. *Nature Genetics*, *36*(2), 167–171. https://doi.org/10.1038/ng1298

Kim, J.-M., Sasaki, T., Ueda, M., Sako, K., & Seki, M. (2015). Chromatin changes in response to drought, salinity, heat, and cold stresses in plants. *Frontiers in Plant Science*, *6*(114). https://doi.org/10.3389/fpls.2015.00114

Kim, J.-M., To, T. K., Ishida, J., Morosawa, T., Kawashima, M., Matsui, A., Toyoda, T., Kimura, H., Shinozaki, K., & Seki, M. (2008). Alterations of Lysine Modifications on the Histone H3 N-Tail under Drought Stress Conditions in Arabidopsis thaliana. *Plant and Cell Physiology*, *49*(10), 1580–1588. https://doi.org/10.1093/pcp/pcn133

Kim, J. H. (2021). Multifaceted chromatin structure and transcription changes in plant stress response. *International Journal of Molecular Sciences*, *22*(4), 1–25. https://doi.org/10.3390/ijms22042013

Kim, J. M., To, T. K., Ishida, J., Matsui, A., Kimura, H., & Seki, M. (2012). Transition of chromatin status during the process of recovery from drought stress in arabidopsis thaliana. *Plant and Cell Physiology*, *53*(5), 847–856. https://doi.org/10.1093/pcp/pcs053

Kim, T.-H., Böhmer, M., Hu, H., Nishimura, N., & Schroeder, J. I. (2010). Guard Cell Signal Transduction Network: Advances in Understanding Abscisic Acid, CO 2 , and Ca 2+ Signaling. *Annual Review of Plant Biology*, *61*(1), 561–591. https://doi.org/10.1146/annurev-arplant-042809-112226

Kleber-Janke, T., & Krupinska, K. (1997). Isolation of cDNA clones for genes showing enhanced expression in harley leaves during dark-induced senescence as well as during senescence under

field conditions. *Planta*, *203*(3), 332–340. https://doi.org/10.1007/s004250050199

Klose, R. J., & Bird, A. P. (2006). Genomic DNA methylation: The mark and its mediators. *Trends in Biochemical Sciences*, *31*(2), 89–97. https://doi.org/10.1016/j.tibs.2005.12.008

Koornneef, M., Reuling, G., & Karssen, C. M. (1984). The isolation and characterization of abscisic acid-insensitive mutants of Arabidopsis thaliana. *Physiologia Plantarum*, *61*(3), 377–383. https://doi.org/10.1111/j.1399-3054.1984.tb06343.x

Kõressaar, T., Lepamets, M., Kaplinski, L., Raime, K., Andreson, R., & Remm, M. (2018). Primer3_masker: integrating masking of template sequence with primer design software. *Bioinformatics*, *34*(11), 1937–1938. https://doi.org/10.1093/bioinformatics/bty036

Kõressaar, T., & Remm, M. (2007). Enhancements and modifications of primer design program Primer3. *Bioinformatics*, *23*(10), 1289–1291. https://doi.org/10.1093/bioinformatics/btm091

Kouzarides, T. (2007). Chromatin Modifications and Their Function. *Cell*, *128*(4), 693–705. https://doi.org/10.1016/j.cell.2007.02.005

Krueger, F., & Andrews, S. R. (2011). Bismark: A flexible aligner and methylation caller for Bisulfite-Seq applications. *Bioinformatics*, *27*(11), 1571–1572. https://doi.org/10.1093/bioinformatics/btr167

Krupinska, K., Dähnhardt, D., Fischer-Kilbienski, I., Kucharewicz, W., Scharrenberg, C., Trösch, M., & Buck, F. (2014). Identification of WHIRLY1 as a Factor Binding to the Promoter of the Stress- and Senescence-Associated Gene HvS40. *Journal of Plant Growth Regulation*, *33*(1), 91–105. https://doi.org/10.1007/s00344-013-9378-9

Krupinska, K., Haussühl, K., Schäfer, A., Van der Kooij, T. A. W., Leckband, G., Lörz, H., & Falk, J. (2002). A novel nucleus-targeted protein is expressed in barley leaves during senescence and pathogen infection. *Plant Physiology*, *130*(3), 1172–1180. https://doi.org/10.1104/pp.008565

Kurdistani, S. K., Tavazoie, S., & Grunstein, M. (2004). Mapping global histone acetylation patterns to gene expression. *Cell*, *117*(6), 721–733. https://doi.org/10.1016/j.cell.2004.05.023

Lämke, J., Brzezinka, K., Altmann, S., & Bäurle, I. (2016). A hit-and-run heat shock factor governs sustained histone methylation and transcriptional stress memory. *The EMBO Journal*, *35*(2), 162–175. https://doi.org/10.15252/embj.201592593

Landt, S. G., Marinov, G. K., Kundaje, A., Kheradpour, P., Pauli, F., Batzoglou, S., Bernstein, B. E., Bickel, P., Brown, J. B., Cayting, P., Chen, Y., DeSalvo, G., Epstein, C., Fisher-Aylor, K. I., Euskirchen, G., Gerstein, M., Gertz, & Snyder, M. (2012). ChIP-seq guidelines and practices of the ENCODE and modENCODE consortia. *Genome Research*, *22*(9), 1813–1831. https://doi.org/10.1101/gr.136184.111

Langmead, B., & Salzberg, S. L. (2012). Fast gapped-read alignment with Bowtie 2. *Nature Methods*, *9*(4), 357–359. https://doi.org/10.1038/nmeth.1923

Law, C. W., Chen, Y., Shi, W., & Smyth, G. K. (2014). voom: precision weights unlock linear model analysis tools for RNA-seq read counts. *Genome Biology*, *15*(2), R29. https://doi.org/10.1186/gb-2014-15-2-r29

Law, J. A., & Jacobsen, S. E. (2010). Establishing, maintaining and modifying DNA methylation patterns in plants and animals. In *Nature Reviews Genetics* (Vol. 11, Issue 3, pp. 204–220). https://doi.org/10.1038/nrg2719

Lee, S. C., Lan, W., Buchanan, B. B., & Luan, S. (2009). A protein kinase-phosphatase pair interacts with an ion channel to regulate ABA signaling in plant guard cells. *Proceedings of the National Academy of Sciences of the United States of America*, *106*(50), 21419–21424. https://doi.org/10.1073/pnas.0910601106

Leung, J., Bouvier-Durand, M., Morris, P.-C., Guerrier, D., Chefdor, F., & Giraudat, J. (1994). Arabidopsis ABA Response Gene ABI1 : Features of a Calcium-Modulated Protein Phosphatase. *Science*, *264*(5164), 1448–1452. https://doi.org/10.1126/science.7910981

Leung, J., Merlot, S., & Giraudat, J. (1997). The Arabidopsis ABSCISIC ACID-INSENSITIVE2 (ABI2) and ABI1 genes encode homologous protein phosphatases 2C involved in abscisic acid signal transduction. *The Plant Cell*, *9*(5), 759–771. https://doi.org/10.1105/tpc.9.5.759

Li, H. (2013). Aligning sequence reads, clone sequences and assembly contigs with BWA-MEM arXiv:1303.3997v1[q-bio.GN].*ArXivPreprint*. https://doi.org/https://doi.org/10.48550/arXiv.1303.3997

Li, H., & Durbin, R. (2010). Fast and accurate long-read alignment with Burrows-Wheeler transform. *Bioinformatics*, *26*(5), 589–595. https://doi.org/10.1093/bioinformatics/btp698

Li, H., Handsaker, B., Wysoker, A., Fennell, T., Ruan, J., Homer, N., Marth, G., Abecasis, G., & Durbin, R. (2009). The Sequence Alignment/Map format and SAMtools. *Bioinformatics*, *25*(16), 2078–2079. https://doi.org/10.1093/bioinformatics/btp352

Li, X., Wang, X., He, K., Ma, Y., Su, N., He, H., Stolc, V., Tongprasit, W., Jin, W., Jiang, J., Terzaghi, W., Li, S., Xing, W. D., & Deng, X. W. (2008). High-resolution mapping of epigenetic modifications of the rice genome uncovers interplay between DNA methylation, histone methylation, and gene expression. *Plant Cell*, *20*(2), 259–276. https://doi.org/10.1105/tpc.107.056879

Li, Z., Jiang, D., Fu, X., Luo, X., Liu, R., & He, Y. (2016). Coupling of histone methylation and RNA processing by the nuclear mRNA cap-binding complex. *Nature Plants*, *2*(3). https://doi.org/10.1038/NPLANTS.2016.15

Liang, D., Zhang, Z., Wu, H., Huang, C., Shuai, P., Ye, C.-Y., Tang, S., Wang, Y., Yang, L., Wang, J., Yin, W., & Xia, X. (2014). Single-base-resolution methylomes of populus trichocarpa reveal the association between DNA methylation and drought stress. *BMC Genetics*, *15*(S1), S9. https://doi.org/10.1186/1471-2156-15-S1-S9

Liang, J., Yi, L., Li, L., Zhang, H., Zhang, Y., Deng, G., Long, H., & Yu, M. (2022). Identification of PP2C Genes in Tibetan Hulless Barley (Hordeum vulgare var. nudum) Under Dehydration Stress and Initiatory Expression and Functional Analysis of HvPP2C59. *Plant Molecular Biology Reporter*, *40*(4), 611–627. https://doi.org/10.1007/s11105-022-01340-y

Lim, C., Baek, W., Jung, J., Kim, J., & Lee, S. (2015). Function of ABA in Stomatal Defense against Biotic and Drought Stresses. *International Journal of Molecular Sciences*, *16*(12), 15251–15270. https://doi.org/10.3390/ijms160715251

Lima-De-Faria, A., & Jaworska, H. (1968). Late DNA synthesis in heterochromatin. *Nature*, *217*(5124), 138–142. https://doi.org/10.1038/217138a0

Lindroth, A. M., Cao, X., Jackson, J. P., Zilberman, D., McCallum, C. M., Henikoff, S., & Jacobsen, S. E. (2001). Requirement of CHROMOMETHYLASE3 for maintenance of CpXpG methylation. *Science*, *292*(5524), 2077–2080. https://doi.org/10.1126/science.1059745

Lister, R., O'Malley, R. C., Tonti-Filippini, J., Gregory, B. D., Berry, C. C., Millar, A. H., & Ecker, J. R. (2008). Highly Integrated Single-Base Resolution Maps of the Epigenome in Arabidopsis. *Cell*, *133*(3), 523–536. https://doi.org/10.1016/j.cell.2008.03.029

Liu, C., Lu, F., Cui, X., & Cao, X. (2010). Histone Methylation in Higher Plants. *Annual Review of Plant Biology*, *61*(1), 395–420. https://doi.org/10.1146/annurev.arplant.043008.091939

Liu, J., & He, Z. (2020). Small DNA Methylation, Big Player in Plant Abiotic Stress Responses and Memory. *Frontiers in Plant Science*, *11*, 595603. https://doi.org/10.3389/fpls.2020.595603

Lu, R. J. H., Lin, P. Y., Yen, M. R., Wu, B. H., & Chen, P. Y. (2023). MethylC-analyzer: a comprehensive downstream pipeline for the analysis of genome-wide DNA methylation. *Botanical Studies*, *64*(1), 1–10. https://doi.org/10.1186/s40529-022-00366-5

Lu, X., Wang, X., Chen, X., Shu, N., Wang, J., Wang, D., Wang, S., Fan, W., Guo, L., Guo, X., & Ye, W. (2017). Single-base resolution methylomes of upland cotton (Gossypium hirsutum L.) reveal epigenome modifications in response to drought stress. *BMC Genomics*, *18*(1), 1–14. https://doi.org/10.1186/s12864-017-3681-y

Lu, Z., & Neumann, P. M. (1998). Water-stressed maize, barley and rice seedlings show species diversity in mechanisms of leaf growth inhibition. *Journal of Experimental Botany*, *49*(329), 1945–1952. https://doi.org/10.1093/jxb/49.329.1945

Luger, K., Mäder, A. W., Richmond, R. K., Sargent, D. F., Richmond, T. J., Mä Der, A. W., Richmond, R. K., Sargent, D. F., Richmond, T. J., Mäder, A. W., Richmond, R. K., Sargent, D. F., & Richmond, T. J. (1997). Crystal structure of the nucleosome core particle at 2.8 Å resolution. *Nature*, *389*(6648), 251–260. https://doi.org/10.1038/38444

Luo, M., Liu, X., Singh, P., Cui, Y., Zimmerli, L., & Wu, K. (2012). Chromatin modifications and remodeling in plant abiotic stress responses. *Biochimica et Biophysica Acta (BBA) - Gene

Regulatory Mechanisms, *1819*(2), 129–136. https://doi.org/10.1016/j.bbagrm.2011.06.008

Lusser, A., Eberharter, A., Loidl, A., Goralik-Schramel, M., Horngacher, M., Haas, H., & Loidl, P. (1999). Analysis of the histone acetyltransferase B complex of maize embryos. *Nucleic Acids Research*, *27*(22), 4427–4435. https://doi.org/10.1093/nar/27.22.4427

Lynch, J. P., Chimungu, J. G., & Brown, K. M. (2014). Root anatomical phenes associated with water acquisition from drying soil : targets for crop improvement. *Journal of Experimental Botany*, *65*(21), 6155–6166. https://doi.org/10.1093/jxb/eru162

Ma, Y., Szostkiewicz, I., Korte, A., Moes, D., Yang, Y., Christmann, A., & Grill, E. (2009). Regulators of PP2C Phosphatase Activity Function as Abscisic Acid Sensors. *Science*, *324*(5930), 1064–1068. https://doi.org/10.1126/science.1172408

Malagnac, F., Bartee, L., Bender, J., West, P. T., Li, Q., Malagnac, F., Bartee, L., & Bender, J. (2002). An Arabidopsis SET domain protein required for maintenance but not establishment of DNA methylation. *EMBO Journal*, *21*(24), 6842–6852. https://doi.org/10.1093/emboj/cdf687

Malapeira, J., Khaitova, L. C., & Mas, P. (2012). Ordered changes in histone modifications at the core of the Arabidopsis circadian clock. *Proceedings of the National Academy of Sciences of the United States of America*, *109*(52), 21540–21545. https://doi.org/10.1073/pnas.1217022110

Malefo, M. B., Mathibela, E. O., Crampton, B. G., & Makgopa, M. E. (2020). Investigating the role of Bowman-Birk serine protease inhibitor in Arabidopsis plants under drought stress. *Plant Physiology and Biochemistry*, *149*, 286–293. https://doi.org/10.1016/j.plaphy.2020.02.007

Malinowska, M., Nagy, I., Wagemaker, C. A. M., Ruud, A. K., Svane, S. F., Thorup-Kristensen, K., Jensen, C. S., Eriksen, B., Krusell, L., Jahoor, A., Jensen, J., Eriksen, L. B., & Asp, T. (2020). The cytosine methylation landscape of spring barley revealed by a new reduced representation bisulfite sequencing pipeline, WellMeth. *Plant Genome*, *13*(3), 1–18. https://doi.org/10.1002/tpg2.20049

Manh, M. B., Ost, C., Peiter, E., Hause, B., Krupinska, K., & Humbeck, K. (2023). WHIRLY1 Acts Upstream of ABA-Related Reprogramming of Drought-Induced Gene Expression in Barley and Affects Stress-Related Histone Modifications. *International Journal of Molecular Sciences*, *24*(7), 6326. https://doi.org/10.3390/ijms24076326

Marmorstein, R., & Zhou, M.-M. (2014). Writers and Readers of Histone Acetylation: Structure, Mechanism, and Inhibition. *Cold Spring Harbor Perspectives in Biology*, *6*(7), a018762–a018762. https://doi.org/10.1101/cshperspect.a018762

Martin, M. (2011). Cutadapt removes adapter sequences from high-throughput sequencing reads. *EMBnet.Journal*, *17*(1), 10. https://doi.org/10.14806/ej.17.1.200

Mascher, M. (2019). *Pseudomolecules and annotation of the second version of the reference genome sequence assembly of barley cv. Morex [Morex V2]*. e!DAL - Plant Genomics and Phenomics Research Data Repository (PGP), IPK Gatersleben, Seeland OT Gatersleben, Corrensstraße 3,

06466, Germany. https://doi.org/10.5447/IPK/2019/8

Mascher, M. (2020). Pseudomolecules and annotation of the third version of the reference genome sequence assembly of barley cv. Morex [Morex V3]. *E!DAL - Plant Genomics and Phenomics Research Data Repository (PGP)*. https://doi.org/https://doi.org/10.5447/ipk/2021/3

Mascher, M., Gundlach, H., Himmelbach, A., Beier, S., Twardziok, S. O., Wicker, T., Radchuk, V., Dockter, C., Hedley, P. E., Russell, J., Bayer, M., Ramsay, L., Liu, H., Haberer, G., Zhang, X.-Q., Zhang, Q., Barrero, R. A., Li, L., Taudien, S., Groth, M., & Stein, N. (2017). A chromosome conformation capture ordered sequence of the barley genome. *Nature*, *544*(7651), 427–433. https://doi.org/10.1038/nature22043

Mascher, M., Wicker, T., Jenkins, J., Plott, C., Lux, T., Koh, C. S., Ens, J., Gundlach, H., Boston, L. B., Tulpová, Z., Holden, S., Hernández-Pinzón, I., Scholz, U., Mayer, K. F. X., Spannagl, M., Pozniak, C. J., Sharpe, A. G., Simková, H., Moscou, M. J., Grimwood, J., Schmutz, J., & Stein, N. (2021). Long-read sequence assembly: A technical evaluation in barley. *Plant Cell*, *33*(6), 1888–1906. https://doi.org/10.1093/plcell/koab077

Mathieu, O., Probst, A. V., & Paszkowski, J. (2005). Distinct regulation of histone H3 methylation at lysines 27 and 9 by CpG methylation in Arabidopsis. *EMBO Journal*, *24*(15), 2783–2791. https://doi.org/10.1038/sj.emboj.7600743

Matzke, M. A., & Mosher, R. A. (2014). RNA-directed DNA methylation: an epigenetic pathway of increasing complexity. *Nature Reviews Genetics*, *15*(6), 394–408. https://doi.org/10.1038/nrg3683

McCarthy, D. J., Chen, Y., & Smyth, G. K. (2012). Differential expression analysis of multifactor RNA-Seq experiments with respect to biological variation. *Nucleic Acids Research*, *40*(10), 4288–4297. https://doi.org/10.1093/nar/gks042

Merlot, S., Gosti, F., Guerrier, D., Vavasseur, A., & Giraudat, J. (2001). The ABI1 and ABI2 protein phosphatases 2C act in a negative feedback regulatory loop of the abscisic acid signalling pathway. *Plant Journal*, *25*(3), 295–303. https://doi.org/10.1046/j.1365-313X.2001.00965.x

Millar, A. A., Jacobsen, J. V., Ross, J. J., Helliwell, C. A., Poole, A. T., Scofield, G., Reid, J. B., & Gubler, F. (2006). Seed dormancy and ABA metabolism in Arabidopsis and barley: The role of ABA 8′-hydroxylase. *Plant Journal*, *45*(6), 942–954. https://doi.org/10.1111/j.1365-313X.2006.02659.x

Monat, C., Padmarasu, S., Lux, T., Wicker, T., Gundlach, H., Himmelbach, A., Ens, J., Li, C., Muehlbauer, G. J., Schulman, A. H., Waugh, R., Braumann, I., Pozniak, C., Scholz, U., Mayer, K. F. X., Spannagl, M., Stein, N., & Mascher, M. (2019). TRITEX: Chromosome-scale sequence assembly of Triticeae genomes with open-source tools. *Genome Biology*, *20*(1), 1–18. https://doi.org/10.1186/s13059-019-1899-5

Moore, J. P., Vicré-Gibouin, M., Farrant, J. M., & Driouich, A. (2008). Adaptations of higher plant cell walls to water loss: Drought vs desiccation. *Physiologia Plantarum*, *134*(2), 237–245.

https://doi.org/10.1111/j.1399-3054.2008.01134.x

Mustilli, A. C., Merlot, S., Vavasseur, A., Fenzi, F., & Giraudat, J. (2002). Arabidopsis OST1 protein kinase mediates the regulation of stomatal aperture by abscisic acid and acts upstream of reactive oxygen species production. *Plant Cell*, *14*(12), 3089–3099. https://doi.org/10.1105/tpc.007906

Nagy, Z., Németh, E., Guóth, A., Bona, L., Wodala, B., & Pécsváradi, A. (2013). Plant Physiology and Biochemistry Metabolic indicators of drought stress tolerance in wheat : Glutamine synthetase isoenzymes and Rubisco. *Plant Physiology et Biochemistry*, *67*, 48–54. https://doi.org/10.1016/j.plaphy.2013.03.001

Nakashima, K., Fujita, Y., Katsura, K., Maruyama, K., Narusaka, Y., Seki, M., Shinozaki, K., & Yamaguchi-Shinozaki, K. (2006). Transcriptional regulation of ABI3- and ABA-responsive genes including RD29B and RD29A in seeds, germinating embryos, and seedlings of Arabidopsis. *Plant Molecular Biology*, *60*(1), 51–68. https://doi.org/10.1007/s11103-005-2418-5

Narusaka, Y., Nakashima, K., Shinwari, Z. K., Sakuma, Y., Furihata, T., Abe, H., Narusaka, M., Shinozaki, K., & Yamaguchi-Shinozaki, K. (2003). Interaction between two cis-acting elements, ABRE and DRE, in ABA-dependent expression of Arabidopsis rd29A gene in response to dehydration and high-salinity stresses. *The Plant Journal*, *34*(2), 137–148. https://doi.org/10.1046/j.1365-313X.2003.01708.x

Nguyen, N. H., Jung, C., & Cheong, J.-J. (2019). Chromatin remodeling for the transcription of type 2C protein phosphatase genes in response to salt stress. *Plant Physiology and Biochemistry*, *141*, 325–331. https://doi.org/10.1016/j.plaphy.2019.06.012

Niederhuth, C. E., Bewick, A. J., Ji, L., Alabady, M. S., Kim, K. Do, Li, Q., Rohr, N. A., Rambani, A., Burke, J. M., Udall, J. A., Egesi, C., Schmutz, J., Grimwood, J., Jackson, S. A., Springer, N. M., & Schmitz, R. J. (2016). Widespread natural variation of DNA methylation within angiosperms. *Genome Biology*, *17*(1), 1–19. https://doi.org/10.1186/s13059-016-1059-0

Nishimura, N., Yoshida, T., Kitahata, N., Asami, T., Shinozaki, K., & Hirayama, T. (2007). ABA-Hypersensitive Germination1 encodes a protein phosphatase 2C, an essential component of abscisic acid signaling in Arabidopsis seed. *Plant Journal*, *50*(6), 935–949. https://doi.org/10.1111/j.1365-313X.2007.03107.x

Ortega-Galisteo, A. P., Morales-Ruiz, T., Ariza, R. R., & Roldán-Arjona, T. (2008). Arabidopsis DEMETER-LIKE proteins DML2 and DML3 are required for appropriate distribution of DNA methylation marks. *Plant Molecular Biology*, *67*(6), 671–681. https://doi.org/10.1007/s11103-008-9346-0

Ost, C., Cao, H. X., Nguyen, T. L., Himmelbach, A., Mascher, M., Stein, N., & Humbeck, K. (2023). Drought-Stress-Related Reprogramming of Gene Expression in Barley Involves Differential Histone Modifications at ABA-Related Genes. *International Journal of Molecular Sciences*, *24*(15). https://doi.org/10.3390/ijms241512065

Pandey, R., Müller, A., Napoli, C. A., Selinger, D. A., Pikaard, C. S., Richards, E. J., Bender, J., Mount, D. W., & Jorgensen, R. A. (2002). Analysis of histone acetyltransferase and histone deacetylase families of Arabidopsis thaliana suggests functional diversification of chromatin modification among multicellular eukaryotes. *Nucleic Acids Research*, *30*(23), 5036–5055. https://doi.org/10.1093/nar/gkf660

Pandian, B. A., Sathishraj, R., Djanaguiraman, M., Prasad, P. V. V., & Jugulam, M. (2020). Role of Cytochrome P450 Enzymes in Plant Stress Response. *Antioxidants*, *9*(5), 454. https://doi.org/10.3390/antiox9050454

Papaefthimiou, D., & Tsaftaris, A. S. (2012). Characterization of a drought inducible trithorax-like H3K4 methyltransferase from barley. *Biologia Plantarum*, *56*(4), 683–692. https://doi.org/10.1007/s10535-012-0125-z

Park, P. J. (2009). ChIP-seq: Advantages and challenges of a maturing technology. *Nature Reviews Genetics*, *10*(10), 669–680. https://doi.org/10.1038/nrg2641

Park, S.-Y., Fung, P., Nishimura, N., Jensen, D. R., Fujii, H., Zhao, Y., Lumba, S., Santiago, J., Rodrigues, A., Chow, T. F., Alfred, S. E., Bonetta, D., Finkelstein, R., Provart, N. J., Desveaux, D., Rodriguez, P. L., McCourt, P., Zhu, J.-K., Schroeder, J. I., Volkman, B. F., & Cutler, S. R. (2009). Abscisic Acid Inhibits Type 2C Protein Phosphatases via the PYR/PYL Family of START Proteins. *Science*, *324*(5930), 1068–1071. https://doi.org/10.1126/science.1173041

Park, Y. D. D., Papp, I., Moscone, E. A., Iglesias, V. A., Vaucheret, H., Matzke, A. J. M., & Matzke, M. A. (1996). Gene silencing mediated by promoter homology occurs at the level of transcription and results in meiotically heritable alterations in methylation and gene activity. *Plant Journal*, *9*(2), 183–194. https://doi.org/10.1046/j.1365-313X.1996.09020183.x

Parthun, M. R., Widom, J., & Gottschling, D. E. (1996). The major cytoplasmic histone acetyltransferase in yeast: Links to chromatin replication and histone metabolism. *Cell*, *87*(1), 85–94. https://doi.org/10.1016/S0092-8674(00)81325-2

Penterman, J., Zilberman, D., Jin, H. H., Ballinger, T., Henikoff, S., & Fischer, R. L. (2007). DNA demethylation in the Arabidopsis genome. *Proceedings of the National Academy of Sciences of the United States of America*, *104*(16), 6752–6757. https://doi.org/10.1073/pnas.0701861104

Pfaffl, M. W. (2002). Relative expression software tool (REST(C)) for group-wise comparison and statistical analysis of relative expression results in real-time PCR. *Nucleic Acids Research*, *30*(9), 36e – 36. https://doi.org/10.1093/nar/30.9.e36

Pfluger, J., & Wagner, D. (2007). Histone modifications and dynamic regulation of genome accessibility in plants. *Current Opinion in Plant Biology*, *10*(6), 645–652. https://doi.org/10.1016/j.pbi.2007.07.013

Pikaard, C. S., & Scheid, O. M. (2014). Epigenetic regulation in plants. *Cold Spring Harbor Perspectives*

in Biology, *6*(12), 1–32. https://doi.org/10.1101/cshperspect.a019315

Pinheiro, C., & Chaves, M. M. (2011). Photosynthesis and drought: Can we make metabolic connections from available data? *Journal of Experimental Botany*, *62*(3), 869–882. https://doi.org/10.1093/jxb/erq340

Pokholok, D. K., Harbison, C. T., Levine, S., Cole, M., Hannett, N. M., Tong, I. L., Bell, G. W., Walker, K., Rolfe, P. A., Herbolsheimer, E., Zeitlinger, J., Lewitter, F., Gifford, D. K., & Young, R. A. (2005). Genome-wide map of nucleosome acetylation and methylation in yeast. *Cell*, *122*(4), 517–527. https://doi.org/10.1016/j.cell.2005.06.026

Probst, A. V., & Mittelsten Scheid, O. (2015). Stress-induced structural changes in plant chromatin. *Current Opinion in Plant Biology*, *27*, 8–16. https://doi.org/10.1016/j.pbi.2015.05.011

Qi, J., Song, C. P., Wang, B., Zhou, J., Kangasjärvi, J., Zhu, J. K., & Gong, Z. (2018). Reactive oxygen species signaling and stomatal movement in plant responses to drought stress and pathogen attack. *Journal of Integrative Plant Biology*, *60*(9), 805–826. https://doi.org/10.1111/jipb.12654

Quinlan, A. R., & Hall, I. M. (2010). BEDTools: A flexible suite of utilities for comparing genomic features. *Bioinformatics*, *26*(6), 841–842. https://doi.org/10.1093/bioinformatics/btq033

Raghavendra, A. S., Gonugunta, V. K., Christmann, A., & Grill, E. (2010). ABA perception and signalling. *Trends in Plant Science*, *15*(7), 395–401. https://doi.org/10.1016/j.tplants.2010.04.006

Ramírez, F., Dündar, F., Diehl, S., Grüning, B. A., & Manke, T. (2014). deepTools: a flexible platform for exploring deep-sequencing data. *Nucleic Acids Research*, *42*(W1), W187–W191. https://doi.org/10.1093/nar/gku365

Rampino, P., Pataleo, S., Gerardi, C., Mita, G., & Perrotta, C. (2006). Drought stress response in wheat: Physiological and molecular analysis of resistant and sensitive genotypes. *Plant, Cell and Environment*, *29*(12), 2143–2152. https://doi.org/10.1111/j.1365-3040.2006.01588.x

Rasmusson, D. C., & Wilcoxson, R. W. (1979). Registration of Morex Barley 1 (Reg. No. 158). *Crop Science*, *19*(2), 293–293. https://doi.org/10.2135/cropsci1979.0011183X001900020032x

Ren, C., Zhu, X., Zhang, P., & Gong, Q. (2016). Arabidopsis COP1-interacting protein 1 is a positive regulator of ABA response. *Biochemical and Biophysical Research Communications*, *477*(4), 847–853. https://doi.org/10.1016/j.bbrc.2016.06.147

Richards, E. J. (1997). DNA methylation and plant development. *Trends in Genetics*, *13*(8), 319–323. https://doi.org/10.1016/S0168-9525(97)01199-2

Ritchie, M. E., Phipson, B., Wu, D., Hu, Y., Law, C. W., Shi, W., & Smyth, G. K. (2015). Limma powers differential expression analyses for RNA-sequencing and microarray studies. *Nucleic Acids Research*, *43*(7), e47. https://doi.org/10.1093/nar/gkv007

Robinson, J. T., Thorvaldsdóttir, H., Winckler, W., Guttman, M., Lander, E. S., Getz, G., & Mesirov, J.

P. (2011). Integrative genomics viewer. *Nature Biotechnology*, *29*(1), 24–26. https://doi.org/10.1038/nbt.1754

Robinson, M. D., McCarthy, D. J., & Smyth, G. K. (2010). edgeR: A Bioconductor package for differential expression analysis of digital gene expression data. *Bioinformatics*, *26*(1), 139–140. https://doi.org/10.1093/bioinformatics/btp616

Rodriguez, P. L., Benning, G., & Grill, E. (1998). ABI2, a second protein phosphatase 2C involved in abscisic acid signal transduction in Arabidopsis. *FEBS Letters*, *421*(3), 185–190. https://doi.org/10.1016/S0014-5793(97)01558-5

Roh, T. Y., Cuddapah, S., & Zhao, K. (2005). Active chromatin domains are defined by acetylation islands revealed by genome-wide mapping. *Genes and Development*, *19*(5), 542–552. https://doi.org/10.1101/gad.1272505

Roth, S. Y., Denu, J. M., & Allis, C. D. (2001). Histone Acetyltransferases. *Annual Review of Biochemistry*, *70*(1), 81–120. https://doi.org/10.1146/annurev.biochem.70.1.81

Roudier, F., Ahmed, I., Bérard, C., Sarazin, A., Mary-Huard, T., Cortijo, S., Bouyer, D., Caillieux, E., Duvernois-Berthet, E., Al-Shikhley, L., Giraut, L., Després, B., Drevensek, S., Barneche, F., Dèrozier, S., Brunaud, V., Aubourg, S., Schnittger, A., Bowler, C., Martin-Magniette, M.-L., Robin, S., Caboche, M., & Colot, V. (2011). Integrative epigenomic mapping defines four main chromatin states in Arabidopsis. *The EMBO Journal*, *30*(10), 1928–1938. https://doi.org/10.1038/emboj.2011.103

Roy, S. (2016). Function of MYB domain transcription factors in abiotic stress and epigenetic control of stress response in plant genome. *Plant Signaling & Behavior*, *11*(1), e1117723. https://doi.org/10.1080/15592324.2015.1117723

Saez, A., Apostolova, N., Gonzalez-Guzman, M., Gonzalez-Garcia, M. P., Nicolas, C., Lorenzo, O., & Rodriguez, P. L. (2004). Gain-of-function and loss-of-function phenotypes of the protein phosphatase 2C HAB1 reveal its role as a negative regulator of abscisic acid signalling. *The Plant Journal*, *37*(3), 354–369. https://doi.org/10.1046/j.1365-313X.2003.01966.x

Samarah, N. H., Alqudah, A. M., Amayreh, J. A., & McAndrews, G. M. (2009). The effect of late-terminal drought stress on yield components of four barley cultivars. *Journal of Agronomy and Crop Science*, *195*(6), 427–441. https://doi.org/10.1111/j.1439-037X.2009.00387.x

SanMiguel, P., Tikhonov, A., Jin, Y. K., Motchoulskaia, N., Zakharov, D., Melake-Berhan, A., Springer, P. S., Edwards, K. J., Lee, M., Avramova, Z., & Bennetzen, J. L. (1996). Nested retrotransposons in the intergenic regions of the maize genome. *Science*, *274*(5288), 765–768. https://doi.org/10.1126/science.274.5288.765

Schauberger, P., Walker, A., & Braglia, L. (2020). Openxlsx: Read, Write and Edit xlsx Files. *R Package Version*, *4*(5).

Schroeder, J. I., Kwak, J. M., & Allen, G. J. (2001). Guard cell abscisic acid signalling and engineering drought hardiness in plants. *Nature*, *410*(6826), 327–330. https://doi.org/10.1038/35066500

Schübeler, D., MacAlpine, D. M., Scalzo, D., Wirbelauer, C., Kooperberg, C., Van Leeuwen, F., Gottschling, D. E., O'Neill, L. P., Turner, B. M., Delrow, J., Bell, S. P., & Groudine, M. (2004). The histone modification pattern of active genes revealed through genome-wide chromatin analysis of a higher eukaryote. *Genes and Development*, *18*(11), 1263–1271. https://doi.org/10.1101/gad.1198204

Schuettengruber, B., Martinez, A. M., Iovino, N., & Cavalli, G. (2011). Trithorax group proteins: Switching genes on and keeping them active. *Nature Reviews Molecular Cell Biology*, *12*(12), 799–814. https://doi.org/10.1038/nrm3230

Schweighofer, A., Hirt, H., & Meskiene, I. (2004). Plant PP2C phosphatases: Emerging functions in stress signaling. *Trends in Plant Science*, *9*(5), 236–243. https://doi.org/10.1016/j.tplants.2004.03.007

Secco, D., Wang, C., Shou, H., Schultz, M. D., Chiarenza, S., Nussaume, L., Ecker, J. R., Whelan, J., & Lister, R. (2015). Stress induced gene expression drives transient DNA methylation changes at adjacent repetitive elements. *ELife*, *4*, 1–26. https://doi.org/10.7554/elife.09343

Seiler, C., Harshavardhan, V. T., Reddy, P. S., Hensel, G., Kumlehn, J., Eschen-lippold, L., Rajesh, K., Korzun, V., Wobus, U., Lee, J., Selvaraj, G., & Sreenivasulu, N. (2014). Abscisic acid flux alterations result in differential abscisic acid signaling responses and impact assimilation efficiency in barley under terminal drought stress. *Plant Physiology*, *164*(4), 1677–1696. https://doi.org/10.1104/pp.113.229062

Shahryary, Y., Hazarika, R. R., & Johannes, F. (2020). MethylStar: A fast and robust pre-processing pipeline for bulk or single-cell whole-genome bisulfite sequencing data. *BMC Genomics*, *21*(1), 1–8. https://doi.org/10.1186/s12864-020-06886-3

Sharma, C., Kumar, S., Saripalli, G., Jain, N., Raghuvanshi, S., Sharma, J. B., Prabhu, K. V., Sharma, P. K., Balyan, H. S., & Gupta, P. K. (2019). H3K4/K9 acetylation and Lr28-mediated expression of six leaf rust responsive genes in wheat (Triticum aestivum). *Molecular Genetics and Genomics*, *294*(1), 227–241. https://doi.org/10.1007/s00438-018-1500-z

Sheen, J. (1998). Mutational analysis of protein phosphatase 2C involved in abscisic acid signal transduction in higher plants. *Proceedings of the National Academy of Sciences of the United States of America*, *95*(3), 975–980. https://doi.org/10.1073/pnas.95.3.975

Shilatifard, A. (2012). The COMPASS family of histone H3K4 methylases: Mechanisms of regulation in development and disease pathogenesis. *Annual Review of Biochemistry*, *81*, 65–95. https://doi.org/10.1146/annurev-biochem-051710-134100

Shinozaki, K., & Yamaguchi-Shinozaki, K. (2007). Gene networks involved in drought stress response

and tolerance. *Journal of Experimental Botany*, *58*(2), 221–227. https://doi.org/10.1093/jxb/erl164

Sims, D., Sudbery, I., Ilott, N. E., Heger, A., & Ponting, C. P. (2014). Sequencing depth and coverage: Key considerations in genomic analyses. *Nature Reviews Genetics*, *15*(2), 121–132. https://doi.org/10.1038/nrg3642

Singh, A., Giri, J., Kapoor, S., Tyagi, A. K., & Pandey, G. K. (2010). Protein phosphatase complement in rice: Genome-wide identification and transcriptional analysis under abiotic stress conditions and reproductive development. *BMC Genomics*, *11*(1). https://doi.org/10.1186/1471-2164-11-435

Singh, A., Jha, S. K., Bagri, J., & Pandey, G. K. (2015). ABA inducible rice protein phosphatase 2C confers ABA insensitivity and abiotic stress tolerance in arabidopsis. *PLoS ONE*, *10*(4), 1–24. https://doi.org/10.1371/journal.pone.0125168

Singh, A., Pandey, A., Srivastava, A. K., Tran, L.-S. S. P., & Pandey, G. K. (2016). Plant protein phosphatases 2C: from genomic diversity to functional multiplicity and importance in stress management. *Critical Reviews in Biotechnology*, *36*(6), 1023–1035. https://doi.org/10.3109/07388551.2015.1083941

Singh, A., & Pandey, G. K. (2012). Protein phosphatases: a genomic outlook to understand their function in plants. *Journal of Plant Biochemistry and Biotechnology*, *21*(S1), 100–107. https://doi.org/10.1007/s13562-012-0150-1

Solomon, E. R., Caldwell, K. K., & Allan, A. M. (2021). A novel method for the normalization of ChIP-qPCR data. *MethodsX*, *8*, 101504. https://doi.org/10.1016/j.mex.2021.101504

Song, J., Henry, H., & Tian, L. (2020). Drought-inducible changes in the histone modification H3K9ac are associated with drought-responsive gene expression in Brachypodium distachyon. *Plant Biology*, *22*(3), 433–440. https://doi.org/10.1111/plb.13057

Song, Y., Ji, D., Li, S., Wang, P., Li, Q., & Xiang, F. (2012). The dynamic changes of DNA methylation and histone modifications of salt responsive transcription factor genes in soybean. *PLoS ONE*, *7*(7), 1–11. https://doi.org/10.1371/journal.pone.0041274

Soon, F. F., Ng, L. M., Zhou, X. E., West, G. M., Kovach, A., Tan, M. H. E., Suino-Powell, K. M., He, Y., Xu, Y., Chalmers, M. J., Brunzelle, J. S., Zhang, H., Yang, H., Jiang, H., Li, J., Yong, E. L., Cutler, S., Zhu, J. K., Griffin, P. R., Melcher, K., & Xu, H. E. (2012). Molecular mimicry regulates ABA signaling by SnRK2 kinases and PP2C phosphatases. *Science*, *335*(6064), 85–88. https://doi.org/10.1126/science.1215106

Stam, M., Viterbo, A., Mol, J. N. M., & Kooter, J. M. (1998). Position-Dependent Methylation and Transcriptional Silencing of Transgenes in Inverted T-DNA Repeats: Implications for Posttranscriptional Silencing of Homologous Host Genes in Plants. *Molecular and Cellular Biology*, *18*(11), 6165–6177. https://doi.org/10.1128/MCB.18.11.6165

Stark, R., & Brown, G. (2011). DiffBind : differential binding analysis of ChIP-Seq peak data. *R Package*

Version 100.4.3, 1–29. https://doi.org/10.18129/B9.bioc.DiffBind.

Sterner, D. E., & Berger, S. L. (2000). Acetylation of Histones and Transcription-Related Factors. *Microbiology and Molecular Biology Reviews*, *64*(2), 435–459. https://doi.org/10.1128/MMBR.64.2.435-459.2000

Straub, P. F., Shen, Q., & Ho, T. hua D. (1994). Structure and promoter analysis of an ABA- and stress-regulated barley gene, HVA1. *Plant Molecular Biology*, *26*(2), 617–630. https://doi.org/10.1007/BF00013748

Strizhov, N., Ábrahám, E., Ökrész, L., Blickling, S., Zilberstein, A., Schell, J., Koncz, C., & Szabados, L. (1997). Differential expression of two P5CS genes controlling proline accumulation during salt-stress requires ABA and is regulated by ABA1, ABI1 and AXR2 in Arabidopsis. *Plant Journal*, *12*(3), 557–569. https://doi.org/10.1046/j.1365-313x.1997.00537.x

Stroud, H., Do, T., Du, J., Zhong, X., Feng, S., Johnson, L., Patel, D. J., & Jacobsen, S. E. (2014). Non-CG methylation patterns shape the epigenetic landscape in Arabidopsis. *Nature Structural and Molecular Biology*, *21*(1), 64–72. https://doi.org/10.1038/nsmb.2735

Stroud, H., Greenberg, M. V. C., Feng, S., Bernatavichute, Y. V., & Jacobsen, S. E. (2013). Comprehensive analysis of silencing mutants reveals complex regulation of the Arabidopsis methylome. *Cell*, *152*(1–2), 352–364. https://doi.org/10.1016/j.cell.2012.10.054

Szostkiewicz, I., Richter, K., Kepka, M., Demmel, S., Ma, Y., Korte, A., Assaad, F. F., Christmann, A., & Grill, E. (2010). Closely related receptor complexes differ in their ABA selectivity and sensitivity. *Plant Journal*, *61*(1), 25–35. https://doi.org/10.1111/j.1365-313X.2009.04025.x

Takuno, S., & Gaut, B. S. (2013). Gene body methylation is conserved between plant orthologs and is of evolutionary consequence. *Proceedings of the National Academy of Sciences*, *110*(5), 1797–1802. https://doi.org/10.1073/pnas.1215380110

Talamè, V., Ozturk, N. Z., Bohnert, H. J., & Tuberosa, R. (2007). Barley transcript profiles under dehydration shock and drought stress treatments: A comparative analysis. *Journal of Experimental Botany*, *58*(2), 229–240. https://doi.org/10.1093/jxb/erl163

Tamada, Y., Yun, J. Y., Woo, S. C., & Amasino, R. M. (2009). ARABIDOPSIS TRITHORAX-RELATED7 is required for methylation of lysine 4 of histone H3 and for transcriptional activation of FLOWERING LOCUS C. *Plant Cell*, *21*(10), 3257–3269. https://doi.org/10.1105/tpc.109.070060

Tamiru, M., Undan, J. R., Takagi, H., Abe, A., Yoshida, K., Undan, J. Q., Natsume, S., Uemura, A., Saitoh, H., Matsumura, H., Urasaki, N., Yokota, T., & Terauchi, R. (2015). A cytochrome P450, OsDSS1, is involved in growth and drought stress responses in rice (Oryza sativa L.). *Plant Molecular Biology*, *88*(1–2), 85–99. https://doi.org/10.1007/s11103-015-0310-5

Tange, O. (2011). GNU parallel-the command-line power tool. *USENIX Mag.*, *36*(1), 42–47.

Team, R. C. (2014). *R: A language and environment for statistical computing. R Foundation for Statistical Computing*. http://www.r-project.org/

Temel, A., Janack, B., & Humbeck, K. (2017). Drought Stress-Related Physiological Changes and Histone Modifications in Barley Primary Leaves at HSP17 Gene. *Agronomy*, *7*(2), 43. https://doi.org/10.3390/agronomy7020043

Tian, L., & Chen, Z. J. (2001). Blocking histone deacetylation in Arabidopsis induces pleiotropic effects on plant gene regulation and development. *Proceedings of the National Academy of Sciences of the United States of America*, *98*(1), 200–205. https://doi.org/10.1073/pnas.98.1.200

Tian, L., Fong, M. P., Wang, J. J., Wei, N. E., Jiang, H., Doerge, R. W., & Chen, Z. J. (2005). Reversible histone acetylation and deacetylation mediate genome-wide, promoter-dependent and locus-specific changes in gene expression during plant development. *Genetics*, *169*(1), 337–345. https://doi.org/10.1534/genetics.104.033142

Tommasini, L., Svensson, J. T., Rodriguez, E. M., Wahid, A., Malatrasi, M., Kato, K., Wanamaker, S., Resnik, J., & Close, T. J. (2008). Dehydrin gene expression provides an indicator of low temperature and drought stress: Transcriptome-based analysis of Barley (Hordeum vulgare L.). *Functional and Integrative Genomics*, *8*(4), 387–405. https://doi.org/10.1007/s10142-008-0081-z

Tsuji, H., Saika, H., Tsutsumi, N., Hirai, A., & Nakazono, M. (2006). Dynamic and reversible changes in histone H3-Lys4 methylation and H3 acetylation occurring at submergence-inducible genes in rice. *Plant and Cell Physiology*, *47*(7), 995–1003. https://doi.org/10.1093/pcp/pcj072

Turner, N. C. (2018). Turgor maintenance by osmotic adjustment : 40 years of progress. *Journal of Experimental Botany*, *69*(13), 3223–3233. https://doi.org/10.1093/jxb/ery181

Ueda, M., & Seki, M. (2020). Histone Modifications Form Epigenetic Regulatory Networks to Regulate Abiotic Stress Response. *Plant Physiology*, *182*(1), 15–26. https://doi.org/10.1104/pp.19.00988

Uga, Y., Sugimoto, K., Ogawa, S., Rane, J., Ishitani, M., Hara, N., Kitomi, Y., Inukai, Y., Ono, K., Kanno, N., Inoue, H., Takehisa, H., Motoyama, R., Nagamura, Y., Wu, J., Matsumoto, T., Takai, T., Okuno, K., & Yano, M. (2013). Control of root system architecture by DEEPER ROOTING 1 increases rice yield under drought conditions. *Nature Genetics*, *45*(9), 1097–1102. https://doi.org/10.1038/ng.2725

Ullah, A., Sun, H., Yang, X., & Zhang, X. (2017). Drought coping strategies in cotton: increased crop per drop. *Plant Biotechnology Journal*, *15*(3), 271–284. https://doi.org/10.1111/pbi.12688

Uno, Y., Furihata, T., Abe, H., Yoshida, R., Shinozaki, K., & Yamaguchi-Shinozaki, K. (2000). Arabidopsis basic leucine zipper transcription factors involved in an abscisic acid-dependent signal transduction pathway under drought and high-salinity conditions. *Proceedings of the National Academy of Sciences of the United States of America*, *97*(21), 11632–11637. https://doi.org/10.1073/pnas.190309197

Untergasser, A., Cutcutache, I., Koressaar, T., Ye, J., Faircloth, B. C., Remm, M., & Rozen, S. G. (2012). Primer3-new capabilities and interfaces. *Nucleic Acids Research*, *40*(15), 1–12. https://doi.org/10.1093/nar/gks596

van Dijk, K., Ding, Y., Malkaram, S., Riethoven, J.-J. M., Liu, R., Yang, J., Laczko, P., Chen, H., Xia, Y., Ladunga, I., Avramova, Z., & Fromm, M. (2010). Dynamic changes in genome-wide histone H3 lysine 4 methylation patterns in response to dehydration stress in Arabidopsis thaliana. *BMC Plant Biology*, *10*(1), 238. https://doi.org/10.1186/1471-2229-10-238

Van Dooren, T. J. M., Silveira, A. B., Gilbault, E., Jiménez-Gómez, J. M., Martin, A., Bach, L., Tisné, S., Quadrana, L., Loudet, O., & Colot, V. (2020). Mild drought in the vegetative stage induces phenotypic, gene expression, and DNA methylation plasticity in Arabidopsis but no transgenerational effects. *Journal of Experimental Botany*, *71*(12), 3588–3602. https://doi.org/10.1093/jxb/eraa132

Vaseva, I. I., Zehirov, G., Kirova, E., & Simova-Stoilova, L. (2016). Transcript profiling of serine- and cysteine protease inhibitors in Triticum aestivum varieties with different drought tolerance. *Cereal Research Communications*, *44*(1), 79–88. https://doi.org/10.1556/0806.43.2015.032

Verbruggen, N., & Hermans, C. (2008). Proline accumulation in plants: A review. *Amino Acids*, *35*(4), 753–759. https://doi.org/10.1007/s00726-008-0061-6

Vergara, Z., & Gutierrez, C. (2017). Emerging roles of chromatin in the maintenance of genome organization and function in plants. In *Genome Biology* (Vol. 18, Issue 1). BioMed Central Ltd. https://doi.org/10.1186/s13059-017-1236-9

Verreault, A., Kaufman, P. D., Kobayashi, R., & Stillman, B. (1998). Nucleosomal DNA regulates the core-histone-binding subunit of the human Hat1 acetyltransferase. *Current Biology*, *8*(2), 96–108. https://doi.org/10.1016/S0960-9822(98)70040-5

Verslues, P. E., & Sharma, S. (2010). Proline Metabolism and Its Implications for Plant-Environment Interaction. *The Arabidopsis Book*, *8*(4), e0140. https://doi.org/10.1199/tab.0140

Wang, Q., Xu, J., Pu, X., Lv, H., Liu, Y., Ma, H., Wu, F., Wang, Q., Feng, X., Liu, T., Tang, Q., Liu, Y., & Lu, Y. (2021). Maize dna methylation in response to drought stress is involved in target gene expression and alternative splicing. *International Journal of Molecular Sciences*, *22*(15). https://doi.org/10.3390/ijms22158285

Wang, W., Qin, Q., Sun, F., Wang, Y., Xu, D., Li, Z., & Fu, B. (2016). Genome-Wide Differences in DNA Methylation Changes in Two Contrasting Rice Genotypes in Response to Drought Conditions. *Frontiers in Plant Science*, *7*, 1–13. https://doi.org/10.3389/fpls.2016.01675

Wasson, A. P., Richards, R. A., Chatrath, R., Misra, S. C., Prasad, S. V. S., Rebetzke, G. J., & Kirkegaard, J. A. (2012). Traits and selection strategies to improve root systems and water uptake in water-limited wheat crops. *Journal of Experimental Botany*, *63*(9), 3485–3498.

https://doi.org/10.1093/jxb/ers111

Wehner, G., Balko, C., Humbeck, K., Zyprian, E., & Ordon, F. (2016). Expression profiling of genes involved in drought stress and leaf senescence in juvenile barley. *BMC Plant Biology*, *16*(1), 1–12. https://doi.org/10.1186/s12870-015-0701-4

Wicker, T., Matthews, D. E., & Keller, B. (2002). TREP: A database for Triticeae repetitive elements. *Trends in Plant Science*, *7*(12), 561–562. https://doi.org/10.1016/S1360-1385(02)02372-5

Wu, Y., & Cosgrove, D. J. (2000). Adaptation of roots to low water potentials by changes in cell wall extensibility and cell wall proteins. *Journal of Experimental Botany*, *51*(350), 1543–1553. https://doi.org/10.1093/jexbot/51.350.1543

Xiang, Y., Sun, X., Gao, S., Qin, F., & Dai, M. (2017). Deletion of an Endoplasmic Reticulum Stress Response Element in a ZmPP2C-A Gene Facilitates Drought Tolerance of Maize Seedlings. *Molecular Plant*, *10*(3), 456–469. https://doi.org/10.1016/j.molp.2016.10.003

Xu, L., & Jiang, H. (2020). Writing and Reading Histone H3 Lysine 9 Methylation in Arabidopsis. *Frontiers in Plant Science*, *11*, 1–10. https://doi.org/10.3389/fpls.2020.00452

Xue, T., Wang, D., Zhang, S., Ehlting, J., Ni, F., Jakab, S., Zheng, C., & Zhong, Y. (2008). Genome-wide and expression analysis of protein phosphatase 2C in rice and Arabidopsis. *BMC Genomics*, *9*, 1–21. https://doi.org/10.1186/1471-2164-9-550

Yamaguchi-Shinozaki, K., & Shinozaki, K. (2005). Organization of cis-acting regulatory elements in osmotic- and cold-stress-responsive promoters. *Trends in Plant Science*, *10*(2), 88–94. https://doi.org/10.1016/j.tplants.2004.12.012

Yan, L., Zhai, X., Zhao, Z., & Fan, G. (2020). Whole-genome landscape of H3K4me3, H3K36me3 and H3K9ac and their association with gene expression during Paulownia witches' broom disease infection and recovery processes. *3 Biotech*, *10*(8), 336. https://doi.org/10.1007/s13205-020-02331-0

Yang, J., Yuan, L., Yen, M., Zheng, F., Ji, R., Peng, T., Gu, D., Yang, S., Cui, Y., Chen, P., Wu, K., & Liu, X. (2020). SWI3B and HDA6 interact and are required for transposon silencing in Arabidopsis. *The Plant Journal*, *102*(4), 809–822. https://doi.org/10.1111/tpj.14666

Yaqoob, U., Jan, N., Raman, P. V., Siddique, K. H. M., & John, R. (2022). Crosstalk between brassinosteroid signaling, ROS signaling and phenylpropanoid pathway during abiotic stress in plants: Does it exist? *Plant Stress*, *4*, 100075. https://doi.org/10.1016/j.stress.2022.100075

Ye, J., Coulouris, G., Zaretskaya, I., Cutcutache, I., Rozen, S., & Madden, T. L. (2012). Primer-BLAST: a tool to design target-specific primers for polymerase chain reaction. *BMC Bioinformatics*, *13*, 134. https://doi.org/10.1186/1471-2105-13-134

Yoder, J. A., Walsh, C. P., & Bestor, T. H. (1997). Cytosine methylation and the ecology of intragenomic

parasites. *Trends in Genetics*, *13*(8), 335–340. https://doi.org/10.1016/S0168-9525(97)01181-5

Yong-Villalobos, L., González-Morales, S. I., Wrobel, K., Gutiérrez-Alanis, D., Cervantes-Peréz, S. A., Hayano-Kanashiro, C., Oropeza-Aburto, A., Cruz-Ramírez, A., Martínez, O., & Herrera-Estrellaa, L. (2015). Methylome analysis reveals an important role for epigenetic changes in the regulation of the Arabidopsis response to phosphate starvation. *Proceedings of the National Academy of Sciences of the United States of America*, *112*(52), E7293–E7302. https://doi.org/10.1073/pnas.1522301112

Yoshida, T., Mogami, J., & Yamaguchi-Shinozaki, K. (2014). ABA-dependent and ABA-independent signaling in response to osmotic stress in plants. *Current Opinion in Plant Biology*, *21*, 133–139. https://doi.org/10.1016/j.pbi.2014.07.009

Yoshida, T., Nishimura, N., Kitahata, N., Kuromori, T., Ito, T., Asami, T., Shinozaki, K., & Hirayama, T. (2006). ABA-hypersensitive germination3 encodes a protein phosphatase 2C (AtPP2CA) that strongly regulates abscisic acid signaling during germination among Arabidopsis protein phosphatase 2Cs. *Plant Physiology*, *140*(1), 115–126. https://doi.org/10.1104/pp.105.070128

Yu, G., Wang, L. G., & He, Q. Y. (2015). ChIP seeker: An R/Bioconductor package for ChIP peak annotation, comparison and visualization. *Bioinformatics*, *31*(14), 2382–2383. https://doi.org/10.1093/bioinformatics/btv145

Yuan, S., Liu, W. J., Zhang, N. H., Wang, M. Bin, Liang, H. G., & Lin, H. H. (2005). Effects of water stress on major photosystem II gene expression and protein metabolism in barley leaves. *Physiologia Plantarum*, *125*(4), 464–473. https://doi.org/10.1111/j.1399-3054.2005.00577.x

Zhang, H., Lang, Z., & Zhu, J.-K. (2018). Dynamics and function of DNA methylation in plants. *Nature Reviews Molecular Cell Biology*, *19*(8), 489–506. https://doi.org/10.1038/s41580-018-0016-z

Zhang, X., Liu, S., & Takano, T. (2008). Two cysteine proteinase inhibitors from Arabidopsis thaliana, AtCYSa and AtCYSb, increasing the salt, drought, oxidation and cold tolerance. *Plant Molecular Biology*, *68*(1–2), 131–143. https://doi.org/10.1007/s11103-008-9357-x

Zhang, X., Yazaki, J., Sundaresan, A., Cokus, S., Chan, S. W. L., Chen, H., Henderson, I. R., Shinn, P., Pellegrini, M., Jacobsen, S. E., & Ecker, J. R. R. (2006). Genome-wide High-Resolution Mapping and Functional Analysis of DNA Methylation in Arabidopsis. *Cell*, *126*(6), 1189–1201. https://doi.org/10.1016/j.cell.2006.08.003

Zhang, Y., Liu, T., Meyer, C. A., Eeckhoute, J., Johnson, D. S., Bernstein, B. E., Nusbaum, C., Myers, R. M., Brown, M., Li, W., & Liu, X. S. (2008). Model-based Analysis of ChIP-Seq (MACS). *Genome Biology*, *9*(9), 1–9. https://doi.org/10.1186/gb-2008-9-9-r137

Zhang, Y. Y., Li, Y., Gao, T., Zhu, H., Wang, D. J., Zhang, H. W., Ning, Y. S., Liu, L. J., Wu, Y. R., Chu, C. C., Guo, H. S., & Xie, Q. (2008). Arabidopsis SDIR1 enhances drought tolerance in crop plants. *Bioscience, Biotechnology and Biochemistry*, *72*(8), 2251–2254.

https://doi.org/10.1271/bbb.80286

Zhao, J., Sun, H., Dai, H., Zhang, G., & Wu, F. (2010). Difference in response to drought stress among Tibet wild barley genotypes. *Euphytica*, *172*(3), 395–403. https://doi.org/10.1007/s10681-009-0064-8

Zhao, P., Ma, B., Cai, C., & Xu, J. (2022). Transcriptome and methylome changes in two contrasting mungbean genotypes in response to drought stress. *BMC Genomics*, *23*(1), 1–16. https://doi.org/10.1186/s12864-022-08315-z

Zheng, B., & Chen, X. (2011). Dynamics of histone H3 lysine 27 trimethylation in plant development. *Current Opinion in Plant Biology*, *14*(2), 123–129. https://doi.org/10.1016/j.pbi.2011.01.001

Zheng, M., Liu, X., Lin, J., Liu, X., Wang, Z., Xin, M., Yao, Y., Peng, H., Zhou, D. X., Ni, Z., Sun, Q., & Hu, Z. (2019). Histone acetyltransferase GCN5 contributes to cell wall integrity and salt stress tolerance by altering the expression of cellulose synthesis genes. *Plant Journal*, *97*(3), 587–602. https://doi.org/10.1111/tpj.14144

Zheng, Y., Huang, Y., Xian, W., Wang, J., & Liao, H. (2012). Identification and expression analysis of the Glycine max CYP707A gene family in response to drought and salt stresses. *Annals of Botany*, *110*(3), 743–756. https://doi.org/10.1093/aob/mcs133

Zhou, J., Wang, X., He, K., Charron, J.-B. F. B. F., Elling, A. A., & Deng, X. W. (2010). Genome-wide profiling of histone H3 lysine 9 acetylation and dimethylation in Arabidopsis reveals correlation between multiple histone marks and gene expression. *Plant Molecular Biology*, *72*(6), 585–595. https://doi.org/10.1007/s11103-009-9594-7

Zhu, J.-K. (2016). Abiotic Stress Signaling and Responses in Plants. *Cell*, *167*(2), 313–324. https://doi.org/10.1016/j.cell.2016.08.029

Zhu, S. Y., Yu, X. C., Wang, X. J., Zhao, R., Li, Y., Fan, R. C., Shang, Y., Du, S. Y., Wang, X. F., Wu, F. Q., Xu, Y. H., Zhang, X. Y., & Zhang, D. P. (2007). Two calcium-dependent protein kinases, CPK4 and CPK11, regulate abscisic acid signal transduction in Arabidopsis. *Plant Cell*, *19*(10), 3019–3036. https://doi.org/10.1105/tpc.107.050666

Zilberman, D., Gehring, M., Tran, R. K., Ballinger, T., & Henikoff, S. (2007). Genome-wide analysis of Arabidopsis thaliana DNA methylation uncovers an interdependence between methylation and transcription. *Nature Genetics*, *39*(1), 61–69. https://doi.org/10.1038/ng1929

Ziller, M. J., Hansen, K. D., Meissner, A., & Aryee, M. J. (2015). Coverage recommendations for methylation analysis by whole-genome bisulfite sequencing. *Nature Methods*, *12*(3), 230–232. https://doi.org/10.1038/nmeth.3152

Zong, W., Zhong, X., You, J., & Xiong, L. (2013). Genome-wide profiling of histone H3K4-tri-methylation and gene expression in rice under drought stress. *Plant Molecular Biology*, *81*(1–2), 175–188. https://doi.org/10.1007/s11103-012-9990-2

6 Appendix

Table 11. GO enrichment analysis results of genes associated with H3K9ac in D2 (M0vsM2vsD2)

#Aspect	GO	Enrichment_log2	q-value	subset_ratio	description
BP	GO:0009628	0.509	1.07E-04	13.103	response to abiotic stimulus
BP	GO:0044281	0.599	4.77E-04	8.690	small molecule metabolic process
BP	GO:0019637	1.040	6.21E-04	3.191	organophosphate metabolic process
BP	GO:0032502	0.406	7.12E-04	15.886	developmental process
BP	GO:0009657	1.223	8.41E-04	2.308	plastid organization
BP	GO:0009790	0.894	1.23E-03	3.802	embryo development
BP	GO:0006629	0.746	1.26E-03	5.227	lipid metabolic process
BP	GO:0048856	0.385	2.23E-03	15.275	anatomical structure development
BP	GO:0032501	0.382	2.84E-03	15.003	multicellular organismal process
BP	GO:0090407	1.102	8.62E-03	2.037	organophosphate biosynthetic process
BP	GO:0007275	0.371	9.30E-03	13.306	multicellular organism development
BP	GO:0044255	0.748	9.47E-03	3.938	cellular lipid metabolic process
BP	GO:0008544	2.209	1.03E-02	0.611	epidermis development
BP	GO:0009793	0.782	1.50E-02	3.327	embryo development ending in seed dormancy
BP	GO:0009584	4.268	1.63E-02	0.204	detection of visible light
BP	GO:0018298	4.268	1.63E-02	0.204	protein-chromophore linkage
BP	GO:1901564	0.244	1.98E-02	22.743	organonitrogen compound metabolic process
BP	GO:0009791	0.425	2.07E-02	9.029	post-embryonic development
BP	GO:0010027	1.995	2.15E-02	0.611	thylakoid membrane organization
BP	GO:0009658	1.074	2.31E-02	1.697	chloroplast organization
BP	GO:0009668	1.922	2.76E-02	0.611	plastid membrane organization
BP	GO:1901135	0.710	2.81E-02	3.394	carbohydrate derivative metabolic process
BP	GO:0043647	2.410	3.51E-02	0.407	inositol phosphate metabolic process
BP	GO:0006066	1.308	3.69E-02	1.086	alcohol metabolic process
BP	GO:0009314	0.525	4.34E-02	5.160	response to radiation
BP	GO:0015979	0.920	4.36E-02	1.901	photosynthesis
BP	GO:0017006	3.683	4.37E-02	0.204	protein-tetrapyrrole linkage
BP	GO:0008610	0.717	4.39E-02	2.919	lipid biosynthetic process
BP	GO:1901615	0.901	4.91E-02	1.901	organic hydroxy compound metabolic process
BP	GO:0098771	1.159	4.93E-02	1.222	inorganic ion homeostasis
BP	GO:0006970	0.550	4.97E-02	4.549	response to osmotic stress
CC	GO:0044444	0.432	8.67E-13	36.253	cytoplasmic part
CC	GO:0005737	0.411	1.63E-12	38.697	cytoplasm
CC	GO:0009536	0.689	9.62E-11	15.954	plastid
CC	GO:0009507	0.673	1.08E-09	15.139	chloroplast
CC	GO:0005829	0.622	3.52E-06	12.016	cytosol
CC	GO:0016020	0.364	1.85E-05	25.526	membrane
CC	GO:0044434	0.656	1.12E-04	8.622	chloroplast part
CC	GO:0044435	0.645	1.18E-04	8.758	plastid part
CC	GO:0009526	0.894	2.61E-04	4.616	plastid envelope
CC	GO:0031967	0.722	6.82E-04	6.042	organelle envelope
CC	GO:0031975	0.722	6.82E-04	6.042	envelope
CC	GO:0009941	0.851	8.61E-04	4.345	chloroplast envelope
CC	GO:0044436	0.910	3.36E-03	3.259	thylakoid part
CC	GO:0071944	0.387	4.92E-03	13.781	cell periphery
CC	GO:0042651	0.928	4.97E-03	2.987	thylakoid membrane
CC	GO:0034357	0.896	6.40E-03	3.055	photosynthetic membrane
CC	GO:0005623	0.138	9.28E-03	52.546	cell
CC	GO:0044464	0.138	9.54E-03	52.546	cell part

| CC	GO:0005739	0.577	1.00E-02	6.110	mitochondrion
CC	GO:0009535	0.893	1.27E-02	2.716	chloroplast thylakoid membrane
CC	GO:0005886	0.387	1.48E-02	11.541	plasma membrane
CC	GO:0055035	0.875	1.49E-02	2.716	plastid thylakoid membrane
CC	GO:0009579	0.698	1.52E-02	4.073	thylakoid
CC	GO:1902555	4.268	1.63E-02	0.204	endoribonuclease complex
CC	GO:1905348	4.268	1.63E-02	0.204	endonuclease complex
CC	GO:0098588	0.566	2.80E-02	5.024	bounding membrane of organelle
CC	GO:0009570	0.578	2.81E-02	4.888	chloroplast stroma
CC	GO:0009534	0.705	3.39E-02	3.259	chloroplast thylakoid
CC	GO:0031976	0.702	3.53E-02	3.259	plastid thylakoid
CC	GO:0031090	0.469	3.68E-02	6.585	organelle membrane
CC	GO:0031984	0.568	4.23E-02	4.549	organelle subcompartment
CC	GO:0009532	0.539	4.30E-02	4.888	plastid stroma
MF	GO:0016863	4.268	4.13E-05	0.407	intramolecular oxidoreductase activity, transposing C=C bonds
MF	GO:0016860	2.588	3.83E-04	0.747	intramolecular oxidoreductase activity
MF	GO:0005515	0.219	2.79E-03	34.691	protein binding
MF	GO:0005509	1.040	6.11E-03	2.376	calcium ion binding
MF	GO:0004197	2.683	8.22E-03	0.475	cysteine-type endopeptidase activity
MF	GO:0004165	4.268	1.63E-02	0.204	dodecenoyl-CoA delta-isomerase activity
MF	GO:0140104	2.223	1.75E-02	0.543	molecular carrier activity
MF	GO:0003824	0.152	1.84E-02	43.449	catalytic activity
MF	GO:0001883	1.140	2.18E-02	1.561	purine nucleoside binding
MF	GO:0005525	1.140	2.18E-02	1.561	GTP binding
MF	GO:0019001	1.140	2.18E-02	1.561	guanyl nucleotide binding
MF	GO:0032550	1.140	2.18E-02	1.561	purine ribonucleoside binding
MF	GO:0032561	1.140	2.18E-02	1.561	guanyl ribonucleotide binding
MF	GO:0070122	3.946	2.86E-02	0.204	isopeptidase activity
MF	GO:0070138	3.946	2.86E-02	0.204	ubiquitin-like protein-specific isopeptidase activity
MF	GO:0070140	3.946	2.86E-02	0.204	SUMO-specific isopeptidase activity
MF	GO:0015211	3.223	2.94E-02	0.272	purine nucleoside transmembrane transporter activity
MF	GO:0032549	1.051	3.82E-02	1.561	ribonucleoside binding
MF	GO:0001882	1.036	4.28E-02	1.561	nucleoside binding
MF	GO:0042578	0.841	4.31E-02	2.240	phosphoric ester hydrolase activity
MF	GO:0032977	3.683	4.37E-02	0.204	membrane insertase activity
MF	GO:0140318	3.683	4.37E-02	0.204	protein carrier activity
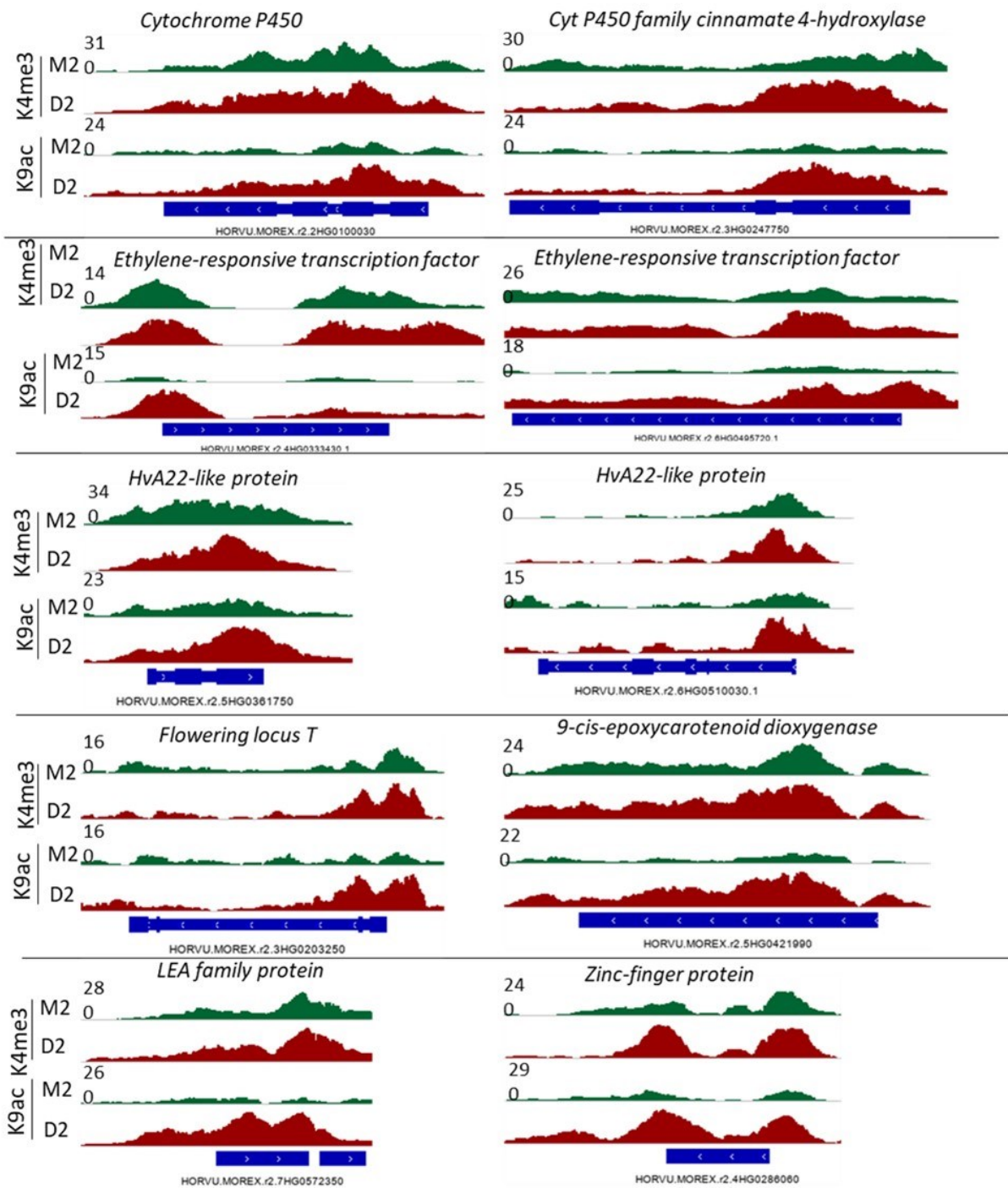
Figure 34. Signal tracks of histone enrichments for selected genes. The increase in H3K9ac in D2 belonging to the GO term 'response to abiotic stimulus' is presented. First two tracks belonging to H3K4me3 and the two bottom tracks to H3K9ac. Green color presents the M2 sample and red the D2 samples.

Table 12. List of DEGs that are upregulated during drought D2 (D2vsM2).

gene	annotation	logFC	adj.P.Val
HORVU.MOREX.r2.3HG0274970	O-methyltransferase	7.48	2.17E-02
HORVU.MOREX.r2.4HG0323160	Laccase	7.10	2.44E-02
HORVU.MOREX.r2.3HG0242240	Coiled-coil domain-containing protein 18, putative isoform 2	7.06	4.48E-02
HORVU.MOREX.r2.2HG0174050	Beta-fructofuranosidase, insoluble protein	6.93	6.55E-03
HORVU.MOREX.r2.3HG0252380	Laccase	6.84	3.43E-02
HORVU.MOREX.r2.6HG0450830	Acid beta-fructofuranosidase	6.77	3.82E-02
HORVU.MOREX.r2.3HG0252410	Laccase	6.55	1.30E-02
HORVU.MOREX.r2.1HG0013640	Peroxidase	6.53	3.35E-02
HORVU.MOREX.r2.2HG0161590	Pectinesterase inhibitor domain containing protein	6.42	1.69E-02
HORVU.MOREX.r2.1HG0059500	Laccase	6.32	1.25E-02
HORVU.MOREX.r2.UnG0626230	C2H2 zinc-finger protein SERRATE (SE)	6.10	1.89E-02
HORVU.MOREX.r2.3HG0253330	DNA glycosylase	6.06	4.93E-02
HORVU.MOREX.r2.4HG0320050	Trichome birefringence-like protein	6.05	2.31E-02
HORVU.MOREX.r2.1HG0070360	Cytochrome b561 and DOMON domain-containing protein	5.95	2.38E-02
HORVU.MOREX.r2.1HG0048800	Trichome birefringence-like protein	5.85	9.33E-03
HORVU.MOREX.r2.4HG0279340	Plasma membrane ATPase	5.80	9.33E-03
HORVU.MOREX.r2.2HG0150910	Retrovirus-related Pol polyprotein from transposon opus	5.70	2.44E-02
HORVU.MOREX.r2.1HG0012120	transcription factor, putative (Protein of unknown function, DUF547)	5.66	2.17E-02
HORVU.MOREX.r2.5HG0400090	Cellulose synthase	5.51	2.44E-02
HORVU.MOREX.r2.3HG0224230	Retrovirus-related Pol polyprotein from transposon TNT 1-94	5.50	9.33E-03
HORVU.MOREX.r2.3HG0274880	Soluble inorganic pyrophosphatase	5.48	1.82E-02
HORVU.MOREX.r2.1HG0068800	Lipid transfer protein	5.41	9.90E-03
HORVU.MOREX.r2.6HG0508020	Myb factor	5.35	2.94E-02
HORVU.MOREX.r2.7HG0619230	Dirigent protein	5.35	1.89E-02
HORVU.MOREX.r2.5HG0434360	RAC-gamma serine/threonine-protein kinase	5.30	1.43E-02
HORVU.MOREX.r2.6HG0510840	Microtubule-associated protein TORTIFOLIA1	5.24	2.90E-02
HORVU.MOREX.r2.2HG0150010	Actin-related protein 2/3 complex subunit 2	5.17	6.55E-03
HORVU.MOREX.r2.5HG0366300	Chaperone DnaJ-domain superfamily protein	5.13	2.17E-02
HORVU.MOREX.r2.2HG0105030	COBRA-like protein	5.13	2.44E-02
HORVU.MOREX.r2.3HG0195770	Fasciclin-like arabinogalactan protein	5.09	2.44E-02
HORVU.MOREX.r2.6HG0449870	Isoflavone reductase-like protein	5.09	2.17E-02
HORVU.MOREX.r2.1HG0068790	Lipid transfer protein	5.06	4.58E-02
HORVU.MOREX.r2.4HG0291960	Heavy metal transport/detoxification superfamily protein	5.05	1.69E-02
HORVU.MOREX.r2.7HG0593340	Serine/threonine-protein kinase atr	4.97	3.31E-02
HORVU.MOREX.r2.1HG0032090	Cellulose synthase	4.94	3.60E-02
HORVU.MOREX.r2.3HG0244020	Methylthioribulose-1-phosphate dehydratase	4.90	3.74E-02
HORVU.MOREX.r2.3HG0242920	branched-chain amino acid transaminase 1	4.89	2.76E-02
HORVU.MOREX.r2.1HG0040740	Purple acid phosphatase	4.81	2.37E-02
HORVU.MOREX.r2.5HG0369430	COBRA-like protein	4.80	1.89E-02
HORVU.MOREX.r2.6HG0489610	FAR1-related sequence 2	4.75	1.39E-02
HORVU.MOREX.r2.7HG0555570	Caleosin	4.74	1.89E-02
HORVU.MOREX.r2.3HG0251960	Gamma-glutamyl phosphate reductase (Delta-1-pyrroline-5-carboxylate synthase)	4.71	3.27E-02
HORVU.MOREX.r2.5HG0447440	Aquaporin-like protein	4.70	2.69E-02
HORVU.MOREX.r2.3HG0184880	Trypsin inhibitor	4.69	2.90E-02
HORVU.MOREX.r2.2HG0174020	Beta-fructofuranosidase, insoluble protein	4.63	3.55E-02
HORVU.MOREX.r2.2HG0126480	Photosystem II 10 kDa polypeptide family protein	4.61	1.89E-02
HORVU.MOREX.r2.3HG0239900	Cellulose synthase	4.61	1.89E-02
HORVU.MOREX.r2.3HG0234850	MYB transcription factor	4.60	2.63E-02
HORVU.MOREX.r2.2HG0149830	Caleosin	4.58	1.82E-02
HORVU.MOREX.r2.3HG0265280	2-oxoglutarate (2OG) and Fe(II)-dependent oxygenase superfamily protein	4.51	3.27E-02
HORVU.MOREX.r2.5HG0399860	C2H2 zinc-finger protein SERRATE (SE)	4.49	3.56E-02
HORVU.MOREX.r2.3HG0224240	Terpenoid cyclases/Protein prenyltransferases superfamily protein	4.47	2.98E-02
HORVU.MOREX.r2.4HG0348600	Heat shock transcription factor	4.46	2.05E-02
HORVU.MOREX.r2.7HG0547450	Thiosulfate sulfurtransferase GlpE	4.36	2.44E-02
HORVU.MOREX.r2.2HG0079450	WEB family protein	4.30	3.85E-02
HORVU.MOREX.r2.2HG0172570	Retrovirus-related Pol polyprotein from transposon TNT 1-94	4.29	1.39E-02
HORVU.MOREX.r2.UnG0633040	Cytochrome P450	4.27	2.05E-02
HORVU.MOREX.r2.1HG0062080	Profilin	4.27	1.56E-02
HORVU.MOREX.r2.5HG0350390	fiber (DUF1218)	4.25	2.90E-02

HORVU.MOREX.r2.6HG0502290	MYB family protein	4.11	4.98E-02
HORVU.MOREX.r2.3HG0234870	RING/U-box superfamily protein	4.08	2.40E-02
HORVU.MOREX.r2.1HG0011450	Proline--tRNA ligase	4.07	2.90E-02
HORVU.MOREX.r2.1HG0071660	Gibberellin 2-oxidase	3.98	2.90E-02
HORVU.MOREX.r2.3HG0224220	Retrovirus-related Pol polyprotein from transposon TNT 1-94	3.98	2.44E-02
HORVU.MOREX.r2.5HG0442690	Patatin	3.95	2.44E-02
HORVU.MOREX.r2.7HG0582870	Senescence-associated protein, putative	3.91	2.44E-02
HORVU.MOREX.r2.7HG0545260	Cytochrome P450	3.89	1.89E-02
HORVU.MOREX.r2.7HG0531800	Sucrose synthase	3.88	1.89E-02
HORVU.MOREX.r2.4HG0332380	Clathrin heavy chain	3.87	3.42E-02
HORVU.MOREX.r2.1HG0028970	Nuclear pore complex protein Nup98	3.85	3.35E-02
HORVU.MOREX.r2.6HG0518300	Transmembrane protein 184C family	3.84	1.89E-02
HORVU.MOREX.r2.1HG0066190	Sulfotransferase	3.84	2.69E-02
HORVU.MOREX.r2.5HG0404790	P-loop containing nucleoside triphosphate hydrolases superfamily protein	3.83	4.92E-02
HORVU.MOREX.r2.6HG0498080	ethylene-responsive transcription factor	3.81	1.89E-02
HORVU.MOREX.r2.2HG0143330	MYB-related transcription factor	3.78	3.75E-02
HORVU.MOREX.r2.2HG0088290	RING/U-box superfamily protein	3.70	3.74E-02
HORVU.MOREX.r2.7HG0595770	Dentin sialophosphoprotein-like	3.70	4.92E-02
HORVU.MOREX.r2.3HG0245240	Disulfide isomerase	3.67	3.35E-02
HORVU.MOREX.r2.2HG0107540	Histone-lysine N-methyltransferase, H3 lysine-9 specific SUVH1	3.66	2.60E-02
HORVU.MOREX.r2.3HG0236180	Protein phosphatase 2C	3.54	9.33E-03
HORVU.MOREX.r2.3HG0258120	Rho GDP-dissociation inhibitor 1	3.53	1.89E-02
HORVU.MOREX.r2.4HG0314890	Vicilin-like protein	3.48	2.91E-02
HORVU.MOREX.r2.7HG0600350	Telomere repeat-binding factor like-protein	3.42	4.31E-02
HORVU.MOREX.r2.4HG0343610	Homeobox protein knotted-1, putative	3.34	3.56E-02
HORVU.MOREX.r2.6HG0519350	Heparanase	3.20	1.89E-02
HORVU.MOREX.r2.4HG0284050	Endoglucanase	3.14	3.38E-02
HORVU.MOREX.r2.7HG0564780	Beta-amylase	3.13	2.44E-02
HORVU.MOREX.r2.5HG0355750	Bidirectional sugar transporter SWEET	3.11	3.35E-02
HORVU.MOREX.r2.3HG0269000	Cysteine-rich receptor kinase	3.10	4.28E-02
HORVU.MOREX.r2.2HG0089370	SCAR family protein	3.06	2.63E-02
HORVU.MOREX.r2.4HG0334210	3-ketoacyl-CoA synthase	2.93	1.90E-02
HORVU.MOREX.r2.4HG0278800	Ankyrin repeat family protein	2.91	3.35E-02
HORVU.MOREX.r2.1HG0052940	Tubulin beta chain	2.91	2.76E-02
HORVU.MOREX.r2.4HG0316930	Hexosyltransferase	2.87	4.29E-02
HORVU.MOREX.r2.5HG0352140	PI-PLC X domain-containing protein	2.69	3.97E-02
HORVU.MOREX.r2.3HG0271440	ABC subfamily C transporter	2.64	2.90E-02
HORVU.MOREX.r2.1HG0031680	Plant/T7N9-9 protein	2.54	4.59E-02
HORVU.MOREX.r2.5HG0399880	Myomodulin neuropeptides 1	2.50	3.00E-02
HORVU.MOREX.r2.3HG0187770	Protein COBRA, putative	2.43	1.90E-02
HORVU.MOREX.r2.3HG0196650	MYB-RELATED transcription factor	2.39	3.57E-02
HORVU.MOREX.r2.6HG0512380	2-oxoglutarate (2OG) and Fe(II)-dependent oxygenase superfamily protein	2.30	2.90E-02
HORVU.MOREX.r2.3HG0226300	Amino acid transporter family protein	2.25	2.17E-02
HORVU.MOREX.r2.3HG0234240	ABC transporter B family protein	2.20	2.33E-02
HORVU.MOREX.r2.5HG0443600	Long-chain-fatty-acid CoA ligase, putative	2.15	2.69E-02
HORVU.MOREX.r2.1HG0066210	Protein phosphatase 2C	2.13	9.33E-03
HORVU.MOREX.r2.6HG0473280	Aldehyde dehydrogenase	2.12	2.44E-02
HORVU.MOREX.r2.3HG0221890	Protein phosphatase 2C	1.99	1.25E-02
HORVU.MOREX.r2.7HG0585130	Negative regulator of sporulation MDS3	1.97	3.55E-02
HORVU.MOREX.r2.1HG0014930	autophagy 2	1.94	1.89E-02
HORVU.MOREX.r2.4HG0281760	UDP-glucose 6-dehydrogenase	1.79	4.02E-02
HORVU.MOREX.r2.2HG0144330	Amino acid permease	1.78	3.27E-02
HORVU.MOREX.r2.5HG0447480	COP1-interacting-like protein	1.72	4.92E-02
HORVU.MOREX.r2.2HG0152870	Kinesin-like protein	1.71	3.75E-02
HORVU.MOREX.r2.3HG0266870	Delta-1-pyrroline-5-carboxylate reductase	1.54	1.69E-02
HORVU.MOREX.r2.3HG0227930	Isoprenylcysteine alpha-carbonyl methylesterase ICME	1.53	4.92E-02
HORVU.MOREX.r2.1HG0067380	Ubiquitin domain-containing protein	1.44	4.48E-02
HORVU.MOREX.r2.6HG0449180	60 kDa chaperonin	1.39	4.20E-02

Table 13. List of genes that are downregulated in D2 (D2vsM2).

gene	annotation	logFC	adj.P.Val
HORVU.MOREX.r2.5HG0356780	Glutaredoxin family protein	-8.93	9.90E-03
HORVU.MOREX.r2.5HG0356760	Glutaredoxin family protein	-7.92	2.05E-02
HORVU.MOREX.r2.1HG0075720	RADIALIS-like transcription factor	-7.53	2.17E-02
HORVU.MOREX.r2.5HG0356890	Glutaredoxin family protein	-7.14	2.94E-02
HORVU.MOREX.r2.1HG0000990	Dirigent protein	-6.83	1.17E-02
HORVU.MOREX.r2.2HG0092470	Peroxidase	-6.53	2.44E-02
HORVU.MOREX.r2.2HG0092500	Peroxidase	-5.92	1.89E-02
HORVU.MOREX.r2.4HG0288340	translation initiation factor	-5.75	3.11E-02
HORVU.MOREX.r2.4HG0337570	ECA1 gametogenesis related family protein	-5.73	2.81E-02
HORVU.MOREX.r2.1HG0076230	Glucan endo-1,3-beta-glucosidase 3	-5.59	2.47E-02
HORVU.MOREX.r2.5HG0356880	Glutaredoxin family protein	-5.38	1.89E-02
HORVU.MOREX.r2.3HG0268330	dicer-like 3	-5.20	1.89E-02
HORVU.MOREX.r2.3HG0188940	AP2/B3 transcription factor family protein	-5.00	2.44E-02
HORVU.MOREX.r2.1HG0075710	RADIALIS-like transcription factor	-4.86	2.44E-02
HORVU.MOREX.r2.5HG0394490	Chaperone protein DNAj, putative	-4.80	2.69E-02
HORVU.MOREX.r2.2HG0149690	Serine/threonine-protein kinase	-4.71	1.97E-02
HORVU.MOREX.r2.5HG0356910	Gag-pol polyprotein	-4.71	2.90E-02
HORVU.MOREX.r2.2HG0149700	Serine/threonine-protein kinase	-4.65	9.33E-03
HORVU.MOREX.r2.5HG0369340	Glutaredoxin family protein	-4.57	3.75E-02
HORVU.MOREX.r2.6HG0503810	Transcription factor RADIALIS	-4.49	3.15E-02
HORVU.MOREX.r2.6HG0521950	Nicotianamine synthase	-4.47	1.89E-02
HORVU.MOREX.r2.1HG0075730	RADIALIS-like transcription factor	-4.37	9.33E-03
HORVU.MOREX.r2.4HG0339950	WAT1-related protein	-4.19	3.85E-02
HORVU.MOREX.r2.6HG0521960	Flagellar hook-basal body complex protein FliE	-4.19	9.90E-03
HORVU.MOREX.r2.7HG0608740	Carbonic anhydrase	-4.14	1.08E-02
HORVU.MOREX.r2.7HG0614600	9-cis epoxycarotenoid dioxygenase	-4.10	3.80E-02
HORVU.MOREX.r2.1HG0073730	RADIALIS-like transcription factor	-4.06	2.17E-02
HORVU.MOREX.r2.2HG0081690	12-oxophytodienoate reductase-like protein	-3.97	3.75E-02
HORVU.MOREX.r2.5HG0356450	Heavy metal transport/detoxification superfamily protein, putative	-3.95	2.47E-02
HORVU.MOREX.r2.2HG0106000	Bifunctional inhibitor/lipid-transfer protein/seed storage 2S albumin superfamily protein	-3.88	4.49E-02
HORVU.MOREX.r2.5HG0358200	Glucan 1,3-beta-glucosidase	-3.87	9.90E-03
HORVU.MOREX.r2.1HG0076300	Receptor-like protein kinase, putative,expressed	-3.84	9.33E-03
HORVU.MOREX.r2.2HG0180810	Purple acid phosphatase	-3.78	2.46E-02
HORVU.MOREX.r2.7HG0527190	50S ribosomal protein L22	-3.77	3.75E-02
HORVU.MOREX.r2.3HG0217920	Retrovirus-related pol polyprotein	-3.68	3.27E-02
HORVU.MOREX.r2.4HG0337410	Cyanate hydratase	-3.65	2.17E-02
HORVU.MOREX.r2.7HG0605570	Receptor kinase	-3.62	2.90E-02
HORVU.MOREX.r2.6HG0513110	1-aminocyclopropane-1-carboxylate oxidase	-3.60	3.17E-02
HORVU.MOREX.r2.7HG0555000	Pathogenesis-related protein 1	-3.49	2.44E-02
HORVU.MOREX.r2.7HG0559290	NAD(P)-binding Rossmann-fold superfamily protein	-3.42	2.90E-02
HORVU.MOREX.r2.3HG0235080	ABC transporter G family member	-3.39	3.74E-02
HORVU.MOREX.r2.7HG0561650	Basic helix-loop-helix transcription factor	-3.38	4.36E-02
HORVU.MOREX.r2.6HG0453710	LINE-1 reverse transcriptase like	-3.38	3.38E-02
HORVU.MOREX.r2.2HG0173970	Allantoinase	-3.32	1.48E-02
HORVU.MOREX.r2.5HG0439240	DNA polymerase epsilon catalytic subunit A, putative	-3.30	2.17E-02
HORVU.MOREX.r2.2HG0153590	Cyclin-like	-3.26	1.05E-02
HORVU.MOREX.r2.4HG0328420	Phytosulfokines 3	-3.26	1.39E-02
HORVU.MOREX.r2.4HG0287220	ENTH/ANTH/VHS superfamily protein	-3.24	3.00E-02
HORVU.MOREX.r2.5HG0446150	Cell wall invertase	-3.20	4.63E-02
HORVU.MOREX.r2.5HG0380960	Fantastic four-like protein	-3.19	3.43E-02
HORVU.MOREX.r2.7HG0592850	Kelch repeat protein	-3.17	3.00E-02
HORVU.MOREX.r2.1HG0068250	transcription initiation factor TFIID subunit, putative (DUF688)	-3.14	3.27E-02
HORVU.MOREX.r2.7HG0618400	proline iminopeptidase	-3.04	3.35E-02
HORVU.MOREX.r2.4HG0295050	Lectin	-3.02	4.38E-02

HORVU.MOREX.r2.3HG0189280	Peptide transporter	-3.00	3.75E-02
HORVU.MOREX.r2.2HG0165650	Anthocyanidin reductase	-2.98	1.39E-02
HORVU.MOREX.r2.3HG0237330	Forkhead box protein O	-2.97	3.97E-02
HORVU.MOREX.r2.1HG0012880	Annexin	-2.93	1.90E-02
HORVU.MOREX.r2.1HG0001860	Leucine-rich repeat receptor-like protein kinase family protein	-2.86	4.09E-02
HORVU.MOREX.r2.6HG0460140	Endoglucanase 11	-2.78	1.25E-02
HORVU.MOREX.r2.1HG0006180	methyl-coenzyme M reductase II subunit gamma, putative (DUF3741)	-2.77	3.29E-02
HORVU.MOREX.r2.2HG0157640	SHR5-receptor-like kinase	-2.74	3.74E-02
HORVU.MOREX.r2.1HG0059820	Plant/T7H20-70 protein	-2.67	1.39E-02
HORVU.MOREX.r2.5HG0401200	O-methyltransferase	-2.63	3.74E-02
HORVU.MOREX.r2.3HG0268300	Two-component response regulator	-2.59	3.56E-02
HORVU.MOREX.r2.5HG0381410	Response regulator	-2.58	3.11E-02
HORVU.MOREX.r2.6HG0454160	Peroxidase	-2.56	3.00E-02
HORVU.MOREX.r2.2HG0143050	Aldose 1-epimerase	-2.47	4.25E-02
HORVU.MOREX.r2.6HG0473100	Sodium transporter	-2.33	2.27E-02
HORVU.MOREX.r2.1HG0070350	O-acyltransferase WSD1	-2.31	2.69E-02
HORVU.MOREX.r2.3HG0193970	Universal stress family protein	-2.26	1.25E-02
HORVU.MOREX.r2.2HG0108690	Lectin receptor kinase	-2.21	3.35E-02
HORVU.MOREX.r2.2HG0079950	Mannose-binding lectin superfamily protein	-2.20	3.74E-02
HORVU.MOREX.r2.4HG0329060	Glutamine synthetase	-2.11	2.49E-02
HORVU.MOREX.r2.3HG0248390	Amino acid permease	-2.09	3.00E-02
HORVU.MOREX.r2.5HG0385870	Chaperone ClpB	-2.06	3.17E-02
HORVU.MOREX.r2.2HG0165270	Cyclin family protein	-2.06	3.35E-02
HORVU.MOREX.r2.1HG0076310	Receptor-like protein kinase, putative,expressed	-2.04	1.39E-02
HORVU.MOREX.r2.1HG0056410	Myb family transcription factor APL	-2.00	4.09E-02
HORVU.MOREX.r2.5HG0363650	Zinc finger protein, putative	-1.98	2.90E-02
HORVU.MOREX.r2.7HG0616140	Leucine-rich repeat receptor-like protein kinase family protein	-1.96	3.27E-02
HORVU.MOREX.r2.6HG0500110	Transcription factor-related family protein	-1.94	2.44E-02
HORVU.MOREX.r2.2HG0172730	Serine/threonine-protein kinase	-1.91	2.90E-02
HORVU.MOREX.r2.3HG0210460	ATPase E1-E2 type family protein / haloacid dehalogenase-like hydrolase family protein	-1.91	2.44E-02
HORVU.MOREX.r2.1HG0077460	Kinase family protein	-1.90	4.29E-02
HORVU.MOREX.r2.7HG0552960	Amino acid transporter, putative	-1.89	2.44E-02
HORVU.MOREX.r2.5HG0439150	Anthranilate synthase	-1.88	3.74E-02
HORVU.MOREX.r2.1HG0077550	Sigma factor sigB regulation protein rsbQ	-1.83	2.52E-02
HORVU.MOREX.r2.6HG0474920	Potassium channel	-1.81	3.27E-02
HORVU.MOREX.r2.5HG0445240	Pantothenate synthetase	-1.79	3.74E-02
HORVU.MOREX.r2.3HG0275510	Jasmonate-induced protein	-1.78	3.22E-02
HORVU.MOREX.r2.5HG0380850	Bifunctional uridylyltransferase/uridylyl-removing enzyme	-1.77	2.38E-02
HORVU.MOREX.r2.2HG0079960	5-methyltetrahydropteroyltriglutamate--homocysteine methyltransferase	-1.70	3.56E-02
HORVU.MOREX.r2.2HG0078890	Cysteine synthase	-1.68	4.18E-02
HORVU.MOREX.r2.2HG0157270	L-allo-threonine aldolase	-1.68	3.05E-02
HORVU.MOREX.r2.2HG0084440	Serine/threonine-protein kinase	-1.64	3.80E-02
HORVU.MOREX.r2.1HG0034100	RING/FYVE/PHD zinc finger superfamily protein	-1.62	2.17E-02
HORVU.MOREX.r2.2HG0160040	Aldose 1-epimerase family protein	-1.58	3.31E-02
HORVU.MOREX.r2.7HG0531260	Autophagy-related protein 22-1	-1.47	2.44E-02
HORVU.MOREX.r2.3HG0187530	Delta(7)-sterol-C5(6)-desaturase	-1.45	2.90E-02
HORVU.MOREX.r2.2HG0085920	Glucose-6-phosphate 1-dehydrogenase	-1.37	3.56E-02
HORVU.MOREX.r2.4HG0276530	Receptor protein kinase, putative	-1.28	2.44E-02
HORVU.MOREX.r2.7HG0617060	Homeobox protein knotted-1, putative	-1.02	4.92E-02

Table 14. PP2Cs associated with H3K9ac in D2. Shown are the TPM-, the bigWigSummary- and the Diffbind values and their corresponding ratios and folds between M2 and D2.

Gene ID	Annotation	RNAseq			BigwigSummary			Diffbind		
		Ø TPM M2	Ø TPM D2	Ratio D2/M2	D2	M2	Ratio D2/M2	D2	M2	Fold (D2-M2)
5HG0392330	PP2C	1.13	28.24	24.94	14.76	2.42	6.11	6.8	4.1	2.7
3HG0236180	PP2C	3.71	51.45	13.86	9.52	3.56	2.67	4.46	1.94	2.53
4HG0323620	PP2C	8.00	73.39	9.18	13.48	4.94	2.73	7.31	5.88	1.43
7HG0604310	PP2C	0.85	10.90	12.84	11.00	2.06	5.35	4	1.2	2.79
3HG0229300	PP2C, putative	1.07	6.08	5.68	9.01	3.03	2.97	6.19	3.82	2.36
3HG0252080	PP2C	9.60	44.45	4.63	13.25	4.33	3.06	8.08	6.71	1.37
1HG0066210	PP2C	20.45	98.72	4.83	10.40	4.74	2.20	7.28	6.17	1.11
7HG0592610	PP2C	1.08	2.94	2.72	14.99	2.32	6.46	4.63	2.9	1.73
2HG0088830	PP2C-like protein	21.14	51.16	2.42	19.80	4.72	4.20	6.18	4.98	1.2
5HG0363800	PP2C family protein	5.64	11.41	2.02	7.73	3.73	2.07	5.05	4.52	0.53
7HG0546220	PP2C, putative	16.94	30.91	1.82	12.66	7.39	1.71	5.83	4.79	1.04
1HG0048630	PP2C family protein	1.41	2.08	1.47	13.04	4.38	2.98	6.11	4.37	1.74
5HG0419590	PP2C family protein	20.79	32.15	1.55	9.56	4.96	1.93	5.24	4.56	0.68
6HG0463090	PP2C, putative	9.28	10.38	1.12	9.17	5.84	1.57	3.55	3.04	0.51
3HG0225580	PP2C family protein	5.75	5.81	1.01	14.77	10.99	1.34	5.06	4.8	0.26
5HG0434880	PP2C	3.87	3.97	1.02	10.02	7.98	1.26	4.48	3.51	0.97
2HG0142110	PP2C family protein	5.46	5.77	1.06	12.33	6.83	1.81	4.12	3.73	0.39
1HG0076850	PP2C family protein	7.87	8.08	1.03	12.03	7.91	1.52	5.03	4.43	0.6
2HG0117550	PP2C	5.67	5.38	0.95	12.60	7.01	1.80	5.27	4.52	0.75
2HG0110630	PP2C, putative	2.47	2.51	1.02	7.97	4.96	1.61	6.33	5.44	0.89
6HG0483290	PP2C containing protein	15.60	14.97	0.96	10.89	4.63	2.35	5.6	4.34	1.27
6HG0487760	PP2C	3.88	3.86	0.99	10.54	4.55	2.31	N/A	N/A	N/A
3HG0275550	PP2C family protein	13.21	11.67	0.88	11.79	8.89	1.33	6.29	5.66	0.62
6HG0501830	PP2C	5.15	4.26	0.83	9.35	3.74	2.50	5.87	5.15	0.71
1HG0068360	PP2C, putative	7.80	6.57	0.84	8.05	5.72	1.41	4.8	4.4	0.4
4HG0333340	PP2C, putative	128.70	41.04	0.32	9.97	6.52	1.53	7.14	6.68	0.47

Table 15. Signal tracks of PP2Cs marked with H3K9ac in D2.

Gene ID	Annotation	Homology	logFC	padj	Signal track
HORVU.MOREX.r2.5HG0392330	Protein phosphatase 2C	OsPP2C68	4.87	7.13E-02	
HORVU.MOREX.r2.3HG0236180	Protein phosphatase 2C		3.54	9.33E-03	
HORVU.MOREX.r2.7HG0604310	Protein phosphatase 2C		3.03	2.09E-01	
HORVU.MOREX.r2.3HG0229300	Protein phosphatase 2c, putative		2.24	1.98E-01	
HORVU.MOREX.r2.1HG0066210	Protein phosphatase 2C		2.13	9.33E-03	
HORVU.MOREX.r2.7HG0592610	Protein phosphatase 2C		1.25	2.13E-01	
HORVU.MOREX.r2.2HG0088830	Protein phosphatase 2C-like protein		1.04	7.68E-01	
HORVU.MOREX.r2.7HG0546220	Protein phosphatase 2c, putative		0.79	6.01E-01	
HORVU.MOREX.r2.6HG0463090	Protein phosphatase 2c, putative		-0.02	9.93E-01	
HORVU.MOREX.r2.3HG0225580	Protein phosphatase 2C family protein		-0.05	9.65E-01	
HORVU.MOREX.r2.5HG0434880	Protein phosphatase 2C		-0.05	9.72E-01	
HORVU.MOREX.r2.1HG0076850	Protein phosphatase 2C family protein		-0.10	8.88E-01	
HORVU.MOREX.r2.2HG0117550	Protein phosphatase 2c		-0.13	8.95E-01	
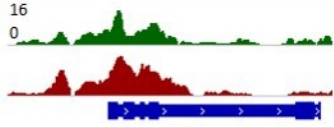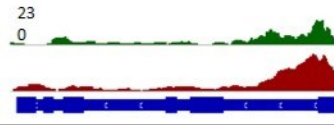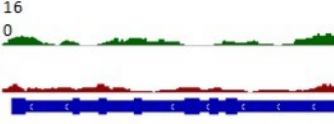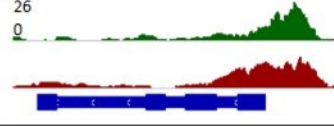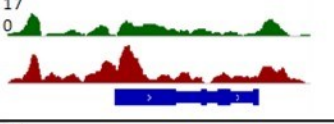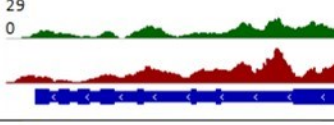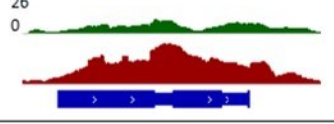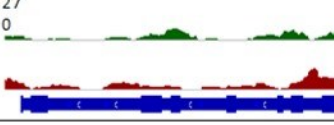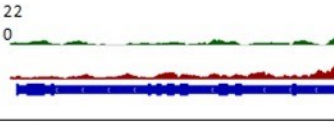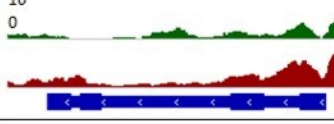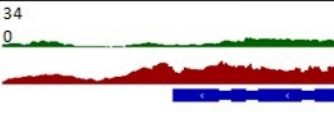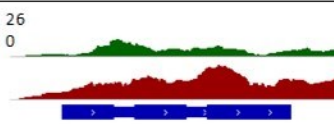
HORVU.MOREX.r2.2HG0110630	Protein phosphatase-2c, putative	-0.16	8.62E-01	
HORVU.MOREX.r2.6HG0483290	Protein phosphatase 2C containing protein	-0.18	8.51E-01	
HORVU.MOREX.r2.6HG0487760	Protein phosphatase 2C	-0.24	7.80E-01	
HORVU.MOREX.r2.3HG0275550	Protein phosphatase 2C family protein	-0.32	6.15E-01	
HORVU.MOREX.r2.6HG0501830	Protein phosphatase 2C	-0.43	4.63E-01	
HORVU.MOREX.r2.1HG0068360	Protein phosphatase 2c, putative	-0.56	6.24E-01	
HORVU.MOREX.r2.4HG0333340	Protein phosphatase 2c, putative	-1.54	2.74E-01	
HORVU.MOREX.r2.1HG0048630	Phosphatase 2C family protein	0.69	8.80E-01	
HORVU.MOREX.r2.2HG0142110	Phosphatase 2C family protein	-0.10	9.56E-01	
HORVU.MOREX.r2.5HG0419590	Phosphatase 2C family protein	0.43	5.73E-01	
HORVU.MOREX.r2.5HG0363800	Phosphatase 2C family protein	0.85	3.11E-01	
Manually				
HORVU.MOREX.r2.3HG0252080	Protein phosphatase 2C	2.20	3.12E-01	
HORVU.MOREX.r2.4HG0323620	Protein phosphatase 2C	3.1	2.03E-01	

Table 16. List of primers used in the qRT-PCR and validation.

Gene ID	Gene annotation	Primer name		Primer sequence (5'->3')
HORVU.MOREX.r2.1HG0067180	senescence regulator (DUF584)	HvS40	for	CGACGGCGACGTCCGATGTA
			rev	CTTTGAGCGTCCTCCCTTTGC
HORVU.MOREX.r2.4HG0329060	Glutamine synthetase	HvGS2	for	ACGAGCGGAGGTTGAGAGG
			rev	CGCCCCACACGAATAGAGCA
HORVU.MOREX.r2.3HG0251960	Delta-1-pyrroline-5-carboxylate synthase	HvP5CS2	for	GGGCGTACCTGCTGTCATTG
			rev	ACTGTCATCTCACGGGGTGTCACT
HORVU.MOREX.r2.1HG0065280	Late embryogenesis abundant protein	HvA1	for	AAGCAGTCGATCCATTCCAAGT
			rev	CATCATCTGCCCGGTCTTCTC
HORVU.MOREX.r2.3HG0187700	Heat shock protein	HvHsp17	for	TCGAGATCTCCGGCTGAATGC
			rev	CGGCAAGAACAACGACACAAC
HORVU.MOREX.r2.3HG0274970	O-methyltransferase		for	TCACCACCACGTACGTAACA
			rev	CATCAGGGTCTCGAGGAGTC
HORVU.MOREX.r2.3HG0234850	MYB transcription factor	MYB TF	for	GGAACAGCTGCCTCAAGAAG
			rev	CCGGGAAAGGGTCGAAAAC
HORVU.MOREX.r2.7HG0545260	Cytochrome P450	CYP 450	for	TCCACAGGCACCTCAATCAT
			rev	TGCTTGAGTTCTGGAGAGGG
HORVU.MOREX.r2.3HG0236180	Protein phosphatase 2C		for	TCCGTCGATCACAAACCTGA
			rev	ACAGACCATCGCTTGCTAGA
HORVU.MOREX.r2.1HG0066210	Protein phosphatase 2C		for	CAGTTGTTCCTCGGGCAAAA
			rev	GATCCATCGCCTCCATCTGA
HORVU.MOREX.r2.3HG0221890	Protein phosphatase 2C	HvABI1	for	TTGTTCCTCGAGCGAAGGAT
			rev	GTTGGGCGGATGACAAGTTT
HORVU.MOREX.r2.5HG0392330	Protein phosphatase 2C	HvPP2C	for	CTACCTCAAGCCGTTCGTGA
			rev	GTTGTCCGAGCTGTTCTTCG
HORVU.MOREX.r2.3HG0238180	Heat shock transcription factor	HSTF	for	CCTCCCCTCCTACTTCAAGC
			rev	ACCTTGCGAAATCCCTGAGA
HORVU.MOREX.r2.5HG0355750	Bidirectional sugar transporter SWEET	SWEET transporter	for	CTCTTCTTCCTCCTCGTCCC
			rev	ATCAACACGCAACGGTCAAA
HORVU.MOREX.r2.4HG0319220	Abscisic acid receptor	ABA receptor	for	CCCCAACCCTACCTTCGAAA
			rev	CTAGGACTCGGTGGTGGTG
HORVU.MOREX.r2.3HG0249890	Transcription factor	BzIP TF	for	TCAAATCAAACCCCGAACCC
			rev	CGAGTGTTACGGAAGGTGC
HORVU.MOREX.r2.1HG0001540	Actin	Actin	for	GGAAATGGCTGACGGTGAGGAC
			rev	GGCGACCAACTATGCTAGGGAAAAC
HORVU.MOREX.r2.4HG0335530	Serine/threonine-protein phosphatase	PP2A	for	CACCATTTCTCAGCTTGTATTG
			rev	CACCCCTTTGTTATTGTTTGTTG
HORVU.MOREX.r2.1HG0027750	Histone acetyltransferase	GCN5	for	CAGGCCGCGTCAACCAAGAAC
			rev	GGACGGCATAACAAGCAAGTCAG
HORVU.MOREX.r2.3HG0229370	WRKY transcription factor	WRKY21	for	CTCTTCGACGTCGTGTACCA
			rev	CACGGAGATCTGCTCCTGTC

Legend of Figures

Legend of Tables

Acknowledgements

First and foremost, I want to thank my supervisor Prof. Dr. Klaus Humbeck for giving me the opportunity to work in his group and fulfill my PhD project. His academic guidance, his scientific experience and his motivation helped me whenever questions and problems arose.

I am deeply grateful to Prof. Dr. Nils Stein, Dr. Martin Mascher, Dr. Axel Himmelbach, Dr. Sudharsan Padmarasu and Ines Walde from IPK Gatersleben. Prof. Nils Stein and Dr. Martin Mascher for taking part in my project and especially Dr. Martin Mascher for guiding me through the complex bioinformatics. Dr. Axel Himmelbach and Ines Walde for processing and sequencing all my samples and Dr. Sudharsan Padmarasu for helping me with the WGBS. You all helped me build the base of this thesis!

I would like to offer my special thanks to former lab member Dr. Xuan Hieu Cao who patiently answered my countless questions and always gave me food for thought with his critical and innovative thinking.

Thanks to the WissenschaftsCampus Halle for funding my project "BEP- Barley Epigenome Project" in the first years and providing me an insight into other interesting projects.

Moreover, I want to express my gratitude to the reviewers for their precious time and expertise to review my work.

Furthermore, I am deeply grateful to get to know and work with the current and former members of the AG Humbeck, namely Dr. Athina Parasyri, Bianka Janack, Linh Thuy Nguyen, Minh Manh Bui, Dr. Nancy Zimmermann, Dr. Olaf Barth, Siska Herklotz, Sylvie Schäfer, Dr. Wiebke Zschiesche and Michael Röser. It was a joyful and nice work atmosphere and regardless whom I asked for help, I always got adequate support. A big thank you to Dr. Olaf Barth, for his detailed and profound explanations and especially helping me with the WGBS data analysis. A very special thanks goes to Athina. I really enjoyed sharing the office with you and our talks about each and everything.

Thank you to my Mum and Dad, Bernhard, Laura, Jojo, Oma, Opa, Heidrun, Marion and Reiner. Your support meant everything to me. Lastly, I want to say thank you to Flo and Carla. Flo, your imperturbable patience and your never-ending support and encouragement helped me through all the ups and downs of this work.

Thank you all for this exciting and instructive time!

Curriculum vitae

Name	Charlotte Ost
Geburtsdatum	18.01.1990
Geburtsort	Berlin-Steglitz
Nationalität	Deutsch

Werdegang

Seit 10/22	**Anfertigung der Promotion**: Drought stress induced changes in the epigenome and transcriptome of barley plants, Martin-Luther Universität Halle-Wittenberg, Fakultät für Biologie, Prof. Dr. Klaus Humbeck
07/21-08/22	**Elternzeit**
Seit 10/16	**Wissenschaftliche Mitarbeiterin** an der Martin-Luther-Universität Halle-Wittenberg, Institutsbereich Pflanzenphysiologie, AG Prof. Dr. Klaus Humbeck
04/16-07/16	**Wissenschaftliche Hilfskraft** an der TU Dresden, Institut für Botanik, Professur für Zell- und Molekularbiologie der Pflanzen, Prof. Dr. Thomas Schmidt
09/15-03/16	**Masterarbeit**: Identifikation und Charakterisierung von Satelliten-DNAs in *Chenopodium quinoa*
10/12-03/16	**Masterstudium der Biologie (M.Sc.)** an der Technischen Universität Dresden
05/12-08/12	**Bachelorarbeit:** Analyse der spleissregulatorischen Funktion des Polypyrimidintrakt-Bindeproteins in Arabidopsis thaliana
10/09-08/12	**Bachelorstudium der Biologie (B.Sc.)** an der Eberhard Karls Universität Tübingen
06/00-06/09	**Allgemeine Hochschulreife** am Gymnasium Nottuln

Veröffentlichungen und Präsentationen

- **Ost, C.**, Cao, H. X., Nguyen, T. L., Himmelbach, A., Mascher, M., Stein, N., & Humbeck, K. (2023). Drought-Stress-Related Reprogramming of Gene Expression in Barley Involves Differential Histone Modifications at ABA-Related Genes. *International Journal of Molecular Sciences*, *24*(15), 12065.

- Manh, M. B., **Ost, C**., Peiter, E., Hause, B., Krupinska, K., & Humbeck, K. (2023). WHIRLY1 Acts Upstream of ABA-Related Reprogramming of Drought-Induced Gene Expression in Barley and Affects Stress-Related Histone Modifications. *International Journal of Molecular Sciences*, *24*(7), 6326.

- Heitkam, T., Weber, B., Walter, I., Liedtke, S., **Ost, C**., & Schmidt, T. (2020). Satellite DNA landscapes after allotetraploidization of quinoa (Chenopodium quinoa) reveal unique A and B subgenomes. *The Plant Journal*, *103*(1), 32-52.

- "BEP - Barley Epigenome Project", 9th International Symposium on Plant Senescence, Berlin, April 2019 (Präsentation)

Eidesstattliche Erklärung

LV

Hiermit versichere ich, dass ich die vorliegende Arbeit mit dem Titel

„Drought-Stress-Related Reprogramming of Gene Expression in Barley Involves Differential Histone Modifications at ABA-related Genes"

in allen Teilen selbstständig und ohne unzulässige fremde Hilfe verfasst habe, dass ich keine anderen als die in der Arbeit angegebenen Quellen und Hilfsmittel, insbesondere keine KI-Software, benutzt habe, und dass ich die Stellen der Arbeit, die ich anderen Werken – auch elektronischen Medien – dem Wortlaut oder Sinn nach entnommen habe, in jedem Fall unter Angabe der Quelle als Entlehnung kenntlich gemacht habe.

Halle (Saale),

(Ort, Datum, Unterschrift)